2017-03-01

Phylogenetic Relationships, Species Boundaries, and Studies of Viviparity and Convergent Evolution in *Liolaemus* Lizards

Cesar Augusto Aguilar
Brigham Young University

Phylogenetic Relationships, Species Boundaries, and Studies of Viviparity and Convergent Evolution in *Liolaemus* Lizards

Cesar Augusto Aguilar

A dissertation submitted to the faculty of
Brigham Young University
in partial fulfillment of the requirements for the degree of

Doctor of Philosophy

Jack W. Sites Jr., Chair
Byron J. Adams
Mark C. Belk
Leigh A. Johnson
Michael R. Stark

Department of Biology

Brigham Young University

ABSTRACT

Phylogenetic Relationships, Species Boundaries, and
Studies of Viviparity and Convergent Evolution
in *Liolaemus* Lizards

Cesar Augusto Aguilar
Department of Biology, BYU
Doctor of Philosophy

In this thesis I have connected different evolutionary studies of *Lioalemus* lizards. In Chapter 1, I followed an integrative approach to delimit species in the *Liolaemus walkeri* complex. Using mitochondrial markers, morphological data, bioclimatic information and methods appropriate for each data type, we found that the name *L. walkeri* was covering three new lineages. Three new species were described and one of them (*L. chavin*) is now categorized as Near Threatened in the IUCN red list.

In Chapter 2, I change the subject from species boundaries to the study of viviparity and placentation. In this paper we employed scanning electron and confocal microscopy to compare the placental ultra-structure and pattern of blood vessels in two *Liolaemus* species. One of the most remarkable traits found is the complete reduction of the eggshell in both placentae, a possible adaptation to improve gas exchange in the hypoxic environments of the high Andes.

In chapter 3, I returned to the issue of species delimitation and employed two integrative approaches: a hypothetical deductive framework and a model-based procedure. I applied both approaches in lowland and highland *Liolaemus* species of the *montanus* group. I found that in only one case (of four) an unnamed lowland lineage ("Nazca") was delimited concordantly by both procedures.

In Chapter 4, I focus on a study of convergent evolution of desert phenotype in *Liolaemus* species and *Ctenoblepharys adspersa*. I performed a Bayesian time calibrated and maximum likelihood tree based on 55 taxa and seven molecular markers. We employed quantitative and categorical traits based on 400 specimens and non-metric multidimensional scaling to obtain new quantitative variables. I used three phylogenetic comparative methods to identify and measure the strength of convergence. My results found a strong case of convergent traits in *C. adspersa, L. lentus, L. manueli, L. poconchilensis* and *L. stolzmanni* that are probably related to predator avoidance in the Peruvian-Atacama and Monte deserts. In addition, my time calibrated tree resolves the origin of these traits first in *C. adspersa* at about 80 million years (My) and later independently in *Liolaemus* species at about 25 My suggesting the present of evolutionary constraints.

Keywords: *Liolaemus*, lizards, species delimitation, placentation, convergence

ACKNOWLEDGMENTS

I would like to express my gratitude to different people and institutions that help me in many ways with my research. First I want to thank my advisor Jack W. Sites Jr. who since 2010 when I started my PhD studies, has been incredibly wise, patient and supportive. I would like to thank my committee for their constant positive attitude towards my research. I want to show appreciation to my friends Ana Almendra, Robert Langstroth, Catherine L. Malone, Cintia Medina and Andrea Roth; all of them in one way or another, and in different moments, shared with me unforgettable moments during my time as PhD student. I am also grateful to Peruvian students and researchers in the Department of Herpetology in San Marcos Natural History Museum for their help with my fieldwork and providing material for my research. I also thank Jesus Cordova, curator of the Department of Herpetology in Peru, for providing me with a loan of specimens and helping me with permits. I would like to thank my lab partners, especially Perry L. Wood Jr., and my colleagues Mariana Morando, Luciano Avila, Ignacio de la Riva and Jaime Troncoso for their help in different aspects of my research.

I am indebted to the BYU Biology Department, Monte L. Bean Life Science Museum, Waitt Foundation-National Geographic Society, BYU Graduate Studies and National Science Foundation for their financial support without which my research would not be possible. I am grateful to researchers of the San Marcos Natural History Museum and friends in the Ministerio de Agricultura for their advice and help in getting permits.

My family deserves special consideration. My brother Alex and sister Silvia as well as my sister's children were always supportive and happily welcomed me every time I went to Peru.

TABLE OF CONTENTS

LIST OF TABLES

Chapter 4

LIST OF FIGURES

Chapter 1

Chapter 2

Chapter 3

Chapter 4

CHAPTER 1: Integrative taxonomy and preliminary assessment of species limits in the *Liolaemus walkeri* complex from Peru (Squamata, Liolaemidae) with descriptions of three new species

ZooKeys 364: 47–91 (2013)
doi: 10.3897/zookeys.364.6109
www.zookeys.org

RESEARCH ARTICLE

A peer-reviewed open-access journal
ZooKeys
Launched to accelerate biodiversity research

Integrative taxonomy and preliminary assessment of species limits in the *Liolaemus walkeri* complex (Squamata, Liolaemidae) with descriptions of three new species from Peru

César Aguilar[1,2,3,†], Perry L. Wood Jr[1,‡], Juan C. Cusi[2,§], Alfredo Guzmán[2,|], Frank Huari[2,¶], Mikael Lundberg[2,#], Emma Mortensen[1,††], César Ramírez[2,‡‡], Daniel Robles[2,§§], Juana Suárez[2,||], Andres Ticona[2,¶¶], Víctor J. Vargas[4,##], Pablo J. Venegas[5,†††], Jack W. Sites Jr[1,‡‡‡]

1 *Department of Biology and Bean Life Science Museum, Brigham Young University (BYU), Provo, UT 84602, USA* **2** *Departamento de Herpetología, Museo de Historia Natural de San Marcos (MUSM), Av. Arenales 1256, Jesús María, Lima, Peru* **3** *Instituto de Ciencias Biológicas Antonio Raimondi, Facultad de Ciencias Biológicas, Universidad Nacional Mayor de San Marcos, Lima, Peru* **4** *Asociación Pro Fauna Silvestre, Urb. Mariscal Cáceres Mz. L - Lt. 48, Huamanga, Ayacucho, Peru* **5** *División de Herpetología-Centro de Ornitología y Biodiversidad (CORBIDI), Santa Rita N°105 Of. 202, Urb. Huertos de San Antonio, Surco, Lima, Peru*

† *http://zoobank.org/6335B1C1-913C-4A2B-B3D4-292EA2D6D92F*
‡ *http://zoobank.org/5E6D0639-94CB-498A-827F-304DE273A804*
§ *http://zoobank.org/6BA95434-F8A0-410D-9F2A-DC35BEF01F2B*
| *http://zoobank.org/FCBAF2C0-9546-4024-8D0E-7A291386D693*
¶ *http://zoobank.org/C4C422E5-9F13-4E38-B740-15A4DBD50316*
# *http://zoobank.org/6EC7C05E-2740-467B-8C0A-A035F13A0ABE*
†† *http://zoobank.org/2BAD6DDD-DA3D-4E4A-AF1B-8F9F9D0E869E*
‡‡ *http://zoobank.org/34A9C3EB-0EA2-468B-9C9E-EC061ABB977F*
§§ *http://zoobank.org/2A708076-1D13-4288-BC7B-5971A3B4C1F3*
|| *http://zoobank.org/5EE8B041-A5C3-4DB9-B3CD-BACC9A31A6AF*
¶¶ *http://zoobank.org/1AFB66B3-85B6-45EE-AA6D-2BCBB505EB98*
http://zoobank.org/9CA58752-DE80-4B17-997E-F7196BCC984F
††† *http://zoobank.org/15AD03E1-9ACF-4F38-AA96-09A5A56A3DC4*
‡‡‡ *http://zoobank.org/7A606DC2-9A3B-4C44-9FD4-C82BB8C2F70E*

Corresponding author: *César Aguilar* (caguilarp@gmail.com)

Academic editor: *L. Penev* | Received 21 August 2013 | Accepted 5 December 2013 | Published 18 December 2013

http://zoobank.org/1D085067-2D94-4404-B0BD-6E6615371BF6

Citation: Aguilar C, Wood PL Jr, Cusi JC, Guzmán A, Huari F, Lundberg M, Mortensen E, Ramírez C, Robles D, Suárez J, Ticona A, Vargas VJ, Venegas PJ, Sites JW Jr (2013) Integrative taxonomy and preliminary assessment of species limits in the *Liolaemus walkeri* complex (Squamata, Liolaemidae) with descriptions of three new species from Peru. ZooKeys 364: 47–91. doi: 10.3897/zookeys.364.6109

Abstract

Species delimitation studies based on integrative taxonomic approaches have received considerable attention in the last few years, and have provided the strongest hypotheses of species boundaries. We used three lines of evidence (molecular, morphological, and niche envelopes) to test for species boundaries in Peruvian populations of the *Liolaemus walkeri* complex. Our results show that different lines of evidence and analyses are congruent in different combinations, for unambiguous delimitation of three lineages that were "hidden" within known species, and now deserve species status. Our phylogenetic analysis shows that *L. walkeri*, *L. tacnae* and the three new species are strongly separated from other species assigned to the *alticolor-bibronii* group. Few conventional morphological characters distinguish the new species from closely related taxa and this highlights the need to integrate other sources of data to erect strong hypothesis of species limits. A taxonomic key for known Peruvian species of the subgenus *Lioalemus* is provided.

Resumen

Los estudios sobre delimitación de especies basados en un enfoque integral han recibido considerable atención en los últimos años, y proveen las hipótesis más robustas sobre límites de especies. Usamos tres líneas de evidencia (molecular, morfológica y modelos de nichos) para evaluar los límites de especies entre poblaciones peruanas del complejo *Liolaemus walkeri*. Nuestros resultados muestran que las diferentes líneas de evidencia y análisis en diferentes combinaciones son congruentes en el descubrimiento no ambiguo de tres linajes que estuvieron confundidos con especies ya conocidas y que ahora merecen reconocimiento específico. Nuestro análisis filogenético muestra que *L. walkeri*, *L. tacnae* y las tres nuevas especies están bien distanciadas de las otras especies asignadas al grupo *alticolor-bibronii*. Pocos caracteres morfológicos convencionales distinguen las nuevas especies de otras estrechamente relacionadas, y esto indica la necesidad de integración de diferentes fuentes de datos para elaborar hipótesis más sólidas sobre límites entre especies. Se proporciona una clave taxonómica para las especies peruanas conocidas del subgénero *Liolaemus*.

Keywords

Liolaemus walkeri complex, integrative taxonomy, new species, viviparity

Introduction

The issue of species delimitation (building explicit hypotheses about species lineages and their geographic boundaries) has received considerable attention in the last decade due in part to an emerging consensus about species concepts and new approaches for testing species boundaries (Sites and Marshall 2003, 2004, de Queiroz 2007, Knowles and Carstens 2007, Wiens 2007, Padial and De la Riva 2010, Padial et al. 2010, Hart 2011, Zapata and Jiménez 2012, Camargo and Sites 2013). The ontological General Lineage Concept (GLC) defines a species as a group of separately evolving meta-population lineages, originally proposed by Mayden (1997, 2002) and de Queiroz (1998, 2005). This definition is generally supported by a consensus view in evolutionary biology (Padial and De la Riva 2010, Padial et al. 2010, Hart 2011, Zapata and Jiménez 2012, but see Hausdorf 2011). The GLC distinguishes the primary property (species are separately evolving meta-population lineages) that is shared by most previous competing species concepts (e.g., biological, phylogenetic, ecological species concept, etc.), from secondary properties (e.g., reproductive isolation, character fixation, niche

differentiation, etc.) that arise at different times during the processes of speciation (de Queiroz 2007). These secondary properties are lines of evidence that are relevant to inferring the species boundaries (de Queiroz 2005, 2007).

In addition to this agreement with respect to GLC, there is a growing number of new empirical methods of species delimitation (SDL; Pons et al. 2006, Knowles and Carstens 2007, Kubatko et al. 2009, Carstens and Dewey 2010, Flot et al. 2010, Hausdorf and Hennig 2010, Martínez-Gordillo et al. 2010, Gurgel-Gonçalves et al. 2011). These new methods for testing hypotheses of species boundaries have been accommodated under the new term "integrative taxonomy" (IT; Dayrat 2005, Padial and De la Riva 2010, Padial et al. 2010). Methods such as the multi-locus coalescent to infer species limits without monophyletic lineages, ecological niche modeling (ENM) to assess spatial distributions of closely related species, and multivariate tolerance regions to test for discontinuities or gaps in morphology, have all been used in new integrative taxonomic studies (Omland et al. 2006, Knowles and Carstens 2007, Raxworthy et al. 2007, Rissler and Apodaca 2007, Vasconcelos et al. 2012, Zapata and Jiménez 2012).

Character fixation as well as discontinuities or gaps have been used as a SDL criterion to assess species limits based on genetic and morphological characters (Marshall et al. 2006, Zapata and Jiménez 2012). Fixed differences and gaps in morphology suggest that some evolutionary force (e.g., absence of gene flow, natural selection) prevent two putative taxa from homogenizing (Wiens and Servedio 2000, Zapata and Jiménez 2012). Often analysis of variance or discriminant analysis have been used to evaluate morphological differentiation in SDL studies, but these statistics, even if significant, evaluate central tendencies and not gaps in morphology, and the latter may be more relevant for testing species boundaries (Zapata and Jiménez 2012). In addition to character fixation and gaps in morphology, niche envelopes can be used to assess the status of uncertain populations which are separated from closely related species by areas that are outside of the climatic niche envelope, and where gene flow between these species is unlikely because it would involve crossing unsuitable habitat (Wiens and Graham 2005). Ecological niche modeling (ENM) can summarize niche envelopes and this approach has also been used in SDL studies (e.g., Raxworthy et al. 2007, Rissler and Apodaca 2007).

Well-supported hypotheses of species boundaries are essential because species are used as basic units of analysis in several areas of biogeography, ecology, and macroevolution, and from the broader perspective of evolutionary theory, delimiting species is important in the context of understanding many evolutionary mechanisms and processes (Sites and Marshall 2003, 2004, Wiens 2007). Among animal groups, lizards have been used extensively in evolutionary studies ranging from community ecology, behavioral ecology, multiple origins of body elongation coupled with limb reduction/loss, multiple origins of novel reproductive modes, including parthenogenesis and viviparity (Sites et al. 2011), as well as phylogeography and speciation studies (Camargo et al. 2010).

SDL studies in lizards have included molecular markers, morphological characters and/or models of species distributions (Camargo et al. 2010). In particular, several clades of the genus *Liolaemus* Wiegmann, 1834 have been studied intensively using

molecular and morphological data to delimit species and infer phylogeographic histories (Morando et al. 2008, Victoriano et al. 2008, Breitman et al. 2011a, 2012), and for testing hypotheses about evolutionary processes (Olave et al. 2011) and performance (in accuracy and precision) of different SDL methods (Camargo et al. 2012). This South American genus includes ~ 230 species (Breitman et al. 2011b), and extends from central Peru to Tierra del Fuego, and from sea level on both Atlantic and Pacific coasts to almost 5000 m in elevation. Species diversity is highest in the Andes and adjacent arid regions, and new species descriptions are published at a rate of 4–5/yr, from moderately well-known areas in Argentina and Chile.

In most cases these studies have demonstrated that populations assigned to single species based on generalized morphological features and limited field sampling, tend to under-represent biodiversity. Distinct lineages have been revealed by molecular data, many of which are later described as new species (e.g., Breitman et al. 2011a, b). The largest poorly-known areas for the genus are the Andean regions of Bolivia, Peru and northern Chile. Intensive fieldwork and molecular phylogenetic studies have never been systematically carried out in these regions, and species descriptions have traditionally been based on gross comparisons of morphological characters from small sample sizes and limited geographic sampling. So SDL studies are needed in the extreme northern range of *Liolaemus* (e.g., Peru) based on intensive geographic sampling and large series for collection of new molecular, coloration, and various classes of morphological data.

Currently, 14 species of *Liolaemus* are known from Peru (*L. montanus* group, 10 spp; *L. alticolor* group, 4 spp), but SDL studies based on an integrative approach have not been carried out in either of these groups. Moreover, several areas in the Peruvian Andes remain completely unexplored, and based on recent studies in the southern range of *Liolaemus*, it is highly probable that the Peruvian Andes harbor many undiscovered species. Here, we use new molecular, morphological, and geographic data from known Peruvian species (*L. alticolor* Barbour, 1909, *L. incaicus* Lobo, Quinteros & Gómez, 2007, *L. tacnae* (Shreve, 1941) and *L. walkeri* Shreve, 1938), assigned to the *L. alticolor* group, and three populations morphologically similar to *L. walkeri* (identified by their regions of occurrence: Ancash, Ayacucho and Cusco), to present the first SDL study based on an IT approach. Our results provide evidence that three new lineages deserve species status, and these are described herein.

Methods

Sampling and DNA extraction

Lizards were collected by hand, photographed and sacrificed with an injection of pentobarbital. After liver tissue was collected for DNA samples, whole specimens were fixed in formaldehyde at 10% and transferred to 70% ethanol for permanent storage in museum collections. Tissue samples were collected in duplicate, stored in 96% ethanol and deposited at the Bean Life Science museum at Brigham Young University (BYU)

and Museo de Historia Natural de San Marcos (MUSM) (see Data resources below). Total genomic DNA is extracted from liver/muscle tissue following the protocol of Fetzner (1999), and using Qiagen DNeasy kits (Qiagen, Inc., Valencia, CA).

Mitochondrial DNA amplification and sequencing

Forty-eight samples from 40 localities were sequenced for 669bp of the mtDNA cytochrome b (cyt-b) region, with LIO742F 5'–TCGACCTVCCYGCCCCATCA–3' and LIO742R 5'–GAGGGGTTACTAAGGGGTTGGC–3' primers (this study), and all unique cyt-b haplotypes were sequenced for a 12S region (752 bp) using primers 12Stphe 5'AAAGCACRGCACTGAAGATGC–3' and 12SE 5'–GTRCGCTTAC-CWTGTTACGACT–3' (Wiens et al. 1999). Double stranded polymerase chain reactions (PCR) were amplified under the following conditions: 1.0 µL of genomic DNA, 1.0 µL of light strand primer 1.0 of µL of heavy strand primer, 1.0 µL of dinucleotide pairs, 2.0 µL of 5x~ buffer, 1.0 µL of MgCl 10x~ buffer, 0.18 µL of Taq polymerase, and 7.5 µL of diH2O. PCR amplification was executed under the following conditions: initial denaturation at 95°C for 2 min, followed by a second denaturation at 95°C for 35 s, annealing at 52°C for 35 s, followed by a cycle extension at 72°C for 35 s, for 31 cycles. PCR products were visualized on a 10% agarose gels to ensure the targeted products were cleanly amplified, and then purified using a MultiScreen PCR (mu) 96 (Millipore Corp., Billerica, MA) and directly sequenced using the BigDye Terminator v 3.1 Cycle Sequencing Ready Reaction (Applied Biosystems, Foster City, CA). The cycle sequencing reactions were purified using Sephadex G-50 Fine (GE Healthcare) and MultiScreen HV plates (Millipore Corp.). Samples were then analyzed on a ABI3730xl DNA Analyzer in the BYU DNA Sequencing Center.

Phylogenetic reconstruction

All sequences were aligned in MUSCLE (Edgar 2004) plugin, and cyt-b sequences were translated to check for premature stop codons in GENEIOUS®PRO v5.6.6. Cyt b haplotype diversity was estimated using DnaSP (Librado and Rozas 2009), and concatenated cyt-b and 12S regions were edited using GENEIOUS®PRO (Drummond et al. 2011). For ingroups and outgroups we used selected species of the subgenus *Liolaemus* that are assigned to different species groups and for which cyt-b and 12S sequences are available in GenBank. Our ingroup samples included taxa that have been assigned to the same species group as *L. tacnae* and *L. walkeri* (*alticolor-bibronii* group), including: *L. abdalai* Quinteros, *L. bibronii* (Bell), *L. gracilis* (Bell), *L. ramirezae* Lobo & Espinoza and *L. saxatilis* Ávila & Cei (Lobo et al. 2010). To further test for monophyly of the *alticolor-bibroni* group, we sampled three species assigned to different species groups (*robertmertensi, pictus* and *monticola* groups), but nested within the subgenus *Liolaemus*; these include: *L. monticola* Müller & Hellmich, *L. pictus* Duméril & Bribon

and *L. robertmertensi* Hellmich (Lobo et al. 2010). We used *L. lineomaculatus* Boulenguer, a species belonging to the subgenus *Eulaemus* (Lobo et al. 2010, Fontanella et al. 2012) as the outgroup. All new sequences were deposited in GenBank (accession numbers KF923633–KF923660 and KF923661–KF923688 for cyt-b and 12s respectively) and a list of all haplotypes, GenBank accession and museum voucher numbers used for the phylogenetic analysis are provided as Supplementary file 1.

Bayesian Information Criteria in JMODELTEST (v 0.01; Posada 2005) identified the best-fit model of evolution for the complete data set of haplotypes as TPM2+ I + Γ. A Maximum-likelihood (ML) search in PHYML (Guindon and Gascuel 2003) was performed with 1000 replicates for bootstrap analyses; we consider strong nodal support for bootstrap values ≥ 70 (Hillis and Bull 1993; with caveats). Because the TPM2+ I + G model is not incorporated in the MRBAYES (Huelsenbeck and Ronquist 2001) plugin of GENEIOUS®PRO v5.6.6, we used a model with the closest likelihood available (GTR + I + Γ). Two parallel runs were performed in MRBAYES using four chains (one cold and three hot) for 1.1×10^6 generations and sampling every 200 generations from the Markov Chain Monte Carlo (MCMC). We determined stationarity by plotting the log likelihood scores of sample points against generation time; when the values reached a stable equilibrium and split frequencies fall below 0.01, stationarity was assumed. We discarded 100,000 samples and 10% of the trees as burn-in. A maximum clade credibility (MCC) tree was constructed using TREEANNOTATOR v1.7.5 (Drummond et al. 2012). We consider Bayesian Posterior Probabilities (BPP) >95% as evidence of significant support for a clade (Huelsenbeck and Ronquist 2001, Wilcox et al. 2002).

Morphological data and analyses

A total of 199 individuals (see species descriptions and Data resources below) representing three putative different populations and four Peruvian species (*L. alticolor*, *L. incaicus*, *L. tacnae* and *L. walkeri*) assigned to the *L. alticolor* group were scored for three classes of morphological characters. We performed a character analysis of 17 discrete binomial characters related to scalation, pattern of coloration and skin folds, including the following: presence/absence of smooth (1) temporal scales and (2) dorsal head scales, contact or not of (3) rostral to nasal scale, presence/absence of (4) mucronate dorsal scales and (5) precloacal pores, (6) preocular scale same or different color as loreal region, presence/absence of (7) spots on dorsal head scales, (8) black line surrounding the interparietal scale, regular spots or marks in (9) paravertebral field and (10) lateral field, presence/absence of dorsolateral stripes (11) and vertebral line (12), marks or spots on throat (13), melanistic belly (14), ringed pattern in ventral tail (15), and presence/absence of antehumeral (16) and neck folds (17). All characters were scored using a stereomicroscope and from photos of live animals taken in the field.

For statistical analyses of these discrete variables we used tolerance intervals as described in the tolerance package of Young (2010), which in a random sample of a univariate population, is an interval expected to contain a specified proportion or

more of the sampled population (Krishnamoorthy and Mathew 2009). We used binomial tolerance intervals to estimate the number of individuals that comprise 95% of the population expected to have one state with a 0.05 level of significance (following Wiens and Servedio 2000, Zapata and Jiménez 2012). One-sided binomial tolerance intervals were estimated using the Wilson method (WS), which is appropriate when the sample sizes are small ($n \leq 40$) (Young 2010).

We scored the following 11 morphometric characters: (SVL) snout-vent length, (AGL) axilla-groin length (between the posterior insertion of forelimb and anterior insertion of thigh), (HL) head length (from snout to anterior border of auditory meatus), (HW), head width (at widest point), (FOL) forelimb length (distance from the attachment of the limb to the body to the terminus of the fourth digit), (HIL) hindlimb length (distance from the attachment of the limb to the body, to the terminus of the fourth digit), (SL) snout length (from snout to anterior border of eye), (AMW) auditory meatus width, (AMH) auditory meatus height, (RW) rostral width, and (RL) rostral length. We also scored five meristic characters, including: (MBS) number of midbody scales (counted transversely at the middle of the body), (DTS) dorsal trunk scales (counted from the level of anterior border of ear to anterior border of thighs), (DHS) dorsal head scales (counted from the rostral scale to anterior border of ear), (VS) ventral scales (counted from the mental scales to the cloaca), and (SCI) number of scales in contact with the interparietal. Measurements and counts were taken from the right side of the animal using a stereomicroscope. Morphometric data were only taken for adult males and females.

After testing for normality in all morphometric and meristic characters with the Shapiro-Wilks test (Shapiro and Francia 1972), we summarized means and ranges for all population samples, and performed Principal Component Analyses (PCA) and Correspondence Analyses (CA) separately for each class of characters and by sex, to summarize patterns. Results of PCA and CA were then compared with the analysis of continuous characters by estimating normal tolerance intervals to find gaps or discontinuities in each class of morphological characters. We used normal tolerance intervals to estimate the lowest and highest values of a continuous character that is contained in 95% of the population with a 0.05 level of significance. Two-sided normal tolerance intervals were estimated using the Howe method (HE), which is considered to be extremely accurate, even for small sample sizes (Young 2010).

For comparison with normal tolerance intervals we assessed the morphometric and meristic characters with univariate ANOVA and Mann-Whitney *U* tests for parametric and non-parametric distributions, respectively. When the assumption of equal-variance was not met for an ANOVA test, the unequal- variance (Welch) version of ANOVA was performed. Each character was tested for intersexual differences, and if present, the sexes were analyzed separately. Results were considered significant when $p \leq 0.05$. However, we didn't use the results of the ANOVA and Mann-Whitney *U* tests in our taxonomic decisions (see Introduction and Discussion). Binomial and tolerance intervals were calculated with the package Tolerance (Young 2010) in R v3.0.1 (R core team 2013). Test of normality, PCA, CA and univariate tests were performed using PASTv. 2.08b, (Hammer et al. 2001).

Distributional models

We used the maximum entropy model implemented in the program MAXENT v3.3.3e (Phillips et al. 2006) to predict where the Peruvian lineages of *L. walkeri* complex are most likely to occur under current climatic conditions. MAXENT generates distributional models (or ecological niche models; ENMs) using presence-only records, contrasting them with background/pseudoabsence data sampled from the remainder of the study area. We chose this approach because of its overall better performance with presence-only data and with small sample sizes (Elith et al. 2006). ENMs were developed from occurrence points used in this study, and records without duplicates are: 22 for Ancash, 31 for Ayacucho, 16 for Cusco, 33 for *L. tacnae* and 52 for *L. walkeri* (see Data resources below). For niche predictions, we used the 19-bioclimatic variables from the WorldClim v1.4 dataset with a resolution of 2.5 min (Hijmans et al. 2005). Bioclimatic variables were derived from monthly temperature and precipitation layers, and represents biologically meaningful properties of climate variation (Hijmans et al. 2005). Layers were trimmed to the areas surrounding each species and populations that might represent new species, and then projected over a larger region (-9.828° to -17.839° and -77.486° to -69.811°).

For model calibration we used the default settings with 1000 iterations, and the minimum training value averaged over the 10 replicates as threshold with the default convergence threshold (10^{-5}). Due to our smaller samples sizes, we used for model calibration and performance the cross-validation option with 10 replicates, and average the results to estimate species niche and distributions. For model significance, 25% of localities were randomly set aside as test points and the area under the curve (AUC) was calculated, which summarizes the model's ability to rank presence localities higher than a sample of random pixels (Peterson et al. 2011). AUC values ≤ 0.5 correspond to predictions that are equal or worse than random. AUC values > 0.5 are generally classed into (1) poor predictions (0.5 to 0.7); (2) reasonable predictions (0.7 to 0.9); and (3) very good predictions (>0.90; but see Peterson et al. 2011, for caveats on use of AUC in presence/background data). Model clamping was checked with the "fade by clamping" option available in MAXENT v 3.3.3e. Estimates of bioclimatic variable importance was performed using the Jackknife test. We used the logistic output (probability values) and mapped the distributional models showing areas from the average minimum logistic values (threshold) to 1 as areas suitable for species.

Schoener's D metric was introduced as a measure of niche similarity between pairs of populations (or species) by Warren et al. (2010), and is calculated using the ENMTOOLS package. We calculated these values by comparing the climatic suitability of each grid cell in the projected area obtained with MAXENT. This similarity measure ranges from 0 (niche models have no overlap) to 1 (niche models identical; Warren et al. 2008). We estimated similarity measures and then tested whether the ENMs produced by two populations or species are identical using the niche identity test in ENMTOOLS. One hundred pseudoreplicate data sets were generated to obtain a distribution of D scores, and we reject the hypothesis of niche identity when the empirically observed value for D is significantly lower than the values expected from the pseudoreplicated data set (Warren et al. 2010).

Species descriptions

Species descriptions follow the terminology of Lobo and Espinoza (1999) and Quinteros (2013). For diagnosis, we selected the following non-Peruvian species assigned to the *L. alticolor* group: *L. aparicioi* Ocampo, Aguilar-Kirigin & Quinteros, *L. bitaeniatus* Laurent, *L. chaltin* Lobo & Espinoza, *L. pagaburoi* Lobo & Espinoza, *L. paulinae* Donoso-Barros, *L. puna* Lobo & Espinoza, *L. pyriphlogos* Quinteros, and *L. variegatus* Laurent. This selection is based on previous phylogenetic analyses (Espinoza et al. 2004, Díaz-Gómez and Lobo 2006, Schulte and Moreno-Roark 2010, Quinteros 2013), and taxonomic revisions and species descriptions of geographically proximate species (Donoso-Barros 1961, Laurent 1984, Lobo and Espinoza 1999, 2004, Quinteros 2012, Ocampo et al. 2012). We assumed that diagnostic characters are "fixed". Color descriptions are based on photographs of live animals taken in the field, and specimens examined are provided in Data resources.

Data resources

The data underpinning the analysis reported in this paper are deposited in the Dryad Data Repository at http://doi.org/10.5061/dryad.0q7pc, and at GBIF, the Global Biodiversity Information Facility, http://ipt.pensoft.net/ipt/resource.do?r=ocurrence_records_liolaemus_walkeri_complex.

Results

Phylogenetic Analysis

A tree with maximum likelihood bootstrap values (logL = -8452.31415, MLB) and Bayesian posterior probabilities (BPP) based on 1421 aligned base pairs is shown in Fig. 1. Differences between both methods are mentioned below. Both ML and Bayesian analyses recovered Ancash, Ayacucho, Cusco, *L. tacnae* and *L. walkeri* haplotypes as monophyletic groups with high support. Both also showed a close relationship between Ayacucho and *L. walkeri* haplotypes, but relationships between Ancash, Cusco and the (*L. walkeri* + Ayacucho) clade were unresolved and with moderate support in the ML tree (MLB 65%). The Bayesian analysis recovers Ancash as the sister to the (*L. walkeri* + Ayacucho) clade with low support (BPP 0.5), and Cusco as the sister clade to the ((*L. walkeri* + Ayacucho) Ancash) clade with moderate support (BPP 0.9). In both analyses, *Liolaemus tacnae* is recovered as the sister group of the (Ancash + Cusco + (*L. walkeri* +Ayacucho)) clade with moderate support (MLB 65%, BPP 0.9). *Liolaemus tacnae* and *L. walkeri* are assigned to the *alticolor-bibronii* group, but the clade (*L. tacnae* (Ancash + Cusco + (*L. walkeri* + Ayacucho))) is strongly differentiated from the other species assigned to the *alticolor-bibronii* group (Fig. 1).

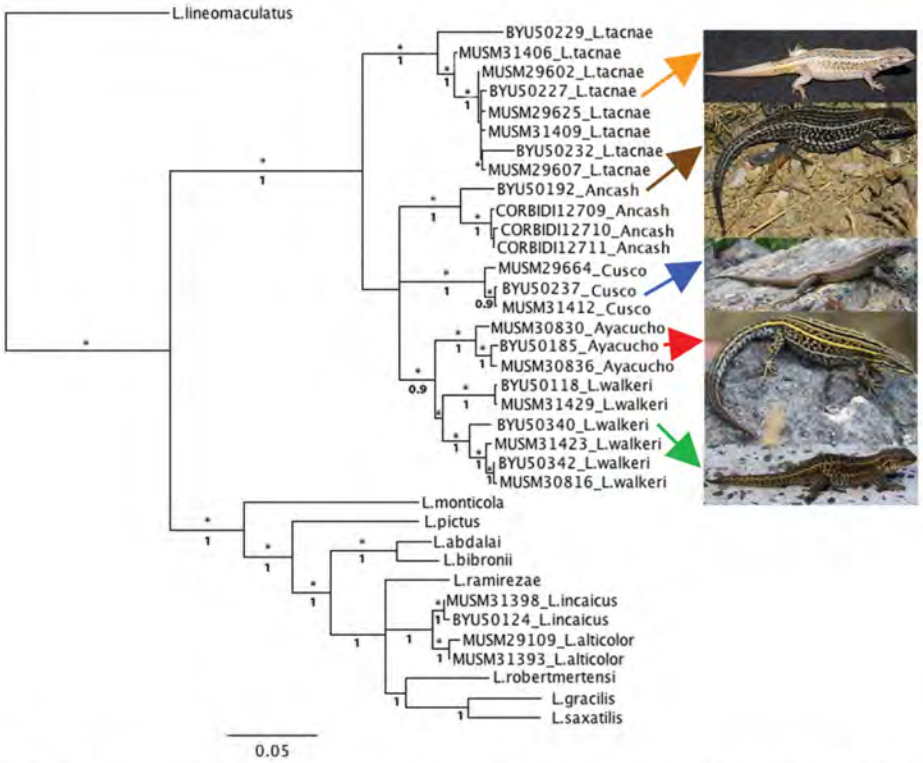

Figure 1. Concatenated maximum likelihood (-Log L = 8452.31415) tree based on cyt-b and 12S haplotypes of focal taxa (Ancash, Ayacucho Cusco) and species assigned to the *alticolor* group and outgroups. Bootstrap ≥ 70 (*) and posterior probabilities values are shown above and below branches respectively.

The monophyletic group (*L. tacnae* (Ancash + Cusco + (*L. walkeri* + Ayacucho))) is the sister group of a clade comprised of taxa assigned to different species groups in the subgenus *Liolaemus,* including species of the *alticolor-bibronii* group. The relationships of these two more inclusive clades showed high MLB, but low BPP values. In this clade, both ML and Bayesian analyses recovered *L. alticolor* and *L. incaicus* haplotypes as monophyletic groups with high support. In our ML analysis, the clade (*L. alticolor* + *L. incaicus*) has unresolved relationships with *L. ramirezae* and the clade (*L. robertmertensi* + (*L. gracilis* + *L. saxatilis*)), and this latter clade has high BPP but low MLB support (Fig. 1). *Liolaemus abdalai* and *L. bibronii* are recovered as sister taxa with high support, and this clade is sister to the clade (*L. ramirezae* + (*L. incaicus* + *L. alticolor*) + (*L. robertmertensi* + (*L. gracilis* + *L. saxatilis*))) also with high support (Fig. 1). *Liolaemus pictus* is sister to the clade ((*Liolaemus abdalai* and *L. bibronii*) + (*L. ramirezae* + (*L. incaicus* + *L. alticolor*) + (*L. robertmertensi* + (*L. gracilis* + *L. saxatilis*)))), and *L. monticola* is basal to a clade that includes *L. pictus* and its sister group.

Morphological analyses

Binomial discrete characters

Because our phylogenetic analysis did not show a close relationship between (*L. alticolor* + *L. incaicus*) and the (*L. tacnae* (Ancash + Cusco + (*L. walkeri* + Ayacucho))) clades, we focus our comparisons on these last five taxa. Of the 17 binomial characters, four were useful for species delimitation among these taxa (Table 1). One-sided binomial tolerance intervals (BTI) for 95% of the population with a 0.05 level of significance is indicated below for each of these four characters.

Ancash (n = 12) and *L. tacnae* (n = 18) males differed from Ayacucho, Cusco and *L. walkeri* males in lacking precloacal pores (Fig. 2A and D; vs. presence in panels B, C, and E). Although these differences are fixed in our samples, the BTI tests showed

Table 1. Binomial characters for females (F) and males (M) of focal populations of *Liolaemus* lizards sampled for this study. Character states useful for species discrimination are in bold, and states only assessed on adults are indicated with an asterisk.

	Ancash		**Ayacucho**		**Cusco**		***L. tacnae***		***L. walkeri***	
	F (n= 18)	M (n =12)	F (n=18)	M (n=10)	F (n=8)	M (n=8)	F (n=23)	M (n=18)	F (n=48)	M (n=21)
Temporal scales smooth	yes	yes/no	yes/no	yes/no	yes	yes	yes/no	yes	yes	yes/no
Dorsal surface of head completely smooth	yes/no	yes/no	yes/no	yes/no	yes	yes/no	yes/no	yes	yes/no	yes/no
Nasal contact rostral scale	yes/no	yes/no	yes/no	yes	yes/no	yes/no	yes/no	yes/no	yes	yes/no
Dorsal scales mucronate	no	no	yes/no	yes/no	no	no	no	no	no	no
Precloacal pores	no	**no**	no	**yes**	no	**yes**	no	**no**	no	**yes**
Sub and preoculars different in color from loreal region	yes/no	yes/no	yes/no	yes/no	yes/no	yes/no	yes/no	yes/no	yes/no	yes/no
Dorsal surface of head with marks or dots	yes	yes	yes/no	yes/no	yes/no	yes	yes/no	yes/no	yes/no	yes/no
Black line surrounds interparietal scale	yes/no	yes/no	yes/no	yes/no	yes/no	yes/no	yes/no	yes/no	yes/no	yes/no
Regular marks or spots in paravertebral field	yes/no	no	yes	yes/no	yes/no	no	yes/no	yes/no	yes/no	yes/no
Regular marks or spots in lateral field	**yes**	**yes**	**yes**	**yes**	**no**	**no**	yes/no	yes/no	yes/no	yes/no
Dorsolateral stripes	yes	yes/no	yes	yes	yes	yes	yes	yes/no	yes	yes
Vertebral line	yes	yes	yes	yes	yes	yes	yes/no	yes/no	yes	yes/no
Throat not immaculate	yes/no	yes/no	yes/no	yes/no	yes	yes	yes/no	yes	no	yes
***Complete or partial melanistic belly**	yes/no	**yes**	no	yes/no	no	**yes**	no	no	no	**yes**
***Ventral tail with ringed pattern**	yes/no	yes/no	yes/no	**yes**	no	**no**	no/yes	yes	yes/no	**no**
Antehumeral fold	yes	yes	yes	yes	yes	yes	yes	yes	yes	yes
Neck folds	yes	yes	yes	yes	yes	yes	yes	yes	yes	yes

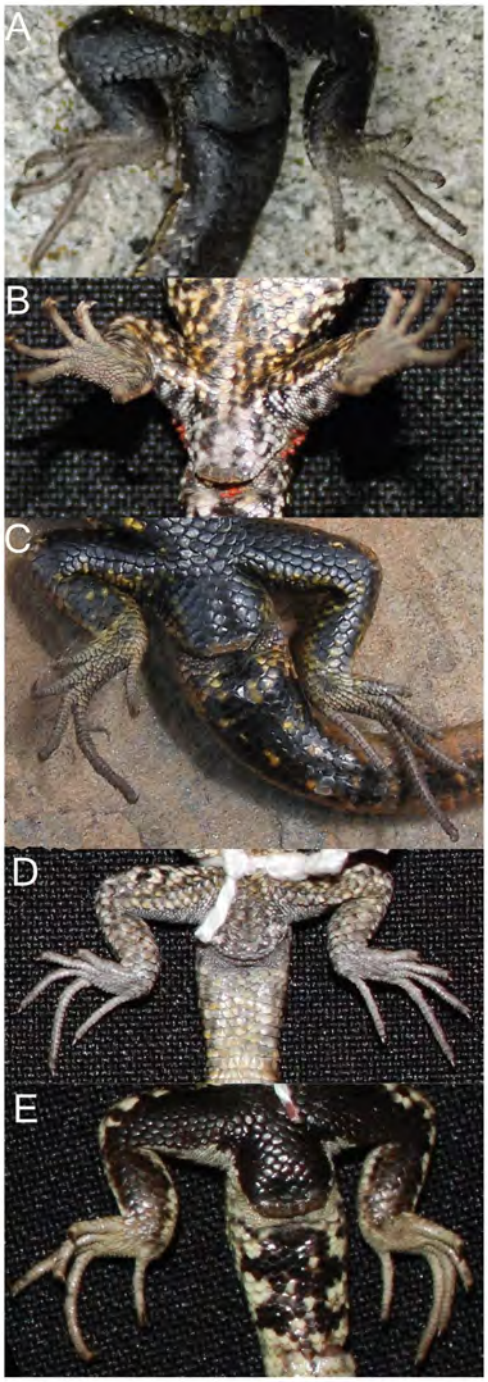

Figure 2. Detailed view of the cloaca region showing absence (**A, D**) or presence (**B, C, E**) of precloacal pores: **A** Ancash **B** Ayacucho **C** Cusco **D** *L. tacnae* and **E** *L. walkeri*.

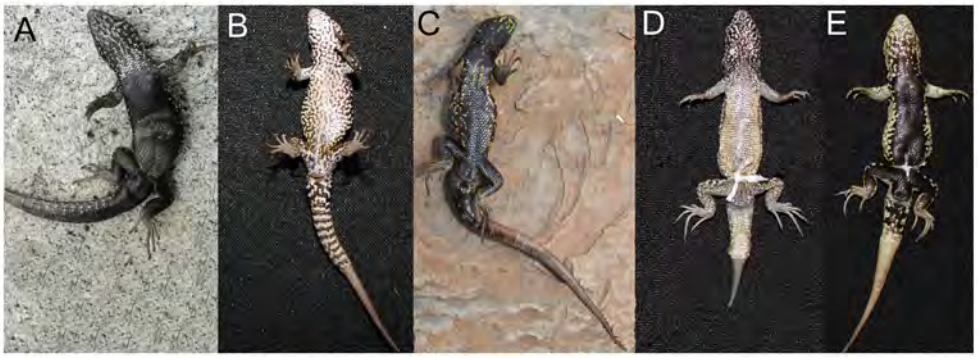

Figure 3. Ventral view showing the color patterns of the belly and tail: **A** Ancash **B** Ayacucho **C** Cusco **D** *L. tacnae* and **E** *L. walkeri*.

that up to 36% and 31% of the Ancash and *L. tacnae* populations, respectively, have a significant probability of possessing the alternative state ($P \leq 0.05$) in a larger sample.

Adult males of Ancash (Fig. 3A) differ from *L. tacnae* (Fig. 3D) in having a melanistic belly, and again while fixed in our samples, BTI showed that up to 36% of the population may have the alternative state ($P \leq 0.05$). Adult males of Ayacucho (Fig. 3B) can be diagnosed by their ringed ventral tail pattern, in contrast to the other four samples (Fig. 3A, C–E), but up to 44% of the population may have the alternative state ($P \leq 0.05$).

Both sexes of the Cusco sample (n = 16; Fig. 4B) differed from all Ayacucho (n = 28; Fig. 4A) and most individuals (90% of n = 69; Fig. 4C) of *L. walkeri*, in lacking regular spots or marks in lateral fields; but up to 33% of the population may have the alternative state ($P \leq 0.05$).

Morphometric and meristic characters

Our empirical results are summarized in Table 2, and tolerance intervals are given in Tables 3 and 4 for morphometric and meristic variables, respectively. Statistical tests rejected normality for HW, AMW, RW and all meristic characters, but we assumed normality because our sample sizes were too small to implement non-parametric tolerance interval tests. We did not find any diagnostic character or gaps in either data set (Tables 3 and 4).

Principal Component and Correspondence Analyses separated by sex or pooled together did not show any differences, so we present the results of the pooled analyses. Principal Component (PC) Analysis revealed that PC1 and PC2 explained 90% of the variance, and the Correspondence Analysis revealed that Correspondence Axis (CA) 1 and CA2 explained 66% of the similarity for morphometric and meristic data, respectively

Figure 4. Lateral view showing the color patterns of **A** Ayacucho **B** Cusco, and **C** *L. walkeri*.

ate plot for the morphometric variables revealed extensive overlap of *L. walkeri* with the remaining four samples, but minimal overlap between the Ancash and Cusco samples, and little overlap between the Ayacucho and Cusco (Fig. 5A). Both of these pairs are differentiated primarily along PC1, for which SVL and AGL contributed the highest loadings (0.85 and 0.47 respectively). The Cusco samples are characterized by shorter SVL and axilla-groin lengths than the Ancash and Ayacucho samples. The PC analyses revealed extensive overlap among all samples along PC2, and the CA for the meristic variables (Fig. 5B) revealed extensive overlap among all five samples along both axes.

Only significant results of ANOVA are mentioned below and the sex of a particular species or population is indicated only if significantly different from the opposite sex. For SVL, there were significant differences between Ancash vs. Cusco, *L. tacnae* and *L. walkeri*; Ayacucho vs. Cusco and *L. tacnae*; Cusco vs. *L. tacnae* and *L. walkeri*.

For AGD, there were significant differences between Ancash males vs. Cusco males and *L. tacnae* males; Ancash females vs. *L. tacnae* females; Ayacucho females vs. Cusco females and *L. tacnae* females; Cusco males vs. *L. tacnae* males and *L. walkeri* males; Cusco females vs. *L. walkeri* females.

Table 2. Descriptive statistics of morphometric and meristic characters for three new species of *Liolaemus* described herein, and *L. tacnae* and *L. walkeri*. First rows show ranges and second rows show means and standard deviations. See methods for abbreviations.

	L. chavin **(Ancash, n=32)**	***L. pachacutec*** **(Cusco, n=18)**	***L. tacnae*** **(n=41)**	***L. walkeri*** **(n=78)**	***L. wari*** **(Ayacucho, n=30)**
SVL	51.0–66.5	33.4–52.0	42.6–56.6	41.5–64.4	50.0–61.4
	57.0±4.0	45.4±4.4	48.6±3.2	54.5±4.6	55.6±3.1
AGL	20.4–34.8	17.8–30.8	14.9–26.5	17.2–33.5	19.8–32.3
	26.5±3.4	22.6±3.6	21.8±2.7	25.3±3.4	25.9±3.9
HL	10.2–15.3	9.2–13.2	9.4–12.0	10.1–14.2	10.3–12.7
	12.4±1.1	10.6±1.0	10.7±0.7	12.2 ±0.9	11.4±0.8
HW	8.8–12.8	6.6–9.7	7.2–9.3	7.8–11.6	8.1–10.7
	10.3±1.1	8.2±0.7	9.6±0.8	9.6±0.9	9.4±0.8
SL	4.2–6.3	3.2–4.7	3.7–5.3	3.5–6.9	4.0–4.9
	5.2±0.5	4.0±0.5	4.5±0.4	5.1±0.5	4.4±0.3
FoL	14.1–19.1	12.9–17.4	13.1–8.3	13.5–21.5	13.9–18.3
	16.2±1.5	15.7±1.3	15.7±1.4	16.7±1.5	15.7±1.2
HiL	22.6–29.5	19.0–27.9	20.8–29.8	19.8–30.7	20.9–28.7
	25.8±1.8	23.4±2.1	24.6±2.2	25.2±2.5	24.2±2.5
AMH	1.7–2.9	1.3–2.4	1.5–2.5	1.4–2.6	1.7–2.5
	2.2±0.26	1.8±0.3	1.9±0.2	2.1±0.3	2.1±0.22
AMW	0.70–1.31	0.8–1.3	0.5–1.5	0.6–1.6	0.76–1.30
	1.0±0.2	1.0±0.1	1.2±0.1	1.2±0.2	1.1±0.1
RH	0.8–1.3	0.6–2.4	0.8–1.3	0.7–1.6	0.9–1.2
	1.0±0.1	1.0±0.3	1.0±0.1	1.1±0.2	1.0±0.1
RW	2.2–3.2	2.1–2.7	1.6 –2.8	1.9–3.1	2.0–2.9
	2.7±0.3	2.6±0.1	2.2±0.2	2.6±0.3	2.5±0.3
MBS	48–69	39–51	42–58	45–60	46–56
	56.8±6.1	46.5.6±3.4	48.1±4.1	53.8±3.6	50.6±3.0
DTS	43–72	42–57	40–55	42–66	40–55
	56.1±7.2	47.2±3.6	47.0±4.1	54.4±4.6	46.4±3.6
DHS	10–19	10–16	11–18	10–19	9–17
	14.6±2.1	13.5±1.5	14.0±1.7	13.7±1.7	12.7±1.8
VS	70–87	56–82	60–87	69–96	71–88
	79.6±4.5	72.8±6.4	76.3±6.5	80.7±5.2	77.7±4.1
SCI	5–12	4–8	5–10	5–9	5–13
	7.9±1.4	6.4±1.2	7.0±1.0	7.1±1.0	7.6±1.4

For HL, there were significant differences between Ancash males vs. Ayacucho males, Cusco, *L. tacnae* and *L. walkeri* males; Ancash females vs. Ayacucho females, Cusco, *L. tacnae* and *L. walkeri* females; Ayacucho males vs. Cusco and *L. tacnae*; Ayacucho females vs. *L. walkeri* females; Cusco vs. *L. walkeri* males and *L. walkeri* females.

For FoL, there were significant differences between Ancash males vs. Cusco and *L. tacnae*; Ancash females vs. *L. walkeri*; Ayacucho females vs. *L. walkeri*; Cusco vs. *L. walkeri*.

Table 3. Normal tolerance intervals for morphometric variables of three species of *Liolaemus* described herein, plus *L. tacnae* and *L. walkeri*; those identified with an asterisk were assumed to follow a normal distribution. See methods for abbreviations.

	Ancash (n=29)	Ayacucho (n=16)	Cusco (n=17)	*L. tacnae* (n=36)	*L. walkeri* (n=74)
SVL	46.7–67.3	46.5–64.6	32.7–58.1	40.5–56.8	44.0–65.1
AGD	17.7–35.3	14.4–37.3	12.3–32.9	15.1–28.6	17.5–33.0
HL	9.6–15.2	9.1–13.8	7.7–13.5	9.1–12.3	10.1–14.3
*HW	7.4–13.1	7.1–11.6	6.0–10.3	7.0–10.0	7.5–11.8
SL	4.0–6.4	3.6–5.2	2.6–5.3	3.5–5.6	3.9–6.4
FoL	12.4–19.9	12.2–19.2	11.9–19.5	12.8–19.0	13.4–20.3
HiL	21.2–30.4	17.1–31.4	17.5–29.3	19.2–30.0	19.5–31.0
AMH	1.6–2.9	1.5–2.7	0.9–2.6	1.4–2.4	1.4–2.8
*AMW	0.6–1.4	0.6–1.5	0.6–1.4	0.6–1.7	0.8–1.7
RH	0.7–1.4	0.8–1.3	0.2–2.1	0.7–1.3	0.7–1.6
*RW	1.9–3.5	1.8–3.3	1.8–2.9	1.6–2.8	2.0–3.2

Table 4. Normal tolerance intervals for meristic characters of three species of *Liolaemus* described herein, plus *L. tacnae* and *L. walkeri*; all variables were assumed to follow a normal distribution. See methods for abbreviations.

	Ancash (n=32)	Ayacucho (n=30)	Cusco (n=18)	*L.tacnae* (n=42)	*L. walkeri* (n=79)
MBS	41.4–72.3	43.1–58.2	36.9–56.1	38.0–58.2	45.6–62.0
DTS	38.0–74.2	37.2–55.7	36.9–57.5	37.0–57.0	43.8–65.3
DHS	9.2–20.0	8.3–17.4	9.2–17.9	9.8–18.3	9.9–17.5
VS	68.2–91.0	67.1–88.3	54.7–91.0	60.5–92.2	68.9–92.5
SCI	4.5–11.3	4.1–11.2	3.0–9.8	4.5–9.5	4.8–9.4

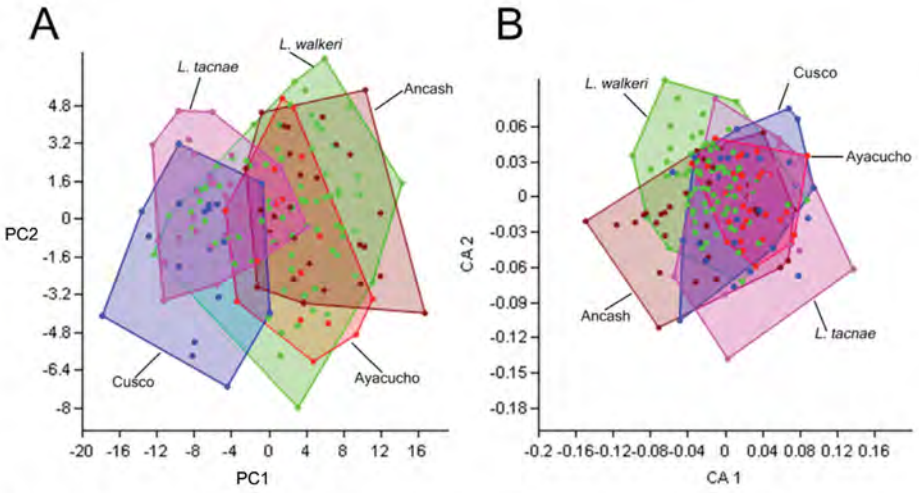

Figure 5. First and second principal components (PC) and correspondence axes (CA) of morphometric (**A**) and meristic (**B**) data of Ancash, Ayacucho, Cusco, *L. tacnae* and *L. walkeri* respectively.

For HiL, there were significant differences between Ancash males vs. Ayacucho, Cusco males and *L. tacnae*; Ancash females vs. Cusco females; Ayacucho vs. Cusco females and *L. walkeri* males; Cusco females vs. *L. tacnae* and *L. walkeri* females.

For SL, there were significant differences between Ancash males vs. Ayacucho males, Cusco, *L. tacnae* and *L. walkeri*; Ancash females vs. Ayacucho females and Cusco; Ayacucho males vs. Cusco; Ayacucho males and females vs. *L. walkeri*; Cusco vs. *L. tacnae* and *L. walkeri*;

For AMH, there were significant differences between Ancash vs. Cusco, *L. tacnae*, *L. walkeri*; Ancash vs. Ayacucho females; Ayacucho males vs. Cusco and *L. tacnae*; Ayacucho females vs. Cusco; Cusco vs. *L. tacnae* and *L. walkeri*.

For RH, there were significant differences between Ancash males vs. *L. tacnae*; Ancash females vs. *L. walkeri*; Ayacucho females vs. *L. walkeri*; Cusco vs. *L. walkeri*.

Only significant results of Mann-Whitney *U* are mentioned below and the sex of a particular species or population is indicated only if significantly different from the opposite sex. For HW, there were significant differences between Ancash males vs. Ayacucho, Cusco, *L. tacnae* and *L. walkeri*; Ancash females vs. Cusco and *L. tacnae*; Ayacucho vs. Cusco and *L. tacnae*; Cusco vs. *L. walkeri*.

For AMW, there were significant differences between Ancash vs. Cusco; Ayacucho vs. *L. tacnae*; Cusco vs. *L. tacnae* and *L. walkeri*.

For RW, there were significant differences between Ancash males vs. Cusco, *L. tacnae* males, and *L. walkeri*; Ancash females vs. Cusco and *L. tacnae* females; Ayacucho males vs. Cusco and *L. tacnae* males; Ayacucho females vs. *L. tacnae* females and *L. walkeri*; Cusco vs. *L. tacnae* females and *L. walkeri*.

For MBS, there were significant differences between Ancash vs. Ayacucho, Cusco, *L. tacnae* and *L. walkeri*; Ayacucho vs. Cusco, *L. tacnae* and *L. walkeri*; Cusco vs. *L. walkeri*.

For DTS, there were significant differences between Ancash vs. Ayacucho, Cusco, *L. tacnae*, *L. walkeri* males and *L. walkeri* females; Ayacucho vs. *L. walkeri* males and *L. walkeri* females; Cusco vs. *L. walkeri* males and *L. walkeri* females.

For DHS, there were significant differences between Ancash vs. Ayacucho females, Cusco females and *L. walkeri*; Ayacucho females vs. *L. tacnae* and *L. walkeri*; Cusco females vs. *L. tacnae*.

For VS, there were significant differences between Ancash vs. Cusco and *L. tacnae*; Ayacucho vs. Cusco and *L. walkeri* females; Cusco vs. *L. tacnae*, *L. walkeri* males and *L. walkeri* females.

For SCI, there were significant differences between Ancash males vs. Ayacucho, Cusco, *L. tacnae* and *L. walkeri*; Ancash females vs. Cusco; Ayacucho vs. Cusco and *L. tacnae*; Cusco vs. *L. walkeri*.

Distributional models

The predicted distribution in all cases matched the known range of each taxon, although some of these overlap. However, the distributional models of Ayacucho vs *L.*

tacnae (Fig. 6; C vs. E), as well as those for *L. walkeri* and *L. tacnae* (Fig. 6; E vs. F) are virtually mutually exclusive. All other combinations of distributional models overlapped, but differed in the contribution of bioclimatic variables to each niche envelope, and in predicting the known distribution of particular taxa (Table 5, Fig. 6). For example, the most important bioclimatic variables for the Ancash model were completely different from those for the *L. walkeri* and Ayacucho models (Table 5). In the same manner, the most important bioclimatic variables contributing to the Ayacucho model were completely different from those for the *L. walkeri* and Cusco models (Table 5). The most important bioclimatic variables for the Cusco model were completely different to those for *L. tacnae* (Table 5). Moreover results from the Niche Identity Test found all pairwise comparison between focal populations and species significantly different, except for Ancash and Cusco (Table 6).

The Ancash model (Fig. 6B) overlapped the known geographic distributions of Ayacucho, Cusco, *L. tacnae*, and partially with *L. walkeri*, but the two most important bioclimatic variables accounting for 94.3% of the contribution to this model were Precipitation of Warmest Quarter (63.3%) and Isothermality (31.0%; Table 5). These were also the most important variables in the permutation and jackknife tests. Thus the Ancash samples are characterized by a niche envelope with relative lower precipitation and more variation in annual temperature. The AUC score for this model = 0.87 (± 0.05), suggesting that the model prediction was reasonable (Fig. 7A).

The Ayacucho model did not overlap known distributions of Ancash, Cusco, *L. tacnae*, and only partially overlapped *L. walkeri* (Fig. 6C); the two most important bioclimatic variables accounting for 75.1% of the contribution to this model were Precipitation of Driest Quarter (64.4%) and Maximum Temperature of Warmest Period (10.7%; Table 5). In the permutation and jackknife tests, Precipitation of Driest Quarter was also the most important variable. In other words, the Ayacucho samples are characterized by a relatively wet and warm niche envelope, and the AUC score = 0.76 (± 0.06), suggesting that model prediction was reasonable (Fig. 7B).

The Cusco model did not overlap the known distribution of Ancash, overlapped most of Ayacucho and *L. walkeri*, and overlapped some of *L. tacnae* (Fig. 6D). The

Table 5. Percentage contributions of most important bioclimatic variables to the ecological niche envelopes for all population samples of three species of *Liolaemus* described herein, plus *L. tacnae* and *L. walkeri*.

	Ancash	Ayacucho	Cusco	*L. tacnae*	*L. walkeri*
Precipitation of the Warmest Quarter	63.3			30.0	
Isotermality	31.0		28.0		
Precipitation of the Driest Quarter		64.4		21.8	
Maximum Temperature of Warmest Period		10.7			
Precipitation of the Wettest Period			55.9		43.6
Precipitation of the Wettest Quarter				12.4	
Precipitation of the Driest Period					40.6

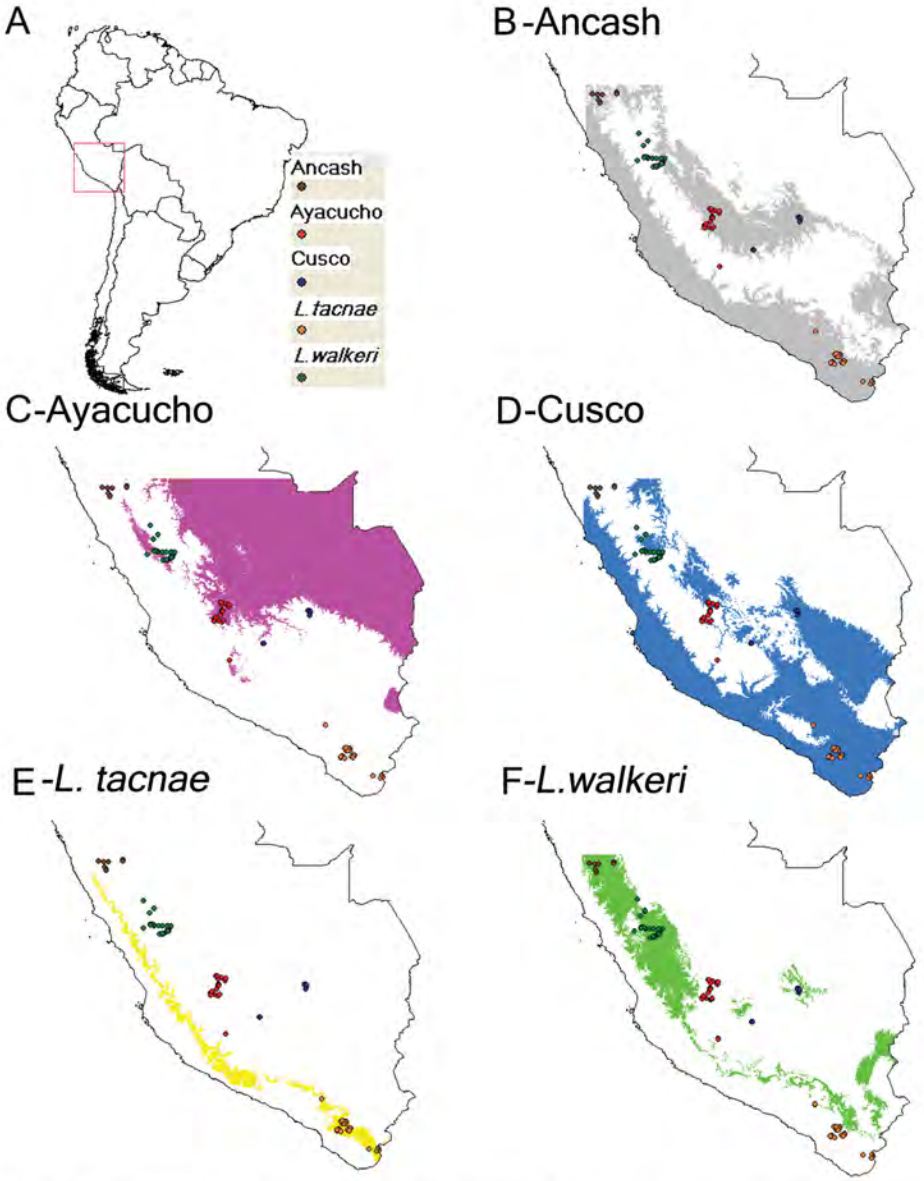

Figure 6. Predicted area and known geographic distribution (**A**) used to develop distributional models of Ancash (**B**) Ayacucho (**C**) Cusco (**D**) *L. tacnae* (**E**) and *L. walkeri* (**F**).

two most important bioclimatic variables accounting for 83.9% of the contribution to the model were Precipitation of the Wettest Period and Isothermality (Table 5). In the permutation and jackknife tests, Precipitation of the Wettest Period was also the most

Table 6. Schoener's D values and Niche Identity test results between focal populations and species. A value in bold denotes a pair of species that has statistically distinct ENMs.

	Ayacucho	Ancash	Cusco	*L. tacnae*	*L. walkeri*
Ayacucho	1	**0.167**	**0.100**	**0.004**	**0.108**
Ancash		1	0.670	**0.346**	**0.300**
Cusco			1	**0.328**	**0.356**
L. tacnae				1	**0.115**
L. walkeri					1

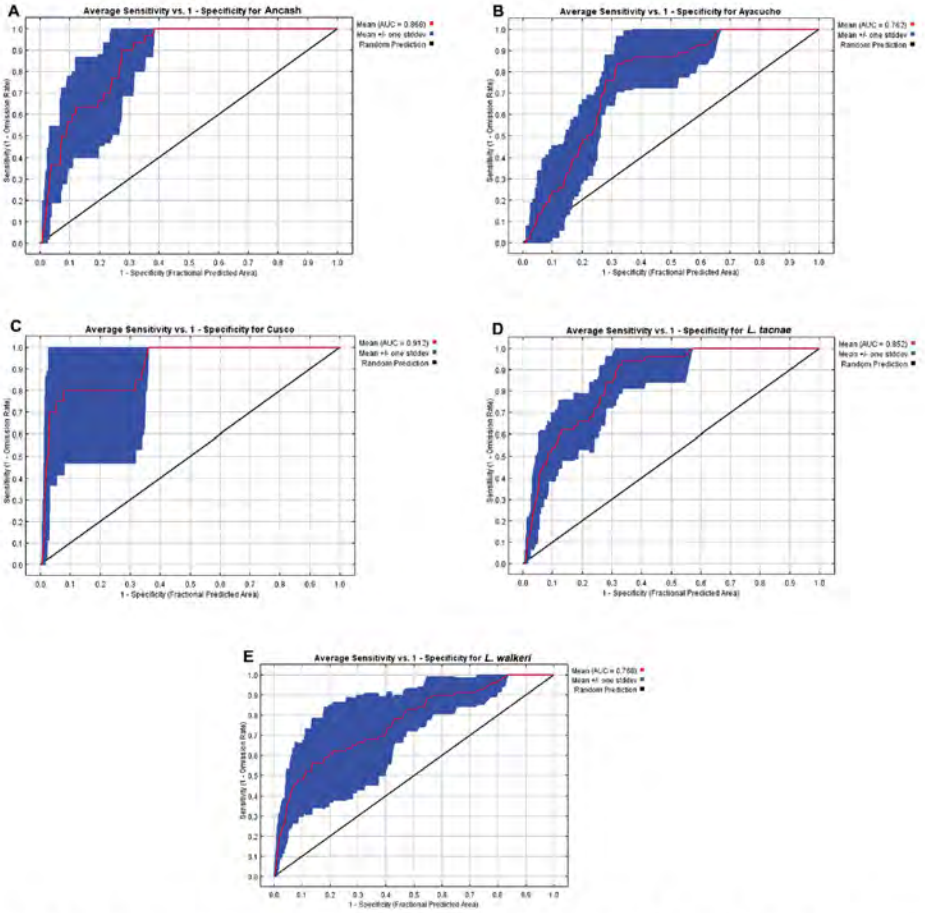

Figure 7. Receiver operating characteristic curves and AUC values for **A** Ancash **B** Ayacucho **C** Cusco **D** *L. tacnae* and **E** *L. walkeri*.

important variable indicating a niche envelope with relative more precipitation in the wettest period of the year. The AUC score = 0.91 (± 0.03), suggesting that model prediction was reasonable (Fig. 7C).

The *L. tacnae* model did not overlap the known distributions of any of the remaining taxa (Fig. 6E); the three most important bioclimatic variables accounting for 64.2% of the contribution to the model are Precipitation of Warmest Quarter, Precipitation of Driest Quarter, and Precipitation of Wettest Quarter (Table 5). In the permutation test, the most important variable was Precipitation of the Coldest Quarter, but in the jackknife tests Precipitation of Warmest Quarter, Precipitation of Wettest Quarter and Annual Precipitation were the most important variables. This indicates that *L. tacnae* samples are characterized by a drier niche envelope relative to all other populations and the AUC score (0.85 ± 0.06) suggests that this model prediction was reasonable (Fig. 7D).

The *L. walkeri* model overlaps the known distribution of the Ancash and partially that of the Cusco samples (Fig. 6F); the two most important bioclimatic variables accounting for 84.2% of the contribution to the model are Precipitation of Driest Period and Precipitation of Wettest Period (Table 5). In the permutation and jackknife tests, Precipitation of Wettest Period also was the most important variable. This suggests a relative wetter niche envelope relative to all other populations, and the AUC score (0.77 ± 0.08) suggests that the model prediction was reasonable (Fig. 7E).

The niche identity test results showed that observed values of Schoener's D between all populations and species were significantly lower than null distribution of pseudoreplicates except for Ancash and Cusco (Table 6).

Integrative taxonomy

Results of mitochondrial haplotypes, binary (presence/absence of precloacal pores, spots or regular marks in lateral field, melanistic belly in adult males, ringed ventral tail pattern), morphometric (snout-vent length, axila-groin length and hindlimb length) characters and niche identity tests in various combinations, differentiated Ancash, Ayacucho and Cusco samples from each other, and from *L. tacnae* and *L. walkeri*. Despite the fact that binomial tolerance intervals showed the possible presence of polymorphisms even at a frequency cut off of 0.5% in discrete characters, we hypothesize that increasing samples sizes will lower the hypothesized frequencies of the alternative states for each taxon. Normal tolerance intervals and distributional models showed overlap between all paired combinations of samples except for the Ayacucho vs. *L. tacnae* distributional models and niche identity tests showed statistical differences between all pairwise comparisons but Ancash vs. Cusco. Note that this is an extremely conservative approach; if we simply look at the data and count the number of "fixed" differences between all combinations of samples, we would conclude that the following pairs are unambiguously diagnosed: Ayacucho, Cusco and *L. walkeri* vs. Ancash (precloacal pores or not), Ancash vs. *L. tacnae* (melanistic belly or not), Ayacucho vs. Cusco and *L. walkeri* (ringed pattern in ventral tail or not), Cusco vs. most *L. walkeri* (lateral markings or not). Based on the integration of molecular, different classes of morphological data, and niche identity test results, we conclude that *Liolaemus* populations from Ancash, Ayacucho, and Cusco can be delimited as separate species, and we describe these new species below.

Species descriptions

***Liolaemus chavin* sp. n.**
http://zoobank.org/47B7926F-7D66-4C0B-9F25-9696C916E6C2
http://species-id.net/wiki/Liolaemus_chavin
Figure 8

2002 *Liolaemus alticolor* Lehr
2007 *Liolaemus incaicus* Lobo, Quinteros and Díaz Gómez
2011 *Liolaemus* aff. *walkeri* Langstroth

Holotype. MUSM 25417, adult male collected at Conococha, Recuay Province, Ancash Department, Peru, -10.123S, -77.293W, elevation 4100 m, on 31 March 2006 by Mikael Lundberg.

Paratypes. Three males (MUSM 20141, 20143, 20146) and twelve females (MUSM 25324, 25327, 25328, 25331, 25333, 25334, 25340, 25423, 25412, 30812, 30813, BYU 50192) from the same locality as the holotype. One male (MUSM 20147) from Carpa, Recuay Province, Ancash Department, on 28 February 2001 by Edgar Lehr and César Aguilar (see Data resources for elevation and coordinates). One female (MUSM 20201) from La Unión, Huánuco Department, on 3 March 1997 by Edgar Lehr (see Data resources for elevation and coordinates). Seven males (CORBIDI 10439, 10450, 10452, 10442, 10441, 10443, 10437) and six females (CORBIDI 10444, 10451, 10440, 10438, 10445, 10449) from Pampas de Huamani, San Marcos District, Huari Province, Ancash Department, on 12 February 2012 by Pablo J. Venegas (see Data resources for elevation and coordinates).

Diagnosis. Small (61.7 mm maximum SVL), slender *Liolaemus* closely related to *L. walkeri*, *L. tacnae, L. pachacutec* sp. n. and *L. wari* sp. n. (described below) (Fig. 1). It differs from *L. walkeri*, *L. pachacutec* sp. n. and *L. wari* sp. n. in the absence of precloacal pores in males. It differs from *L. tacnae* in having a melanistic belly in adult males (not melanistic in adult *L. tacnae* males). In comparison with other species assigned to the *L. alticolor* group, *L. chavin* sp. n. differs from *L. bitaeniatus* and *L. pagaburoi* in having a smooth dorsal surface of the head (rough to slightly rough dorsal surface). It differs from *L. alticolor*, *L. aparicioi*, *L. incaicus*, *L. paulinae*, *L. pyriphlogos, L. puna,* and *L. variegatus* in the absence of precloacal pores in males. *Liolaemus chaltin* also lacks precloacal pores in males, but *L. chavin* sp. n. differs in having also a melanistic belly in adult males.

Description of holotype. Adult male; SVL 56.8 mm; head length 13.7 mm; head width 11.3 mm; head height 7.7 mm; axilla-groin 21.0 mm (37% of SVL); foot length 10.3 mm (18.3% of SVL); tail length (regenerated) 35.2 mm (0.6 times SVL).

Fifteen dorsal head scales (from a line drawn horizontally between anterior edges of external auditory meatus to anterior border of rostral). Dorsal head scales smooth except for the interparietal and surrounding scales, scale organs more abundant in prefrontal, internasal, and supralabial regions. Five scale organs on postrostral. Nasal scale in contact

Figure 8. Dorsal (**A**) and ventral (**B**) views of the holotype of *Liolaemus chavin* sp. n. (**C**) Type locality.

with rostral, separated from first supralabial by one scale, nasal bordered by eight scales; canthus separated from nasal by one scale. Six supralabials. Six lorilabial scales, three in contact with the subocular. Six infralabials. Auditory meatus oval (height 2.3 mm, width 1.2 mm), with three small, projecting scales on anterior margin. Seven convex, smooth temporals. Orbit–auditory meatus distance 4.9 mm. Orbit–anterior margin of rostral distance 6.3 mm. Rostral almost three times wider than high (width 2.9 mm; height 1.2 mm). Mental subpentagonal, about two times as wide as high (width 3.2 mm; height 1.7 mm). Interparietal pentagonal with an elongated posterior apex, bordered by eight scales, the parietal slightly smaller. Frontal quadrangular. Supraorbital semicircles complete on both sides. Semicircles formed by 6 scales. Four enlarged supraoculars. Six distinctly imbricate superciliaries on both sides. Eleven upper and ten lower ciliaries.

Subocular elongate, 3.8 mm, longer than eye diameter (2.9 mm), separated from supralabials by a single, but interrupted row of lorilabials. Second supralabial elongate, 1.9 mm. Six lorilabials with single and double rows of scale organs. Sixth, fifth and fourth lorilabials contacting subocular. Preocular small, separated from lorilabial row by one scale. Postocular as large as preocular. Mental in contact with four scales: first infralabials (on each side) and two enlarged chin shields. Chin shields forming a longitudinal row of three enlarged scales separated one from the other by seven smaller scales. Scales of throat round, flat, and imbricate. Twenty-four gulars between auditory meatus. Longitudinal neck fold without keeled scales, that are similar to dorsal in size scales. Antehumeral pocket and antehumeral neck fold well developed. Forty-two scales between auditory meatus and shoulder (counting along postauricular and longitudinal neck fold), thirty-two scales between auditory meatus and antehumeral neck fold. Gular folds absent.

Dorsal scales rhomboidal, keeled, and imbricate. Sixty-six dorsal scales between occiput and level of groin. Sixty-two scales around midbody. Thirty rows of keeled scales on dorsum at midtrunk. Scales become smooth along flank and toward belly. Ventral scales slightly wider than dorsals. Eighty-two ventral scales between mental and cloaca; no precloacal pores. Supracarpals laminar, round, and smooth. Subdigital lamellae of fingers with three keels, in number I: 6; II: 11; III: 14; IV: 15; V: 10 (right hand). Claws moderately long. Supradigital lamellae convex, smooth, and imbricate. Infracarpals and infratarsals keeled, distinctly imbricate. Supratarsals smooth. Subdigital lamellae of toes I: 13; II: 13; III: 13; IV: 12; V: 6 (right foot).

Color pattern in preservation. Dorsal background color from occiput to base of tail greenish brown. Black continuous vertebral stripe present. Dark paravertebral marks. Paravertebral and vertebral fields of same background color. Dorsolateral stripes distinctly cream-color. Small dark cream-colored markings scattered in lateral field. Cream ventrolateral stripe, beginning on the upper auricular meatus, continuing across the longitudinal neck fold, through the shoulders, ending in the groin. Dark and small cream-colored marks in the ventral field. Black ventral color from about second third of head to femur, tibia and first third of tail. Dark and cream-colored small markings in first third of ventral head and two posterior thirds of tail.

Color pattern in life. Head dorsally brown with black and light brown dots. Subocular cream colored, dorsum bisected by a dark vertebral line. Vertebral field not conspicuous, bordering the vertebral line with a tenuous yellowish line. Paravertebral field with dark marks, bordered dorsally by a yellowish cream dorsolateral stripe. Lateral field with black and yellow reticulated pattern and white dots. Inconspicuous ventrolateral stripe, beginning on upper margin of auricular meatus, continuing from the longitudinal neck fold, through the shoulders, ending in the groin. Ventrolateral similar to lateral field but with more white dots. Fore and hind limbs same color as the paravertebral field, with diffuse dorsal markings. Dark, melanistic ventral color from about second third of head to femur, tibia and first third of tail. Dark and white dots in first third of ventral head and two posterior thirds of tail.

Variation. Variation in characters is summarized in Tables 1–4. There is sexual dichromatism. Adult males exhibit melanistic belly, cloacal region and throat, or mela-

nistic belly only; adult females exhibit black and white spots on belly, cloacal region and throat, or yellowish belly and tail.

Etymology. The specific epithet *chavin* refers to the pre-Inca culture Chavin, which had its center close to the type locality and frequently depicted reptile figures on some of its most remarkable sculptures. The species name is in the nominative singular.

Distribution and natural history. *Liolaemus chavin* sp. n. is known from four localities in the central Andes, at elevations of 3535–4450 m in Ancash and Huánuco Departments in western central Peru (Fig. 11). It is the northernmost species of the subgenus *Liolaemus*.

Liolaemus chavin sp. n. was found active and under rocks in grassland and shrubland habitats at higher and lower elevations respectively (Fig. 8). In Pampas de Huamani the new species was usually found basking on grass up to 60 cm above the ground, and when they were disturbed they escaped into the base of grass clumps. Individuals basking on rocks were very rare in all localities. On cloudy days we found this species inactive hidden in the base of grass clumps, although some individuals were also found inactive under rocks. This species is viviparous; one female showed two uterine chambers per side with developed embryos, yolk and no visible shell in either chamber, and three females showed two uterine chambers per side with yolk, without developed embryos and no visible shell in each chamber. At the type locality no sympatric species of reptiles were found, but four amphibians are known: *Pleurodema marmoratum* (Duméril & Bibron, 1840), *Telmatobius mayoloi* Salas & Sinsch, 1996, *Gastrotheca peruana* and *Rhinella (Bufo) spinulosa* (Wiegmann, 1834) (Lehr, 2002; personal observations). Sympatric species at Catac include the anurans *G. peruana*, *R. (Bufo) spinulosa*, *Telmatobius rimac* Schmidt, 1954, *T. mayoloi*, and the lizard *Stenocercus chrysopygus* Boulenger, 1900; at Carpa, *G. peruana* (Boulenger, 1900), *R. (Bufo) spinulosa* and *P. marmoratum*; at Pampas de Huamani, *G. peruana, P. marmoratum* and *R. (Bufo) spinulosa*; and at La Unión, *Gastrotheca griswoldi* Shreve, 1941, *G. peruana*, *R. (Bufo) spinulosa* and *S. chrysopygus* (Lehr, 2002).

***Liolaemus pachacutec* sp. n.**
http://zoobank.org/A979BB00-3CA1-47C9-8EB0-F605166FBF1A
http://species-id.net/wiki/Liolaemus_pachacutec
Figure 9

Holotype. MUSM 29683, adult male collected at Challabamba, Paucartambo Province, Cusco Department, Peru, -13.254S, -71.838W, elevation 4364 m, on 1 April 2009 by César Ramírez.

Paratypes. Three males (MUSM 29681, 29687, 29678) and four females (MUSM 29679, 29689, 29680, 29682) from the same locality as the holotype. Two males MUSM (29665, 29668) and one female (MUSM 29669) from Lamay, Calca Province, Cusco Department, on 12 October 2009 by César Ramírez (see Data resources for elevations and coordinates). One male (MUSM 29664), two females (MUSM

29688, BYU 50237) and one juvenile (MUSM 31412) from Pisac, Calca Province, Cusco Department, on 4 July and 11 October 2009 by César Ramírez, and on 28 June 2012 by César Aguilar, Perry Wood and Juan Carlos Cusi (see Data resources for elevations and coordinates). One male (MUSM 31540), two females (MUSM 31538-39) and one juvenile (MUSM 31537) from Tiaparo, Pocohuanca District, Aymaraes Province, Apurímac Department, on 11 June 2013 by Alfredo Guzmán (see Data resources for elevations and coordinates).

Diagnosis. Small (51.9 mm maximum SVL) *Liolaemus* closely related to *L. chavin* sp. n., *L. tacnae, L. walkeri,* and *L. wari* sp. n. (described below) (Fig. 1). It differs from *L. chavin* sp. n. and *L. tacnae* in having precloacal pores (males). *Liolaemus pachacutec* differs from *L. wari* sp. n. in having a partial or complete melanistic belly in adult males and in lacking a ringed pattern in ventral tail. *Liolaemus pachacutec* differs from most individuals (90%) of *L. walkeri* in lacking spots in the lateral field. In comparison with other species assigned to the *L. alticolor* group, *L. pachacutec* differs from *L. chaltin* in having precloacal pores in males. It differs from *L. paulinae* in the presence of a vertebral line and smooth neck scales. It differs from *L. puna, L. alticolor* and *L. incaicus* in having a partial or complete melanistic belly in adult males. It differs from *L. aparicioi* in lacking keeled temporal scales. It differs from *L. bitaeniatus* and *L. pagaburoi* in having a smooth dorsal surface of the head. It differs from *L. pyriphlogos* in the absence of red marks in lateral fields. It differs from *L. variegatus* in lacking keeled temporal scales, rugose dorsal head scales, and precloacal pores in females.

Description of holotype. Adult male; SVL 44.8 mm; head length 11.0 mm; head width 8.2 mm; head height 6.2 mm; axilla-groin distance 18.4 mm (41.1% of SVL); foot length 13.6 mm (30.4% of SVL); tail length 74.9 mm. (1.7 times SVL).

Dorsal head scales 16, dorsal head scales smooth, scale organs more abundant in loreal and supralabial regions. Two scale organs on postrostral. Nasal scale in contact with rostral, separated from first supralabial by one scale, nasal bordered by six scales; canthus separated from nasal by one scale. Four supralabials. Four lorilabials scales and one in contact with the subocular. Five infralabials. Auditory meatus oval (height 2.0 mm, width 1.0 mm), with two small, projecting scales on anterior margin. Six convex, smooth temporals (counting vertically from buccal commissure to posterior corner of orbit). Orbit–auditory meatus distance 3.9 mm. Orbit–anterior margin of rostral distance 4.3 mm. Rostral about two times wider than high (width 2.3 mm; height 1.0 mm). Mental subpentagonal, about two times as wide as high (width 2.5 mm; height 1.0 mm). Interparietal pentagonal with an elongated posterior apex, bordered by five scales, the parietal of similar size. Frontal trapezoidal.

Supraorbital semicircles complete on both sides. Semicircles formed by six scales. Five enlarged supraoculars. Six distinctly imbricate superciliaries on both sides. Eleven upper and lower ciliaries. Subocular elongate, 2.8 mm, longer than eye diameter (2.1 mm; measured between anterior and posterior commissure of ciliaries), separated from supralabials by a single, but interrupted row of lorilabials. Fourth supralabial elongate, 2.0 mm. Four lorilabials with single row of scale organs. Fourth lorilabial contacting subocular. Preocular small, separated from lorilabial row by one scale. Postocular as

Figure 9. Lateral (**A**) dorsal (**B**) and ventral (**C**) views of the holotype of *Liolaemus pachacutec* sp. n. (**D**) Habitat of *L. pachacutec*

large as preocular. Mental in contact with four scales: first infralabials (on each side) and two enlarged chin shields. Chin shields forming a longitudinal row of four enlarged scales separated one from the other by six smaller scales. Scales of throat round, flat, and imbricate. Twenty-two gulars between auditory meatus. Longitudinal neck

fold without keeled scales and smaller in size than dorsal scales. Antehumeral pocket and antehumeral neck fold well developed. Thirty-six scales between auditory meatus and shoulder (counting along postauricular and longitudinal neck fold), twenty-six scales between auditory meatus and antehumeral neck fold. Gular folds absent.

Dorsal scales rhomboidal, keeled, and imbricate. Forty-two dorsal scales between occiput and level of groin. Forty-five scales around midbody. Nineteen rows of keeled scales on dorsum at midtrunk. Scales becoming smooth along flank and toward belly. Ventral scales slightly wider than dorsals. Seventy-seven ventral scales between mental and precloacal pores. Five precloacal pores. Supracarpals laminar, round, and smooth. Subdigital lamellae of fingers with three keels, in number I: 8; II: 12; III: 16; IV: 18; V: 12 (right fingers). Claws moderately long. Supradigital lamellae convex, smooth, and imbricate. Infracarpals and infratarsals keeled, distinctly imbricate. Supratarsals smooth. Subdigital lamellae of toes I: 10; II: 14; III: 18; IV: 22; V: 15 (right toes).

Color in preservation. Dorsal background color from occiput to base of tail brownish-green. Black thin continuous vertebral line present. No dark paravertebral marks. Paravertebral and vertebral fields with same background color. Distinct cream dorsalateral stripes. No marks in lateral field. Cream ventrolateral stripes, beginning on the posterior corner of the eye, continuing across the upper auricular meatus, the longitudinal neck fold, through the shoulders, ending in the groin. No marks in the ventral field. Melanistic venter on throat, femur, tibia, and belly. Small and scattered dark marks in chin area and ventrolateraly. Ventral tail melanistic near the cloaca, with a thin longitudinal stripe, first half with small marks lateral to the stripe.

Color pattern in life. Head dorsally brown with scattered black dots. Subocular white. Thin and faint black vertebral line. Paravertebral field without dark marks. Creamy dorsolateral stripes. Lateral field without marks. Faint cream-white ventrolateral stripe, beginning on upper margin of eye, continuing from auricular meatus, the longitudinal neck fold, through the shoulders, ending in the groin. Ventral field yellow. Forelimbs and chin scales white with scattered black dots. Melanistic belly, hind limbs, posterior two thirds of throat. Belly with scattered yellow dots laterally. Tail with a black region close to the cloaca, black longitudinal stripe and dots at each side of the stripe.

Variation. Variation in characters is summarized in Table 1–4. There is sexual dichromatism. Males have a complete or partial melanistic belly and throat, while females have a white or yellow belly and black spots on throat. Some males have orange and yellow dots on lateral belly and yellow dots on chin scales, and ventral field with orange and black dots.

Etymology. The specific epithet *pachacutec* refers to one of most important Inca rulers, Pachacutec, who built the best known Inca ruins, including Machu Picchu and Pisac, this last site at a higher elevation just above the type locality. The species name is in the nominative singular.

Distribution and natural history. *Liolaemus pachacutec* sp. n. is known from four localities in the central Andes, at elevations of 4023–4972 m in the departments of Cusco and Apurímac in southeastern Peru (Fig. 11). The species was found under

rocks in grassland habitats (Fig. 9). It was found in sympatry at similar elevations with *Liolaemus ortizi* Laurent, 1982 and *Tachymenis peruviana* Wiegmann, 1835. This species is probably viviparous; two females showed one or two uterine chambers per side, with an embryo and abundant yolk in each chamber, but without a visible shell.

***Liolaemus wari* sp. n.**
http://zoobank.org/67A997B8-5854-4D0D-B1E0-77680FF47512
http://species-id.net/wiki/Liolaemus_wari
Figure 10

1999 *Liolaemus walkeri* Lobo and Espinoza
2002 *Liolaemus walkeri* Martínez Oliver and Lobo
2007 *Liolaemus walkeri* Lobo, Quinteros and Díaz Gómez
2012 *Liolaemus walkeri* Quinteros
2012 *Liolaemus walkeri* Ocampo, Aguilar-Kirigin and Quinteros

Holotype. MUSM 30837, adult male collected at Abra Toccto, Huamanga Province, Ayacucho Department, Peru, -13.345S, -74.167W, elevation 4231 m, on 4 June 2012 by César Aguilar and Víctor Vargas.

Paratypes. Three males (MUSM 30823, BYU 50184, 50185) and ten females (MUSM 30824, 30825, 30826, 30827, 30828, 30831, BYU 50186, 50187, 50191, 50243) from the same locality as the holotype. Two males (MUSM 30830, 30834) and three females (MUSM 30829, BYU 50188, 50190) from high area above the Historic Sanctuary Pampas, Huamanga Province, Ayacucho Department, on 3 June 2012 by César Aguilar and Víctor Vargas (see Data resources for elevations and coordinates). Two males (MUSM 25703, 25704) and one female (MUSM 25702) from Yanacocha Lake, La Mar Province, Ayacucho Department, on 24 November 2010 by Margarita Medina (see Data resources for elevations and coordinates). Two females (MUSM 25719, BYU 50189) from Huaychao, Huamanga Province, Ayacucho Department, on 1 December 2010 by Margarita Medina (see Data resources for elevations and coordinates). Two females (MUSM 30243, 30244) from Tambo, San Miguel Province, Ayacucho Department, by Michael Harvey. One male (MUSM 31411) and two juveniles (BYU 50235-36) from about 45 Km west Puquio-Cusco roadway, Lucanas Province, Ayacucho Department, on 11 June 2012 by César Aguilar and Víctor Vargas (see Data resources for elevations and coordinates).

Diagnosis. Small (61.4 mm maximum SVL), slender *Liolaemus*, closely related to *L. chavin* sp. n., *L. pachacutec* sp. n., *L. tacnae* and *L. walkeri* (Fig. 1). It differs from *L. chavin* sp. n., *L. pachacutec* sp. n. and *L. walkeri* in having a ringed pattern on the ventral tail of adult males. It differs from *L. pachacutec* sp. n. in having spots in the lateral fields. *Liolaemus wari* differs from *L. tacnae* and *L. chavin* in having precloacal pores in males. In comparison with other species assigned to the *L. alticolor* group, *L. wari* sp. n. differs from *L. chaltin* in having precloacal pores in males. It differs from

L. paulinae in lacking keeled neck scales. It differs from *L. puna, L. alticolor* and *L. incaicus* in having black spots on belly of adult males. It differs from *L. aparicioi* in lacking keeled temporal scales. It differs from *L. bitaeniatus* and *L. pagaburoi* in having a smooth dorsal surface of the head (rough to slightly dorsal surface of the head). It differs from *L. pyriphlogos* in the absence of red marks in the lateral field (red marks in the lateral fields present). It differs from *L. variegatus* in the absence of keeled temporal scales, rugose dorsal head scales and precloacal pores in females.

Description of holotype. Adult male; SVL 55.4 mm; head length 11.4 mm; head width 9.8 mm; head height 6.2 mm; axilla–groin distance 23.3 mm (42% of SVL); foot length 15.0 mm. (27.1% of SVL); tail length 83.7 mm. (1.5 times SVL).

Dorsal head scales 14, dorsal head scales smooth, scale organs more abundant in loreal and supralabial regions. Five scale organs on postrostral. Nasal scale in contact with rostral, separated from first supralabial by one scale, nasal bordered by seven scales; canthus separated from nasal by one scale. Four supralabials. Five lorilabials scales and two in contact with the subocular. Four infralabials. Auditory meatus oval (height 2.0 mm, width 1.9 mm), with two small, projecting scales on anterior margin. Seven convex, smooth temporals (counting vertically from buccal commissure to posterior corner of orbit). Orbit–auditory meatus distance 4.6 mm. Orbit–anterior margin of rostral distance 7.9 mm. Rostral almost three times wider than high (width 2.7 mm; height 1.0 mm). Mental subpentagonal, about two times as wide as high (width 2.6 mm; height 1.2 mm). Interparietal pentagonal with an elongated posterior apex, bordered by seven scales, the parietal slightly smaller. Frontal trapezoidal. Supraorbital semicircles complete on both sides. Semicircles formed by 6 scales. Four enlarged supraoculars. Five distinctly imbricate superciliaries on both sides. Eleven upper and lower ciliaries. Subocular elongate, 3.2 mm, longer than eye diameter (2.3 mm; measured between anterior and posterior commissure of ciliaries), separated from supralabials by a single, but interrupted row of lorilabials. Second supralabial elongate, 1.6 mm. Five lorilabials with single and double rows of scale organs. Fifth and fourth lorilabials contacting subocular. Preocular small, separated from lorilabial row by one scale. Postocular as large as preocular. Mental in contact with four scales: first infralabials (on each side) and two enlarged chin shields. Chin shields forming a longitudinal row of three enlarged scales separated one from the other by six smaller scales. Scales of throat round, flat, and imbricate. Twenty-one gulars between auditory meatus. Longitudinal neck fold without keeled scales and smaller in size than dorsal scales. Antehumeral pocket and antehumeral neck fold well developed. Twenty-nine scales between auditory meatus and shoulder (counting along postauricular and longitudinal neck fold), 21 scales between auditory meatus and antehumeral neck fold. Gular folds absent.

Dorsal scales rhomboidal, keeled, and imbricate. Forty-four dorsal scales between occiput and level of groin. Fifty-three scales around midbody. Twenty-two rows of keeled scales on dorsum at midtrunk. Scales becoming smooth along flank and toward belly. Ventral scales slightly wider than dorsals. Seventy-three ventral scales between mental and precloacal pores. Five precloacal pores. Supracarpals laminar, round, and smooth. Subdigital lamellae of fingers with three keels, in number I: 8; II: 12; III: 16;

Figure 10. Lateral (**A**) dorsal (**B**) and ventral (**C**) views of the holotype of *Liolaemus wari* sp. n. (**D**) Type locality.

IV: 16; V: 10 (right fingers). Claws moderately long. Supradigital lamellae convex, smooth, and imbricate. Infracarpals and infratarsals keeled, distinctly imbricate. Supratarsals smooth. Subdigital lamellae of toes I: 8; II: 12; III: 16; IV: 20; V: 13 (left toes).

Color pattern in preservation. Dorsal background color from occiput to base of tail brownish-green. Black continuous vertebral line present. Dark paravertebral marks. Paravertebral and vertebral fields with same background color. Highly distinct creamy-yellow dorsalateral stripes. Large dark and small cream marks in lateral field. Cream ventrolateral stripe, beginning on the posterior corner of the eye, continuing across the upper auricular meatus, the longitudinal neck fold, through the shoulders, ending in the groin. Dark and cream small marks in the ventral field. Black spots

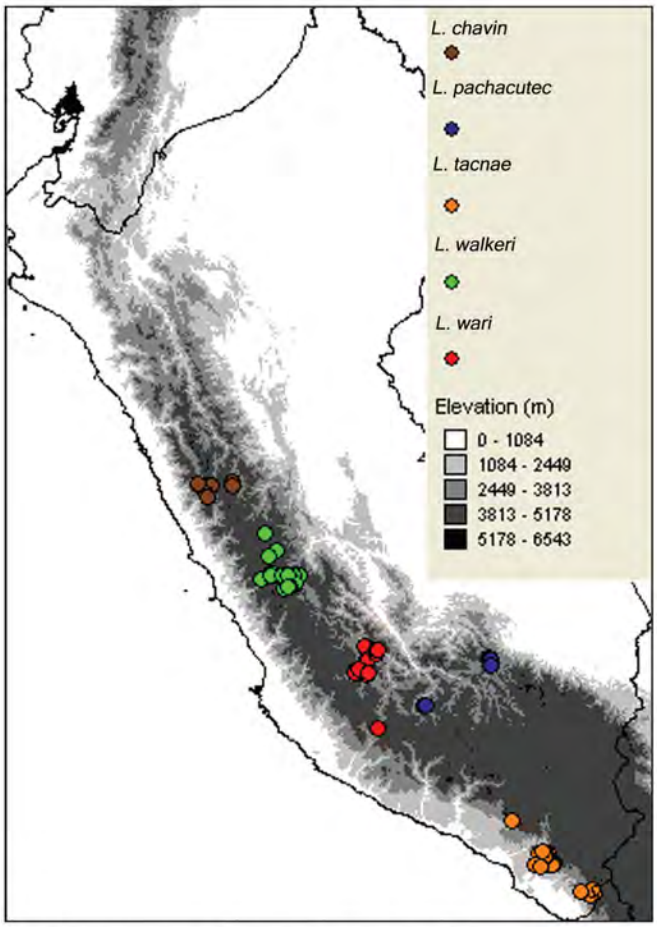

Figure 11. Geographic distribution of *L. chavin, L. pachacutec, L. tacnae, L. walkeri,* and *L. wari.*

on throat, femur, tibia, posterior third of belly and laterally in anterior two thirds of belly. Small and scattered dark marks in chest and anterior two thirds of belly. Tail with dark horizontal rows.

Color pattern in life. Head dorsally brown with black dots. Subocular cream. A black vertebral band with a thin yellow stripe on the middle. The vertebral band has a thin white stripe on each side. Paravertebral field with dark marks with posterior white dots. Creamy-yellow dorsolateral stripes. Lateral field with black marks separated by cream diagonal stripes. Yellowhish-white ventrolateral stripe, beginning on upper margin of eye, continuing from auricular meatus, the longitudinal neck fold, through the shoulders, ending in the groin. Ventrolateral similar to lateral field and same color as the paravertebral field, with diffuse dorsal markings. Forelimbs, chest and belly yellowish-white with scattered and diffuse black dots. Black marks on hind

limbs, throat, and posterior third of belly. Tail with black horizontal bands separated by white bands.

Variation. The variation in morphological characters is shown in Tables 1–4. There is sexual dichromatism. Males have white or yellow belly and throat covered completely with black spots, yellowish belly and throat with black spots on posterior third of belly, or a melanistic belly on posterior third and cloacal region, with black dots on a white throat; females have white belly and yellowish throat with faint black dots, yellowish belly and throat with faint black spots, or yellowish belly and throat without spots. Adult males have white, yellowish and yellow tails with a conspicuous ringed pattern; adult females have white, yellowish or reddish ventral tails with or without a faint ringed pattern.

Etymology. The specific epithet *wari* refers to the pre-Inca culture Wari (600–850 AD), which had its center close to the type locality. The species name is in the nominative singular.

Distribution and natural history. *Liolaemus wari* sp. n. is known from seven localities in the central Andes, at elevations of 3768–4246 m in Ayacucho Department in eastern southern Peru (Fig. 11).

Liolaemus wari sp. n. was active on the ground or found under rocks in grassland (Fig. 10) and shrubland habitats. It was found in sympatry with another *Liolaemus* species belonging to the *L. montanus* series and the snake *Tachymenis peruviana*. This species is probably viviparous; three females each showed three uterine chambers per side; each chamber showed yolk, but with no developed embryos or visible shell.

Discussion

Phylogenetic relationships

Surprisingly, our phylogenetic analysis showed that the three new species described herein plus *L. tacnae* and *L. walkeri,* assigned to *alticolor-bibronii* group, are strongly separated from the other members of this species group included in this study. Specifically, the species *L. alticolor* and *L. incaicus* assigned to the *alticolor-bibronii* group (Lobo et al. 2010, Quinteros 2013) were not recovered with *L. tacnae*, *L. walkeri*, and the three new species.

Previous molecular based phylogenies did not include *L. alticolor*, *L. tacnae* and/or *L. walkeri* (Espinoza et al. 2004, Morando et al. 2007, Schulte and Moreno-Roark 2010) and much of what these different topologies show (including ours) is probably an artifact of incomplete taxon/population sampling. Previous morphology-based phylogenies included better taxon sampling, but all of them recovered clades with low or no statistical support, and relationships of *L. tacnae*, *L. walkeri*, *L. alticolor,* and *L. incaicus* with each other and other species assigned to the *alticolor-bibronii* group are ambiguous.

Species delimitation and integrative taxonomy

We take our results based the mtDNA gene tree as a first step in species "discovery" (Carstens et al. 2013), and identify the Ancash, Ayacucho, and Cusco clades as "candidate species" (Morando et al. 2003, Avila et al. 2004). Comparative morphological and niche envelope assessments of these three clades revealed combinations of characters from three different lines of evidence, that unambiguously diagnose these groups as distinct from each other and from *L. tacnae* and *L. walkeri* (this is the second step of species delimitation – "validation" – following Carstens et al. 2013). This result highlights the need for using an integrative approach rather than a single line of evidence (e.g. morphology, usually meristic data only) to delimit species.

Our results show that normal tolerance intervals of continuous morphometric and meristic characters could not discriminate between any of these new species nor between *L. tacnae* and *L. walkeri*. On the other hand, discrete character analysis revealed some diagnostic characters, including: (1) the presence/absence of pre-cloacal pores in males distinguishing *L. chavin* and *L. tacnae* from *L. pachacutec*, *L. walkeri*, and *L. wari*; (2) the presence/absence of a complete or partial melanistic belly in adult males distinguishing *L. chavin* from *L. tacnae*; (3) the presence/absence of a ringed ventral tail pattern of adult males distinguishing *L. wari* from *L. pachacutec* and *L. walkeri*; and (4) the presence/absence of regular marks or spots in lateral fields distinguishing *L. pachacutec* from *L. wari* and from most (90%) individuals of *L. walkeri*. However, binomial tolerance intervals showed that all these "fixed" character states in our samples have a high probably of non-fixation when statistical inference is extended to consider large sample sizes. Despite these findings, we encourage the use of these binomial tests to place empirical evidence into a broader context, and to make investigators aware that tolerance intervals will become narrower as sample sizes increase, and that taxonomic decisions should be based on statistical populations not on samples (Zapata and Jiménez 2012). Moreover, samples taken at random are important for strong statistical inferences, but obtaining random samples in observational studies (such as in most taxonomic studies) is often impractical or impossible, and thus potential for bias is a serious concern (Ramsey and Schafer 2002). Besides this limitation, a statistical inference (such as those based on tolerance intervals) is better than no inference at all. However, statistic tests that evaluate differences in central tendencies (e.g., the ANOVA and Mann-Whitney *U* tests we used here) do not seem relevant as SDL criteria or for practical taxonomic purposes. For instance, most pairwise comparisons of SVL between focal populations (Ancash, Ayacucho, Cusco) and species (*L. tacnae* and *L. walkeri*) are significant in an ANOVA test at a confidence level of 0.05, giving the false impression that this character is useful for species delimitation or taxonomic identification, but tolerance intervals indicate that these populations and species completely overlap with respect to this character (Table 2).

Molecular analysis and, in most cases, niche identity tests, support our species units based on these few morphological characters, and in combination provide more

robust hypotheses. Our model-based molecular phylogenetic analysis provided the basis for our "candidate species" hypotheses, but molecular phylogenetic analysis relies on the assumption that a chosen evolutionary model is a correct one (Posada 2009), and we recognize that in the absence of corroboration from independent data sets, mtDNA may often over-split species (Miralles and Vences 2013). However, assumptions are also pervasive in morphological and ENM analyses. Discovery of gaps in morphology assumes that discontinuities are not due polymorphisms, ontogenetic variation or phenotypic plasticity (Wiens and Servedio 2000, Zapata and Jiménez 2012), and ENM (especially those models based on background data and not true absence records) assumes that occupied distribution of a species is not reduced by biotic interactions and dispersal limitations (Peterson et al. 2011). Despite these assumptions, we think that robust hypotheses of species delimitation based on different data sets give stability to scientific names, provide the strongest inference about species boundaries, overcome overlapping character variation in any particular character system, and should be a prioritized research theme in systematics (Balakrishnan 2005, Will et al. 2005, Padial and De la Riva 2006, Padial et al. 2010). In addition, we expect more exciting results when new molecular coalescent-based multi-locus and morphological multivariate methods can be applied to our data (Zapata and Jiménez 2012, Camargo and Sites 2013).

Northern limits of squamate viviparity in the high Andes

Liolaemus chavin is the northernmost viviparous species of the subgenus *Liolaemus*. Two recognized *Liolaemus* species present in the extreme northern range of the genus are *L. robustus* Laurent, 1992 and *L. disjunctus* Laurent, 1990 (subgenus *Eulaemus*). In the case of *L. disjunctus*, our recent fieldwork in the area of the species' type locality did not locate any specimen. The same result was found when we revisited localities near the type locality of *L. disjunctus* in 2012, and to our knowledge this species has not been collected at least since its original description and data on its reproductive mode are still lacking (Laurent 1990). On the other hand, the colubrid snake *Tachymenis peruviana* is another viviparous squamate widely distributed in the high Andes of Argentina, Bolivia, Chile and Peru. Its northern limits are in the department of La Libertad, Peru at about latitude 7°S, and no other viviparous squamate species are present in the high Andes of northernmost Peru, Ecuador, and Colombia.

What selective pressures might have limited the distribution of viviparous squamates in the high Andes? Although there are no field or experimental studies that have addressed this question in particular, one distributional pattern seems to be evident in the northern distributional limit of *Liolaemus*. For instance, on the Pacific Andean slopes at about latitude 15°S and south in Peru, viviparous *Liolaemus* species are present in lower, middle and higher elevations (C. Aguilar, personal observations), and oviparous lizards (genera *Phyllodactylus*, *Ctenoblepharys* and *Microlophus* but not *Stenocercus*) are only present at lower and middle elevations. However, on the Pacific

Andean slopes at about latitude 12°S, *Liolaemus* species are only present at higher elevations and oviparous *Stenocercus* (Tropiduridae) species become common at lower and middle elevations, together with the above-mentioned oviparous genera. If we consider the actual northern limits of *Liolaemus* as represented by *L. chavin*, viviparous lizards in the high Andes do not extend north beyond about latitude 8–9°S. North of latitude 8°S, oviparous *Stenocercus, Petracola* and *Riama* (Gymnophthalmidae) species are the only lizard genera present in the high Andes of Peru and Ecuador. One interesting distributional and reproductive pattern that matches this change in reproductive mode in lizards is the distribution pattern of amphibians with direct development (genus *Pristimantis*). No *Pristimantis* species have been found in sympatry with northernmost *Liolaemus* species. At high elevations on the Pacific slopes, the northernmost *Liolaemus* species (*L. chavin* and *L. robustus*) have always been found with anurans having complete (genera *Rhinella*, *Pleurodema* and *Telmatobius*) or partial (*Gastrotheca*) indirect development.

Direct-development *Pristimantis* rely on high humidity substrates for egg development (Duellman and Lehr 2009), and what may have limited the distribution of direct-development frogs in the Pacific basin of southern Peru and northern Chile, and the Andean Plateau, is the formation of an Arid Diagonal area due to the interaction of the Humboldt Current and uplift of the Andes. If so, then a working hypothesis for the evolution of viviparity and placentation in some clades of *Liolaemus* is their relationship to the presence of these arid and hypoxic conditions. Arid environments in hypoxic middle and high elevations might be lethal to the development of oviparous lizard eggs. However, origins of viviparity in *Liolaemus* seem to be associated with shifts to cold climates (e.g., in the Oligocene; Schulte and Moreno-Roark 2010), thus supporting the cold climate hypothesis (CCH; Tinkle and Gibbons 1977). According to this hypothesis, viviparity has evolved to avoid lethal ambient temperatures in high elevations and latitudes, and through retention of eggs in the uterus coupled with female behavioral thermoregulation, this mode accelerates embryonic development (for a recent review see Sites et al. 2011). The CCH is a special case of a more general maternal manipulation hypothesis (MMH) where females can enhance fitness-related phenotypic attributes in offspring by manipulating thermal conditions during embryogenesis (Shine 1995). However, arid environments may be more important with increasing hypoxic conditions in high altitudes for the evolution of viviparity than cold climates, as has been suggested for *Phrynosoma* lizards (Hodges 2004, but see Lambert and Wiens 2013). In other words, altitude may be a surrogate of other selective factors important for the evolution of viviparity, not only cold climates (Hodges 2004). High altitude environments tend to be drier and have low oxygen conditions, and viviparous species may be able to provide a better oxygen environment for developing embryos via placental structures (Hodges 2004). Whether shifts in cold climates and/or appearance of arid zones along with Andean uplift are correlated with the origin of viviparity in *Liolaemus* should be tested with coalescent based multi-locus phylogenetic studies and a time-calibrated hypothesis of species relationships.

Key to Peruvian species of the subgenus *Liolaemus*

1a Dorsal body with mucronated scales, no melanistic or without black spots on throat or belly in males ..... ***Liolaemus alticolor* group**
1b Dorsal body usually without mucronated scales, melanistic or with spots on throat or belly in males **3**
2a Dorsal pattern without spots..... ***Liolaemus alticolor***
2b Dorsal pattern with spots..... ***Liolaemus incaicus***
3a Males without precloacal pores **4**
3b Males with precloacal pores **5**
4a Males with black spots on throat, no melanistic belly..... ***Liolaemus tacnae***
4b Males with melanistic belly..... ***Liolaemus chavin***
5a Males with ringed pattern in ventral tail, mucronated scales present or absent..... ***Liolaemus wari***
5b Males without ringed pattern in ventral tail, mucronated scales absent **6**
6a Spots absent in the lateral fields ..... ***Liolaemus pachacutec***
6b Spots present in the lateral fields (most individuals)..... ***Liolaemus walkeri***

Acknowledgements

We thank J. Córdova, C. Torres (MUSM), J. Losos, J. Rosado (MCZ), F. Glaw and J. Koepcke (ZSM) for loans and accessions of specimens under their care, E. Lehr, A. Ticona, S. Ríos, D. Olivera, C. Salas, E. Coronado, M. Angeles, F. Ortiz and M. Medina for field assistance, and R. Langstroth, L. Ávila and Juan Carlos Ortiz for providing valuable literature. A. Almendra, M. Morando and F. Fontanella helped with different parts of molecular lab protocols, sequence edition and alignment, and implementation of niche models. Fieldwork was made possible by the Waitt Foundation-National Geographic Society (award W195-11 to CA and JWS), the BYU Bean Life Museum (JWS), and a NSF-Emerging Frontiers award (EF 1241885) to JWS. Collecting and exportation permits were issued by the DGFFS in Lima, Peru. We thank Ignacio De la Riva and an anonymous reviewer for providing valuable comments to our manuscript.

References

Avila LJ, Morando M, Pérez CHF, Sites JW Jr (2004) Phylogenetic relationships of lizards of the *Liolaemus petrophilus* group (Squamata, Liolaemidae), with description of two new species from western Argentina. Herpetologica 60: 187–203. doi: 10.1655/03-04

Balakrishnan R (2005) Species concepts, species boundaries and species identification: a view from the tropics. Systematic Biology 54: 689–693. doi: 10.1080/10635150590950308

Breitman MF, Parra M, Pérez CHF, Sites JW Jr (2011a) Two new species of lizards from the *Liolaemus lineomaculatus* section (Squamata: Iguania: Liolaemidae) from southern Patagonia. Zootaxa 3120: 1–28.

Breitman MF, Perez CHF, Parra M, Morando M, Sites JW Jr, Avila LJ (2011b) New species of lizard from the *magellanicus* clade of the *Liolaemus lineomaculatus* section (Squamata: Iguania: Liolaemidae) from southern Patagonia. Zootaxa 3123: 32–48.

Breitman MF, Avila LJ, Sites JW Jr, Morando M (2012) How lizards survived blizzards: phylogeography of the *Liolaemus lineomaculatus* group (Liolaemidae) reveals multiple breaks and refugia in southern Patagonia and their concordance with other codistributed taxa. Molecular Ecology 21: 6068–6085. doi: 10.1111/mec.12075

Camargo A, Sinervo B, Sites Jr. JW (2010) Lizards as model organisms for linking phylogeographic and speciation studies. Molecular Ecology 19: 3250–3270. doi: 10.1111/j.1365-294X.2010.04722.x

Camargo A, Ávila LJ, Morando M, Sites JW Jr (2012) Accuracy and Precision of Species Trees: Effects of Locus, Individual, and Base Pair Sampling on Inference of Species Trees in Lizards of the *Liolaemus darwinii* Group (Squamata, Liolaemidae). Systematic Biology 61: 272–288. doi: 10.1093/sysbio/syr105

Camargo A, Sites JW Jr (2013) Species Delimitation: A Decade After the Renaissance. Intech. doi: 10.5772/52664

Carstens BC, Dewey TA (2010) Species delimitation using a combined coalescent and information-theoretic approach: an example from North American *Myotis* bats. Systematic Biology 59: 400–414. doi: 10.1093/sysbio/syq024

Carstens BC, Pelletier TA, Reid NM, Satler JD (2013) How to fail at species delimitation. Molecular Ecology 22: 4369–4383. doi: 10.1111/mec.12413

Dayrat B (2005) Towards integrative taxonomy. Biological Journal of the Linnean Society 85: 407–415. doi: 10.1111/j.1095-8312.2005.00503.x

de Queiroz K (1998) The general lineage concept of species, species criteria, and the process of speciation. In: Howard DJ, Berlocher SH (Eds) Endless Forms: Species and Speciation. Oxford University Press, New York, 57–75.

de Queiroz K (2005) A Unified Concept of Species and Its Consequences for the Future of Taxonomy. Proceedings of the California Academy of Sciences 56: 196–215.

Díaz-Gómez JM, Lobo F (2006) Historical biogeography of a clade of *Liolaemus* (Iguania: Liolaemidae) based on ancestral areas and dispersal-vicariance analysis (DIVA). Papeis Avulsos de Zoologia 46: 261–274. www.scielo.br/paz, doi: 10.1590/S0031-10492006002400001

Donoso-Barros R (1961) Three New Lizards of the Genus *Liolaemus* from the Highest Andes of Chile and Argentina. Copeia 1961: 387–391. doi: 10.2307/1439578

Drummond AJ, Ashton B, Buxton S, Cheung M, Cooper A, Duran C, Field M, Heled J, Kearse M, Markowitz S, Moir R, Stones-Havas S, Sturrock S, Thierer T, Wilson A (2011) Geneious v5.6.6.

Drummond AJ, Suchard MA, Xie D, Rambaut A (2012) Bayesian phylogenetics with BEAUti and the BEAST 1.7. Molecular Biology and Evolution 29: 1969–1973. doi: 10.1093/molbev/mss075

Duellman WE, Lehr E (2009) Terrestrial-Breeding Frogs (Strabomantidae) in Peru. Natur-und Tier-Verlag, Münster, 384 pp.

Edgar RC (2004) MUSCLE: multiple sequence alignment with high accuracy and high throughput. Nucleic Acids Research 32: 1792–1797. doi: 10.1093/nar/gkh340

Elith J, Graham CH, Anderson RP, Dudik M, Ferrier S, Guisan A, Hijmans RJ, Huettmann F, Lethwick JR, Lehmann A, Li J, Lohmann, G, Loiselle BA, Manion G, Moritz C, Nakamura M, Nakazawa Y, Overton JMc, Peterson AT, Phillips SJ, Richardson K, Scachetti-Pereira R, Schapire RE, Soberon J, Williams S, Wisz MS, Zimmermann NE (2006) Novel methods improve prediction of species' distributions from occurrence data. Ecography 29: 129–151. doi: 10.1111/j.2006.0906-7590.04596.x

Espinoza RE, Wiens JJ, Tracy CR (2004) Recurrent evolution of herbivory in small, cold-climate lizards: Breaking the ecophysiological rules of reptilian herbivory. Proceedings of the National Academy of Sciences of the United States of America 48: 16819–16824. doi: 10.1073/pnas.0401226101

Fetzner J (1999) Extracting high-quality DNA from shed reptile skins: a simplified method. BioTechniques 26: 1052–1054.

Flot JF, Couloux A, Tillier S (2010) Haplowebs as a graphical tool for delimiting species: a revival of Doyle's "field for recombination" approach and its application to the coral genus *Pocillopora* in Clipperton. BMC Evolutionary Biology 10: 372. doi: 10.1186/1471-2148-10-372

Fontanella F, Olave M, Ávila LJ, Sites JW Jr, Morando M (2012) Molecular dating and diversification of the South American lizard genus *Liolaemus* (subgenus *Eulaemus*) based on nuclear and mitochondrial DNA sequences. Zoological Journal of the Linnean Society 164: 825–835. doi: 10.1111/j.1096-3642.2011.00786.x

Guindon S, Gascuel O (2003) A Simple, Fast, and Accurate Algorithm to Estimate Large Phylogenies by Maximum Likelihood. Systematic Biology 52: 696–704. doi: 10.1080/10635150390235520

Gurgel-Gonçalves R, Ferreira JBC, Rosa AF, Bar ME, Galvâo C (2011) Geometric morphometrics and ecological niche modelling for delimitation of near-sibling triatomine species. Medical and Veterinary Entomology 25: 84–93. doi: 10.1111/j.1365-2915.2010.00920.x

Hammer Ø, Harper DAT, Ryan PD (2001) PAST: Paleontological Statistics Software Package for Education and Data Analsis. Palaeontological Electrronica 4: 1–9.

Hart MW (2011) The species concept as an emergent property of population biology. Evolution 65: 613–616. doi: 10.1111/j.1558-5646.2010.01202.x

Hausdorf B (2011) Progress Toward A General Species Concept. Evolution 65: 923–931. doi: 10.1111/j.1558-5646.2011.01231.x

Hausdorf B, Hennig C (2010) Species delimitation using dominant and codominant multilocus markers. Systematic Biology 59: 491–503. doi: 10.1093/sysbio/syq039

Hijmans RJ, Cameron SE, Parra JL, Jones PG, Jarvis A (2005) Very high resolution interpolated climate surfaces for global land areas. International Journal of Climatolology 25: 1965–1978. doi: 10.1002/joc.1276

Hillis DM, Bull JJ (1993) An empirical test of bootstrapping as a method for assessing confidence in phylogenetic analysis. Systematic Biology 42: 182–192.

Hodges WL (2004) Evolution of viviparity in horned lizards (*Phrynosoma*): testing the cold-climate hypothesis. Journal of Evolutionary Biology 17: 1230–1237. doi: 10.1111/j.1420-9101.2004.00770.x

Huelsenbeck JP, Ronquist F (2001) MRBAYES: Bayesian inference of phylogeny. Bioinformatics 17: 754–755. doi: 10.1093/bioinformatics/17.8.754

Knowles LL, Carstens BC (2007) Delimiting species without monophyletic gene trees. Systematic Biology 56: 887–895. doi: 10.1080/10635150701701091

Krishnamoorthy K, Mathew T (2009) Statistical Tolerance Regions. Wiley Series in Probability and Statistics, New Jersey, 461 pp. doi: 10.1002/9780470473900

Kubatko L, Carstens BC, Knowles LL (2009) STEM: species tree estimation using maximum likelihood for gene trees under coalescence. Bioinformatics 25: 971–973. doi: 10.1093/bioinformatics/btp079

Lambert SM, Wiens JJ (2013) Evolution of viviparity: A phylogenetic test of the cold-climate hypothesis in Phrynosomatid lizards. Evolution 67: 2614–2630. doi: 10.1111/evo.12130

Langstroth R (2011) On the species identities of a complex *Liolaemus* fauna from the Altiplano and Atacama Desert: insights on *Liolaemus stolzmanni*, *L. reichei*, *L. jamesi pachecoi*, and *L. poconchilensis* (Squamata: Liolaemidae). Zootaxa 2809: 20–32

Laurent R (1984) Tres especies nuevas del genero *Liolaemus* (Reptilia, Iguanidae). Acta Zoologica Lilloana 37: 273–299.

Laurent R (1990) Una especie apartada del genero *Liolaemus* Wiegmann (Iguanidae, Lacertilia). Acta Zoologica Lilloana 39: 79–84.

Lehr E (2002) Amphibien und Reptilien in Peru. Natur und Tier-Verlag, Münster, 208 pp.

Librado P, Rozas J (2009) DnaSP v5: A software for comprehensive analysis of DNA polymorphism data. Bioinformatics 25: 1451–1452. doi: 10.1093/bioinformatics/btp187

Lobo F, Quinteros S, Díaz-Gómez JM (2007) Description of a new species of the *Liolaemus alticolor* group (Iguania: Liolaemidae) from Cuzco, Peru. Herpetologica 63: 537–543. doi: 10.1655/0018-0831(2007)63[537:DOANSO]2.0.CO;2

Lobo F, Espinoza RE, Quinteros S (2010) A critical review and systematic discussion of recent classification proposals for liolaemid lizards. Zootaxa 2549: 1–30.

Lobo F, Espinoza RE (1999) Two new cryptic species of *Liolaemus* (Iguania: Tropiduridae) from northwestern Argentina: Resolution of the purported reproductive bimodality of *Liolaemus alticolor*. Copeia 1999: 122–140. doi: 10.2307/1447393

Lobo F, Espinoza RE (2004) Two new *Liolaemus* from the puna region of Argentina and Chile: Further resolution of purported reproductive bimodality in *Liolaemus alticolor* (Iguania: Liolaemidae). Copeia 2004: 850–867. doi: 10.1643/CH-03-241R1

Marshall J, Arévalo E, Benavides E, Sites JL, Sites JW Jr (2006) Delimiting species: comparing methods for mendelian characters using lizards of the *Sceloropus grammicus* complex. Evolution 60: 1050–1065.

Martínez Oliver I, Lobo F (2002) Una nueva especies de *Liolaemus* del grupo *alticolor* (Iguania: Liolaemidae) de la puna salteña, Argentina. Cuadernos de Herpetología 16: 47–64.

Martínez-Gordillo D, Rojas-Soto O, de los Monteros AE (2010) Ecological niche modelling as an exploratory tool for identifying species limits: an example based on Mexican muroid rodents. Journal of Evolutionary Biology 23: 259–270. doi: 10.1111/j.1420-9101.2009.01897.x

Mayden RL (1997) A hierarchy of species concepts: the denouement in the saga of the species problem. In: Claridge MF, Dawah HA, Wilson MR (Eds) Species: the Units of Biodiversity. Chapman & Hall Ltd., London, 381–424.

Mayden RL (2002) On biological species, species concepts and individuation in the natural world. Fish and Fisheries 3: 171–196. doi: 10.1046/j.1467-2979.2002.00086.x

Miralles A, Vences M (2013) New Metrics for Comparison of Taxonomies Reveal Striking Discrepancies among Species Delimitation Methods in *Madascincus* Lizards. PLoS ONE 8: e68242. doi: 10.1371/journal.pone.0068242

Morando M, Ávila LJ, Sites JW Jr (2003) Sampling Strategies for Delimiting Species: Genes, Individuals, and Populations in the *Liolaemus elongatus-kriegi* Complex (Squamata: Liolaemidae) in Andean–Patagonian South America. Systematic Biology 52: 159–185. doi: 10.1080/10635150390192717

Morando M, Avila LJ, Turner CR, Sites JW Jr (2007) Molecular evidence for a species complex in the patagonian lizard *Liolaemus bibronii* and phylogeography of the closely related *Liolaemus gracilis* (Squamata : Liolaemini). Molecular Phylogenetics and Evolution 43: 952–973. doi: 10.1016/j.ympev.2006.09.012

Morando M, Ávila LJ, Turner C, Sites JW Jr (2008) Phylogeography between valleys and mountains: the history of populations of *Liolaemus koslowskyi* (Squamata, Liolaemini). Zoologica Scripta 37: 603–618. doi: 10.1111/j.1463-6409.2008.00350.x

Ocampo M, Aguilar-Kirigin A, Quinteros S (2012) A New Species of *Liolaemus* (Iguania: Liolaemidae) of the *alticolor* group from La Paz, Bolivia. Herpetologica 68: 410–417. doi: 10.1655/HERPETOLOGICA-D-12-00001.1

Olave M, Martínez LE, Ávila LJ, Sites JW Jr, Morando M (2011) Evidence of hybridization in the Argentinean lizards *Liolaemus gracilis* and *Liolaemus bibronii* (Iguania: Liolaemini): An integrative approach based on genes and morphology. Molecular Phylogenetics and Evolution 61: 381–391. doi: 10.1016/j.ympev.2011.07.006

Omland KE, Baker JM, Peters JL (2006) Genetic signatures of intermediate divergence: population history of Old and New World Holarctic ravens (*Corvus corax*). Molecular Ecology 15: 795–808. doi: 10.1111/j.1365-294X.2005.02827.x

Padial JM, De la Riva I (2006) Taxonomic inflation and the stability of species lists: The perils of ostrich's behavior. Systematic Biology 55: 859–867. doi: 10.1080/1063515060081588

Padial JM, De la Riva I (2010) A response to recent proposals for integrative taxonomy. Biological Journal of the Linnean Society 101: 747–756. doi: 10.1111/j.1095-8312.2010.01528.x

Padial JM, Miralles A, De la Riva I, Vences M (2010) The integrative future of taxonomy. Frontiers in Zoology 7: 16. doi: 10.1186/1742-9994-7-16

Peterson AT, Soberon J, Pearson R, Anderson RP, Martínez-Meyer E, Nakamura M, Araujo MB (2011) Ecological Niches and Geographic Distributions. Princeton University Press, Princeton, 314 pp.

Phillips S, Anderson RP, Schapire RE (2006) Maximum entropy modeling of species geographic distributions. Ecological Modelling 190: 231–259. doi: 10.1016/j.ecolmodel.2005.03.026

Pons J, Barraclough TG, Gómez-Zurita J, Cardoso A, Duran DP, Hazell S, Kamoun S, Sumlin WD, Vogler AP (2006) Sequence-based species delimitation for the DNA taxonomy of undescribed insects. Systematic Biology 55: 595–609. doi: 10.1080/10635150600852011

Posada D (2005) JModelTest v.0.01: phylogenetic model averaging. Molecular Biology and Evolution 25: 1253–1256. doi: 10.1093/molbev/msn083

Posada D (2009) Selecting models of evolution. In: Lemey P, Salemi M, Vandamme AM (Eds) The Phylogenetic Handbook: a Practical Approach to Phylogenetic Analysis and Hypotesis Testing. Cambridge University Press, Cambridge, 345–361. doi: 10.1017/CBO9780511819049.012

Quinteros S (2012) Taxonomy of the *Liolaemus alticolor–bibronii* Group (Iguania: Liolaemidae), with Descriptions of Two New Species. Herpetologica 68: 100–120. doi: 10.1655/HERPETOLOGICA-D-10-00065.1

Quinteros S (2013) A morphology-based phylogeny of the *Liolaemus alticolor–bibronii* group (Iguania: Liolaemidae). Zootaxa 3670: 1–32.

R Core Team (2013) R: A language and environment for statistical computing. R Foundation for Statistical Computing, Vienna, Austria. http://www.R-project.org

Ramsey FL, Schafer DF (2002) The Statistical Sleuth. A course in Methods of Data Analysis. Duxbury, USA, 742 pp.

Raxworthy CJ, Ingram CM, Rabibisoa N, Pearson RG (2007) Applications of ecological niche modeling for species delimitation: A review and empirical evaluation using day geckos (*Phelsuma*) from Madagascar. Systematic Biology 56: 907–923. doi: 10.1080/10635150701775111

Rissler LJ, Apodaca JJ (2007) Adding more ecology into species delimitation: Ecological niche models and phylogeography help define cryptic species in the black salamander (*Aneides flavipunctatus*). Systematic Biology 56: 924–942. doi: 10.1080/10635150701703063

Schulte JA, Moreno-Roark F (2010) Live birth among Iguanian lizards predates Pliocene-Pleistocene glaciations. Biology Letters 6: 216–218. doi: 10.1098/rsbl.2009.0707

Shapiro SS, Francia RS (1972) An approximate analysis of variance test for normality. Journal of the American Statistical Association 67: 215–216. doi: 10.1080/01621459.1972.10481232

Shine R (1995) A New hypothesis for the evolution of viviparity in reptiles. American Naturalist 145: 809–823. doi: 10.1086/285769

Sites JW, Marshall JC (2003) Delimiting species: a Renaissance issue in systematic biology. Trends in Ecology and Evolution 8: 462–470. doi: 10.1016/S0169-5347(03)00184-8

Sites JW, Marshall JC (2004) Operational criteria for delimiting species. Annual Review of Ecology Evolution and Systematics 35: 199–227. doi: 10.1146/annurev.ecolsys.35.112202.130128

Sites JW, Reeder TW, Wiens JJ (2011) Phylogenetic Insights on Evolutionary Novelties in Lizards and Snakes: Sex, Birth, Bodies, Niches, and Venom. In: Futuyma DJ, Shaffer HB, Simberloff D (Eds) Annual Review of Ecology, Evolution, and Systematics 42: 227–244. doi: 10.1146/annurev-ecolsys-102710-145051

Tinkle DW, Gibbons JW (1977) The distribution and evolution of viviparity in reptiles. Miscellanous Publications Museum of Zoology, University of Michigan 154: 1–55.

Vasconcelos R, Perera A, Geniez P, Harris DJ, Carranza S (2012) An integrative taxonomic revision of the *Tarentola* geckos (Squamata, Phyllodactylidae) of the Cape Verde Islands. Zoological Journal of the Linnean Society 164: 328–360. doi: 10.1111/j.1096-3642.2011.00768.x

Victoriano PF, Ortíz JC, Benavides E, Adams BJ, Sites JW Jr (2008) Comparative phylogeography of codistributed species of Chilean *Liolaemus* (Squamata: Tropiduridae) from the central-southern Andean range. Molecular Ecology 17: 2397–2416. doi: 10.1111/j.1365-294X.2008.03741.x

Warren DL, Glor RE, Turelli M (2008) Environmental niche equivalency versus conservatism: quantitative approaches to niche evolution. Evolution 62: 2868–2883. doi: 10.1111/j.1558-5646.2008.00482.x

Warren DL, Glor RE, Turelli M (2010) ENMTools: a toolbox for comparative studies of environmental niche models. Ecography 33: 607–611. doi: 10.1111/j.1600-0587.2009.06142.x

Wiens JJ, Reeder TW, Montes de Oca AN (1999) Molecular phylogenetics and evolution of sexual dichromatism among populations of the Yarrow's spiny lizard (*Sceloporus jarrovii*). Evolution 53: 1884–1897. doi: 10.2307/2640448

Wiens JJ, Servedio MR (2000) Species delimitation in systematics: inferring diagnostic differences between species. Proceedings of the Royal Society of London B 267: 631–636. doi: 10.1098/rspb.2000.1049

Wiens JJ, Graham CH (2005) Niche Conservatism: Integrating Evolution, Ecology, and Conservation Biology. Annual Review of Ecology, Evolution and Systematics 36: 519–539.

Wiens JJ (2007) Species delimitation: New approaches for discovering diversity. Systematic Biology 56: 875–878. doi: 10.1080/10635150701748506

Wilcox TP, Zwickl DJ, Heath TA, Hillis DM (2002) Phylogenetic relationships of the dwarf Boas and a comparison of Bayesian and bootstrap measures of phylogenetic support. Molecular Phylogenetics and Evolution 25: 361–371. doi: 10.1016/S1055-7903(02)00244-0

Will KW, Mishler BD, Wheeler QD (2005) The Perils of DNA Barcoding and the Need for Integrative Taxonomy. Systematic Biology 5: 844–851. doi: 10.1080/10635150500354878

Young D (2010) Tolerance: An R Package for Estimating Tolerance Intervals. Journal of Statistical Software 36: 1–39. http://www.jstatsoft.org/

Zapata F, Jiménez I (2012) Species delimitation: Inferring Gaps in Morphology across Geography. Systematic Biology 61: 179–194. doi: 10.1093/sysbio/syr084

Appendix 1

Supplementary file 1. (doi: 10.3897/zookeys.364.6109.app1) File format: Microsoft Excel (xls).

Explanation note: GenBank accesion and museum voucher numbers of haplotypes used in this study.

Citation: Aguilar C, Wood PL Jr, Cusi JC, Guzmán A, Huari F, Lundberg M, Mortensen E, Ramírez C, Robles D, Suárez J, Ticona A, Vargas VJ, Venegas PJ, Sites JW Jr (2013) Integrative taxonomy and preliminary assessment of species limits in the *Liolaemus walkeri* complex (Squamata, Liolaemidae) with descriptions of three new species from Peru. ZooKeys 364: 47–91. doi: 10.3897/zookeys.364.6109 Supplementary file 1. doi: 10.3897/zookeys.364.6109.app1

Appendix 2

Supplementary file 2. (doi: 10.3897/zookeys.364.6109.app2) File format: Microsoft Excel (xls).

Explanation note: Museum voucher data of specimens used in the morphological analyses.

Citation: Aguilar C, Wood PL Jr, Cusi JC, Guzmán A, Huari F, Lundberg M, Mortensen E, Ramírez C, Robles D, Suárez J, Ticona A, Vargas VJ, Venegas PJ, Sites JW Jr (2013) Integrative taxonomy and preliminary assessment of species limits in the *Liolaemus walkeri* complex (Squamata, Liolaemidae) with descriptions of three new species from Peru. ZooKeys 364: 47–91. doi: 10.3897/zookeys.364.6109 Supplementary file 2. doi: 10.3897/zookeys.364.6109.app2

Appendix 3

Supplementary file 3. (doi: 10.3897/zookeys.364.6109.app3) File format: Microsoft Excel (xls).

Explanation note: Occurrence records and locality information of *Liolaemus tacnae, L. walkeri* and the three new species described in this study, and used to develop ecological niche models.

Citation: Aguilar C, Wood PL Jr, Cusi JC, Guzmán A, Huari F, Lundberg M, Mortensen E, Ramírez C, Robles D, Suárez J, Ticona A, Vargas VJ, Venegas PJ, Sites JW Jr (2013) Integrative taxonomy and preliminary assessment of species limits in the *Liolaemus walkeri* complex (Squamata, Liolaemidae) with descriptions of three new species from Peru. ZooKeys 364: 47–91. doi: 10.3897/zookeys.364.6109 Supplementary file 3. doi: 10.3897/zookeys.364.6109.app3

Appendix 4

Supplementary file 4. (doi: 10.3897/zookeys.364.6109.app4) File format: Microsoft Excel (xls).

Explanation note: Eigenvalues, percentage of variance and similarity accounted by principal components and correspondence axes 1 and 2 respectively.

Citation: Aguilar C, Wood PL Jr, Cusi JC, Guzmán A, Huari F, Lundberg M, Mortensen E, Ramírez C, Robles D, Suárez J, Ticona A, Vargas VJ, Venegas PJ, Sites JW Jr (2013) Integrative taxonomy and preliminary assessment of species limits in the *Liolaemus walkeri* complex (Squamata, Liolaemidae) with descriptions of three new species from Peru. ZooKeys 364: 47–91. doi: 10.3897/zookeys.364.6109 Supplementary file 4. doi: 10.3897/zookeys.364.6109.app4

CHAPTER 2: Placental Morphology in Two Sympatric Andean Lizards of the Genus *Liolaemus* (Reptilia: Liolaemidae)

JOURNAL OF MORPHOLOGY 276:1205–1217 (2015)

Placental Morphology in Two Sympatric Andean Lizards of the Genus *Liolaemus* (Reptilia: Liolaemidae)

César Aguilar,[1,2,3]* Michael R. Stark,[4] Juan A. Arroyo,[4] Michael D. Standing,[5] Shary Rios,[2] Trevor Washburn,[4] and Jack W. Sites, Jr.[1]

[1]*Department of Biology and Bean Life Science Museum, Brigham Young University (BYU), Provo, Utah 84602*
[2]*Departamento de Herpetologia, Museo De Historia Natural De San Marcos (MUSM), Av. Arenales 1256, Jesus María, Lima, Perú*
[3]*Instituto de Ciencias Biologicas Antonio Raimondi, Department of Zoology, Facultad De Ciencias Biologicas, Universidad Nacional Mayor De San Marcos, Lima, Perú*
[4]*Department of Physiology and Developmental Biology, BYU, Provo, Utah 84602*
[5]*Microscopy Lab, BYU, Provo, Utah 84602*

ABSTRACT Viviparity is a remarkable feature in squamate sauropsids and it has evolved multiple times in parallel with the formation of a placenta. One example of this repeated evolution of viviparity and placentation occurs in the species-rich South American genus *Liolaemus* with at least six independent origins of viviparity. However, evolutionary studies of placentation in this genus are limited by a lack of data on placental morphology. The aim of this study is to describe and compare the microanatomy and vessel diameter (Dv, a function of blood flow) of the placenta using scanning electron microscopy (SEM) and confocal laser scanning microscopy (cLSM) in two sympatric Andean viviparous but highly divergent species, *Liolaemus robustus* and *Liolaemus walkeri*. We found interspecific differences in cell types in the chorion, allantois, and omphalopleure that may be explained by divergent phylogenetic history. Time elapsed since divergence may also explain the pronounced interspecific differences in vessel diameter, and within each species, there are strong differences in Dv between tissue locations. Both species show features to improve gas exchange in the chorioallantoic placenta including absence of eggshell, large Dv in the allantois (*L. robustus*) or embryonic side of the uterus (*L. walkeri*), and when present, microvillous cells in the allantois (*L. walkeri*). Both species also show features that suggest transfer of nutrients or water in the omphaloplacenta, including an almost complete reduction of the eggshell, secretive material (*L. robustus*), or vesicles (*L. walkeri*) on cell surface uterus, and when present specialized cells in the omphalopleure (*L. walkeri*). No statistical differences in Dv were found among stages 32–39 in each species, suggesting that a different mechanism, other than enhanced blood flow, might satisfy the increased oxygen demand of the developing embryos in the hypoxic environments of the high Andes. J. Morphol. 276:1205–1217, 2015. © 2015 Wiley Periodicals, Inc.

KEY WORDS: viviparity; blood vessels; scanning electron microscopy; confocal microscopy; high Andes

INTRODUCTION

The evolution of placentation depends on the advantages of viviparity, or live birth, to the species. One main advantage of viviparity is the ability to protect and maintain a suitable thermal environment and nutrition for embryos during the most vulnerable stage of their development (Wooding and Burton, 2008; Lodé, 2012). In amniotes (sauropsids and mammals), viviparity is based on similar repertoire of fetal membrane structures (chorioallantois, yolk sac, and amnion) to interact with adjacent uterine tissues to develop placentae (Ferner and Mess, 2011; Van Dyke et al., 2014). Viviparity is a remarkable feature in squamate sauropsids (lizards and snakes), and evolved multiple times before or in parallel with the formation of a placenta (Guillette, 1993; Blackburn, 2005; Stewart and Blackburn, 2014).

Two types of placenta are present in viviparous squamates and formed either through: 1) apposition of the chorioallantois (dorsal embryo or embryonic side); or 2) apposition of the omphalopleure (ventral embryo or abembryonic side), to the inner tissue of the uterine oviduct; these are the chorioallantoic and yolk sac placentae, respectively (Thompson and Speake 2006; Blackburn and Flemming 2009).

Additional Supporting Information may be found in the online version of this article.

Contract grant sponsor: Waitt Foundation-National Geographic Society (award W195-11 to CA and JWS); Contract grant sponsor: The BYU Bean Life Science Museum (JWS); Contract grant sponsor: A NSF-Emerging Frontiers award (EF 1241885) to JWS.

*Correspondence to: Cesar Aguilar, Department of Biology, Brigham Young University, Provo, UT 84602. E-mail: caguilarp@gmail.com

Received 4 December 2014; Revised 18 April 2015; Accepted 11 May 2015.

Published online 29 July 2015 in Wiley Online Library (wileyonlinelibrary.com). DOI 10.1002/jmor.20412

In addition to the types of placentae, the morphology of the placenta in viviparous squamates can be simple or complex, depending on the mode of nutrient provision. Species with complex placentae ovulate small eggs with little yolk, and transport nutrients to the developing embryos across the placenta (the placentotrophic condition; Thompson and Speake 2006; Blackburn and Flemming 2009). In contrast, species with simple morphological placentae retain (or not) a thin eggshell in the uterus, provide few types of nutrients across the placenta, and sustain embryos wholly or predominantly by nutrients in the yolk (the lecithotrophic condition; Thompson and Speake 2006; Blackburn and Flemming 2009). Within the squamates, placentotrophy has evolved only in one lizard family (Scincidae), while simple lecithotrophic placentae are more widespread among squamate families, but for most of them little is known about placental morphology and function (e.g., the South American lizard family Liolaemidae; Stewart and Blackburn, 2014).

Liolaemidae includes three genera, the monotypic oviparous *Ctenoblepharys*, viviparous *Phymaturus* (~38 species; Morando et al., 2013) and the species rich *Liolaemus* (255 species; Quinteros et al., 2014). *Liolameus* is divided into two subgenera (*Eulaemus* and *Liolaemus*) which diverged in the early-Miocene (~20 million years ago; Olave et al., 2015). Both subgenera include oviparous and viviparous taxa, and comprise the most diverse groups of viviparous species in the family Liolaemidae (Schulte et al., 2000). Six independent origins of viviparity have been proposed in the genus, and at least in the subgenus *Eulaemus* viviparous species are distributed from lowlands to highlands in the central Andes (Schulte et al., 2000; Aguilar et al., 2013), making *Liolaemus* a model group for studies of the evolution of viviparity and placentation.

The goal of this study is to describe and compare the blood vessel diameter (Dv, a function of blood flow; Parker et al., 2010) and microanatomy of the placenta, in two highly divergent viviparous species of this genus, *Liolaemus robustus* and *Liolaemus walkeri*. These species belong to different subgenera (*Eulaemus* and *Liolaemus*, respectively), and are sympatric in most of their geographic ranges in the central Andean highlands. Tools such as scanning electron microscopy (SEM) and confocal laser scanning microscopy (cLSM) have improved functional and evolutionary studies of placental morphology (Blackburn et al., 2002; Adams et al., 2005; Adams et al., 2007a,b; Blackburn et al., 2009; Murphy et al., 2010; Parker et al., 2010; Anderson et al., 2011; Ramirez-Pinilla et al., 2012; Wu et al., 2014), but no comparative studies using these tools have focused on the lecithotrophic placentae of any species of *Liolaemus*. To date, the only previous study of placental morphology in any species of *Liolaemus* was based on a light microscope histological study of *L. elongatus* (Crocco et al., 2008), but here we also extend studies of this genus using cLSM and SEM methods as a starting point for further studies of the evolution of placentation and viviparity at the northern geographic limit of the distribution of *Liolaemus* (Aguilar et al., 2013). *L. robustus* and *L. walkeri* together with *L. chavin* (subgenus *Liolaemus*) represent the northern-most species of the genus, after which no viviparous lizards inhabit the northern high Andes, but only oviparous taxa (e.g., the Tropidurid genus *Stenocercus*; Aguilar et al., 2013). This study can provide an example for future phylogenetically based comparative studies of the microanatomy and vascularization of the embryonic tissues of viviparous and oviparous *Liolaemus* that will contribute to the understanding of the evolutionary selective pressures and constraints for each reproductive mode on clades in the high Andes.

METHODS

A total of 16 pregnant females were collected for this study, including five *L. robustus* Laurent, 1992 and 11 *L. walkeri* Shreve, 1938 from Peru. For *L. robustus*, one female was collected on April 26, 2011 in Junin Department, and four females were collected on August 17, 2012 in Lima Department. For *L. walkeri*, all females were collected on August 11–13, 2012 in Junin Department. See Table 1 for specific locality names, coordinates, and elevations. Collecting permit was issued by the DGFFS-MINAG (RD N° 0280-2012-AG-DGFFS-DGEFFS), Lima, Peru, and the work was approved by the BYU Institutional Animal Care and Use Committee protocol number 12001 and in accordance with US law.

Specimens were euthanized with 0.1 ml pentobarbital 60 mg/ml (Halatal, Lima, Peru) intrathoracically and dissected ventrally to expose the uteri. The right uteri were fixed in 2% buffered glutaraldehyde for SEM preparation, and the left uteri were fixed in 10% buffered formaldehyde for cLSM. All voucher specimens were deposited in research collections of the Museo de la Universidad de San Marcos (MUSM), or the Bean Life Science Museum, Brigham Young University (BYU) (Table 1). Uterine incubation chambers were dissected into embryonic (dorsal) and abembryonic (ventral) hemispheres, and the enclosed embryos and yolks were removed. Embryos were staged according to Dufaure and Hubert (1961). Fetal and maternal components were peeled apart and processed separately.

Five embryos (stages 33–39) of *L. robustus* and five of *L. walkeri* (stages 34–37) were used for SEM (Table 2). Placental tissues were washed six times in 0.03 mol l^{-1} sodium cacodylate buffer for 10 min, treated with 1% osmium tetraoxide in 0.06 mol l^{-1} sodium cacodylate buffer for 3 h, washed six times in distilled water for 10 min, dehydrated in a graded acetone series (one time at 10, 30, 50, 70, 95, and 3 times 100%) for 10 min each, and processed in a Tousimis Auto Samdri series 931 critical point dryer with CO_2. Dried samples were mounted onto metal stubs and coated with gold–palladium (10–15 nm thickness) in a Quorum Q 150T ES sputter coater. Samples were examined and photographed using a FEI XL30 ESEM FEG scanning electron microscope operating at 10 kV, spot size 3, and working distance about 10 mm.

Four embryos (stages 33–39) of *L. robustus* and 11 of *L. walkeri* (stages 32–39) were used for cLSM (Table 2). Fetal chorioallantois and uterine maternal components were peeled apart and dissections were made close to the area surrounding the embryo in the embryonic hemisphere, and close to the area of the egg pole in the abembryonic hemisphere. Dissected areas were placed on glass chamber slides and covered with 10% buffered formaldehyde. Autofluorescent light emissions from

TABLE 1. Female adult specimens used in this study and their locality information

Species	Museum number	Department	Province	Coordinates		Elevation
				Latitude	Longitude	
L. robustus	BYU 50485	Junin	Junin	11°05.152′	76°09.418′	4260
L. robustus	MUSM 31506	Lima	Yauyos	12°14.852′	75°38.467′	4641
L. robustus	BYU 50482	Lima	Yauyos	12°14.805′	75°38.452′	4657
L. robustus	MUSM 31505	Lima	Yauyos	12°14.805′	75°38.452′	4657
L. robustus	BYU 50480	Lima	Yauyos	12°14.703′	75°38.468′	4647
L. walkeri	BYU 50330	Junin	Jauja	11°38.060′	75°30.029′	3966
L. walkeri	MUSM 31420	Junin	Jauja	11°40.707′	75°32.664′	4027
L. walkeri	MUSM 31415	Junin	Jauja	11°40.649′	75°32.643′	4032
L. walkeri	MUSM 31417	Junin	Jauja	11°40.706′	75°32.618′	4025
L. walkeri	BYU 50337	Junin	La Oroya	11°32.270′	75°56.540′	4054
L. walkeri	BYU 50331	Junin	Jauja	11°37.974′	75°35.878′	3996
L. walkeri	BYU 50334	Junin	Jauja	11°38.553′	75°29.338′	4178
L. walkeri	BYU 50240	Junin	Jauja	11°40.658′	75°32.645′	4030
L. walkeri	MUSM 31424	Junin	Jauja	11°38.054′	75°36.028′	3963
L. walkeri	BYU 50242	Junin	La Oroya	11°32.325′	75°56.532′	4018
L. walkeri	MUSM 31419	Junin	La Oroya	11°32.349′	75°56.501′	4001

BYU, Brigham Young University; MUSM, Museo de Historia Natural de San Marcos.

erythrocytes were used to detect blood vessels in uterine and chorioallantoic tissues. Stacks of images (3,170 × 3,170 μm^2) in the embryonic and abembryonic uteri, and in the chorioallantois were obtained using an Olympus FV-1000 confocal microscope with a TRITC preset of 543-nm laser excitation, a BA 560–660 nm emission filter, 4× lens, and 640 × 640 μm^2 pixel size. Stacks then were flattened to produce images of two-dimensional projections. Images were measured and red "stained" using an Olympus Fluoriew v.3.1 viewer. After careful evaluation of the entire tissue sample, images were captured from several representative areas for comparison of the two species with each other. One image per section and slide were taken to estimate mean Dv, which was calculated by measuring diameters of blood vessels in selected transect across each image. Transects that crossed the maximum number of blood vessels per image were selected. Because of the low resolution for small blood vessels obtained with erythrocyte autofluorescence, measurements were considered reliable only for vessels ≥20 μm. A total of 145 and 161 measurements were made in the embryonic and abembryonic uteri, respectively, and 170 measurements were made in the chorioallantois (a total of 114 and 362 measurements for *L. robustus* and *L. walkeri*, respectively; Table 3). Measurements of all embryos with the same stage and belonging to the same mother were pooled together. Data are reported as mean ± standard errors (Table 3).

TABLE 2. Sample size and embryonic stages (see text for details) of L. robustus and L. walkeri used for SEM and cLSM in this study

Stages	*L. robustus*		*L. walkeri*	
	SEM	cLSM	SEM	cLSM
32	—	—	—	3
33	2	2	—	2
33/34	—	—	1	1
35	1	2	1	1
36	—	—	—	2
37	1	2	3	5
39	1	2	—	3
Total	5	8	5	17

Statistical Analyses

Statistical analyses of Dv measurements were performed using the package lmPerm (Permutation tests for linear models) v1.1-2 (Wheeler, 2010) in R v.3.0.3 (R Core Team, 2014). A permutation test was used because it makes fewer assumptions than standard parametric tests, and is more powerful than nonparametric tests (Whitlock and Schluter, 2009). In a permutation test, the assignment to individuals of the values of one of the variables is scrambled, which "randomizes" the dataset so that every individual keeps its original measurement for one variable but has a randomly reassigned value for the second variable. This randomization procedure is repeated many times, and the test statistic of association is calculated for each randomized dataset (Whitlock and Schluter, 2009).

A linear model with an ANOVA approach and Tukey honest significance difference (HSD) post hoc test, using placental tissue (uterus on the embryonic and abembryonic sides, and the chorioallantoic side), stage and the interaction of stage, and placental tissue as factors, was used to test for differences for the response variable Dv. When a model with an interaction factor was not significant, a model with only stage and placental tissue as factors was used. Probability values less than 0.05 were considered statistically significant.

RESULTS

General Features

Embryos used in this study ranged from stages 33 to 39 in *L. robustus*, and from 32 to 39 in *L. walkeri* (40 being the final stage of development). Each embryo lies on its left side and is sunken into the yolk (Fig. 1). Embryos occupy the dorsal (mesometrial) hemisphere of the uterus and the yolk occupies the ventral (abembryonic) hemisphere (Fig. 1). Throughout development, oviductal tissues are very thin and nearly transparent (Fig. 1A,B). At stages 32 and 33 in *L. walkeri* and *L. robustus*, respectively, the uterus is already expanded into separate "incubation chambers" that house each conceptus. In *L. robustus*,

TABLE 3. Means ± standard errors of vessel diameter (Dv) and number of measured blood vessels (n) in embryonic uterine (EU), allantoic (A), and abembryonic uterine (AU) tissues

Species	Museum number	Stages	Placenta tissue Dv		
			EU	A	AU
L. robustus	MUSM 31506	33	60.9 ± 14.6 (n = 11)	93 ± 16.1(n = 10)	64.3 ± 9.2 (n = 7)
	BYU 50482	35	40 ± 5.2 (n = 11)	78 ± 15.7 (n = 10)	62.9 ± 15.8 (n = 7)
	MUSM 31505	37	55.7 ± 16.6 (n = 7)	85.8 ± 29.6 (n = 12)	68.3 ± 25.9 (n = 6)
	BYU 50480	39	58.2 ± 12.6 (n = 11)	85.4 ± 15.3 (n = 13)	54.4 ± 16.2 (n = 9)
L. walkeri	BYU 50330	32	112.2 ± 36.3 (n = 9)	46.6 ± 4.8 (n = 25)	33.9 ± 4.2 (n = 18)
	MUSM 31420	33	31.3 ± 5.5 (n = 8)	39.1 ± 13.1 (n = 11)	26.5 ± 2.3 (n = 17)
	MUSM 31415	33	112 ± 52 (n = 5)	32.8 ± 8.9 (n = 7)	57.1 ± 13.6 (n = 7)
	MUSM 31417	33/34	60 ± 20.5 (n = 7)	55 ± 16.8 (n = 8)	52.9 ± 10.2 (n = 7)
	BYU 50337	35	62.2 ± 9.4 (n = 5)	51.7 ± 4.8 (n = 6)	21.9 ± 1.2 (n = 11)
	BYU 50331	36	35 ± 11 (n = 15)	62 ± 14.7 (n = 15)	40.9 ± 6 (n = 16)
	BYU 50334	37	62.2 ± 9.4 (n = 9)	59 ± 12.6 (n = 10)	26.4 ± 2.3 (n = 14)
	BYU 50240	37	35 ± 11.0 (n = 8)	32.5 ± 6.5 (n = 8)	30 ± 10 (n = 4)
	MUSM 31424	37	56.3 ± 11.2 (n = 8)	58.7 ± 10.6 (n = 15)	40 ± 8 (n = 13)
	BYU 50242	39	66 ± 14.7 (n = 15)	50 ± 8.3 (n = 13)	40 ± 7.8 (n = 18)
	MUSM 31419	39	45.6 ± 6.25 (n = 16)	28.6 ± 5.9 (n = 7)	28.6 ± 5.9 (n = 7)

the number of embryos per side is three, and in *L. walkeri*, this number varies from one to three. The uterine artery and vein lie along the mesometrial aspect of the uterus, and connect with numerous small blood vessels that pass around each incubation chamber to supply the maternal portion of the placentae. The isolated yolk mass (IYM) is obvious in the abembryonic hemisphere (Fig. 1C,D), and is progressively depleted during gestation. In *L. robustus*, the IYM is a thin mass separated from a continuous yolk mass (YM) by a yolk cleft (YC; Fig. 1C); in *L. walkeri*, the IYM is a smaller mass separated from a partially divided YM and a YC (Fig. 1D).

Liolaemus robustus

Scanning electron microscopy. *Chorioallantoic placenta.* SEM reveals that the chorion is lined externally by a continuous layer of broad, flat epithelial cells (Fig. 2A). In surface view, most cells appear as irregular polygons with angular borders and low ridges or small projections (more evident between stages 35–39). These cells range from about 20 to 50 μm in width. Scattered among these flat cells are small triangular cells with rounded apices and also with small projections; these measure ~4 μm in width × 6 μm in length (Fig. 2A,C).

In the inner surface of the chorioallantoic membrane, allantoic blood vessels are visible as prominent longitudinal ridges. The large vessels (Fig. 3A) branch into progressively smaller vessels (not shown). The allantoic endoderm consists of broad, flattened cells with angular borders (Fig. 3A) which measure ~48–55 μm in width. The surfaces of these cells bear elaborate interconnecting surface ridges (Fig. 3C). Nuclei of the cells are sometimes apparent as centrally located bulges in cell surface.

In surface view, the uterine epithelium of the chorioallantoic placenta consists of continuous and intact flat cells with rounded or pointed borders (Fig. 4A). The cells measure ~8–12 μm in width and lack surface features (Fig. 4A).

Yolk sac placenta. The surface of the omphalopleure epithelium (OE) consists of a continuous layer of broad cells with flattened apices and angular borders; these are ~9–16 μm in width (Fig. 5A). Other components of the omphaloplacenta are visible with SEM (Fig. 5C,E). The IYM is made of spherical bodies of various sizes that are interspersed with endodermal cells and bordered internally by intravitelline cells. Both endodermal and intravitelline cells are usually difficult to visualize. Allantoic blood vessels are visible dorsal to the IYM (Fig. 5E) and OE.

The uterus of this placental region is lined by a continuous layer of epithelial cells with rounded borders (Fig. 6A). The abembryonic uterus seems to show secretory activity. Often a thin layer of uterine secretion covers the underlying epithelium (Fig. 6A,C). SEM of fetal and maternal membranes show absence of an eggshell membrane (SM) between them, but a strip of SM is visible in the abembryonic pole.

Confocal laser scanning microscopy. In *L. robustus*, there is no significant variation in blood Dv as a function of developmental stage X placental tissue interaction. A model without this interaction but with placental tissue and stage as explanatory variables also shows that there is no significant variation in Dv among stages (Figs. 7A,C,E,G and 8A,C), but significant differences are present in Dv among placenta tissues (Supporting Information Table S1). A Tukey HSD shows significant differences between Dv of allantois and uterine embryonic tissue (P = 0.0007), and between allantois and uterine abembryonic tissue (P = 0.004; Supporting Information Table S1).

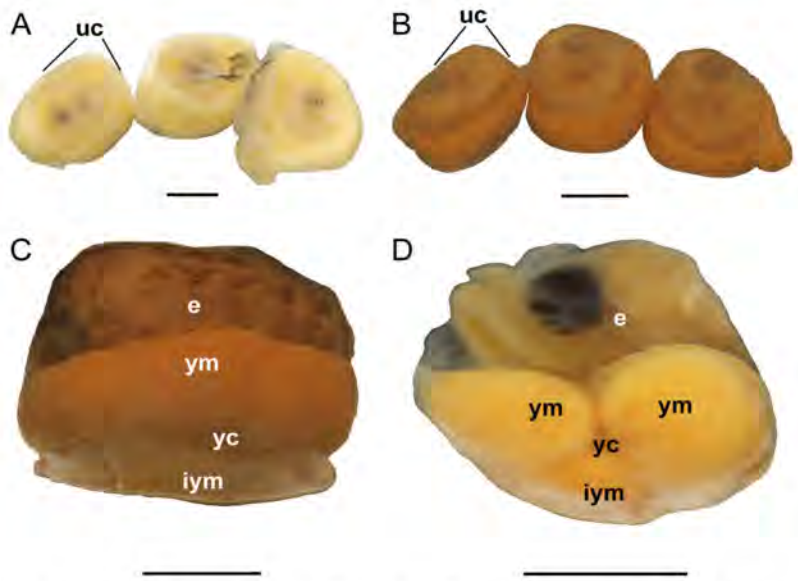

Fig. 1. Uterine chambers (uc) of (**A**) *L. robustus* and (**B**) *L. walkeri*. The embryos are enclosed in the uterine tissue and in their own fetal membranes. Embryos (e) without the uterine tissue and with the chorioallantois partially removed in (**C**) *L. robustus* (stage 39) and (**D**) *L. walkeri* (stage 37). The isolated yolk mass (iym) can be seen as a membrane in *L. robustus* (C) or as a small ventral mass in *L. walkeri* (D). In both cases the iym is separated from the yolk mass (ym) by a yolk cleft (yc). Note that the ym is divided in *L. walkeri* but not in *L. robustus*. Scale bar: A–D = 50 mm. [Color figure can be viewed in the online issue, which is available at wileyonlinelibrary.com.]

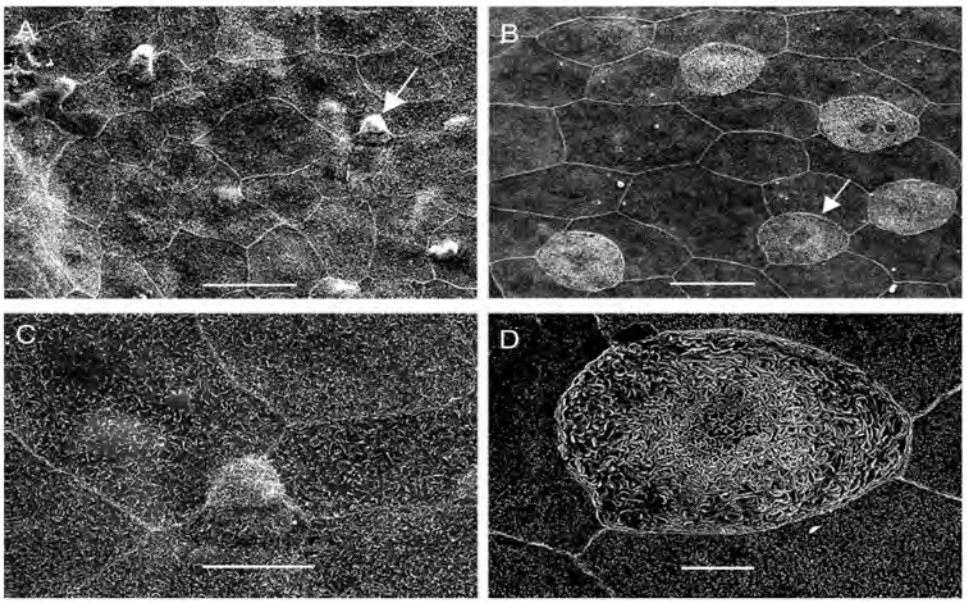

Fig. 2. Fetal components of the chorioallantoic; SEM. External surface of chorion in *L. robustus* (**A, C**) and *L. walkeri* (**B, D**). Arrows show small cells with apical extensions (A and C) and larger cells with complex ridged surfaces (B and D) in *L. robustus* and *L. walkeri* respectively. Embryonic stages: A–D = 34. Scale bar: A–B = 50 μm; C = 20 μm; D = 10 μm.

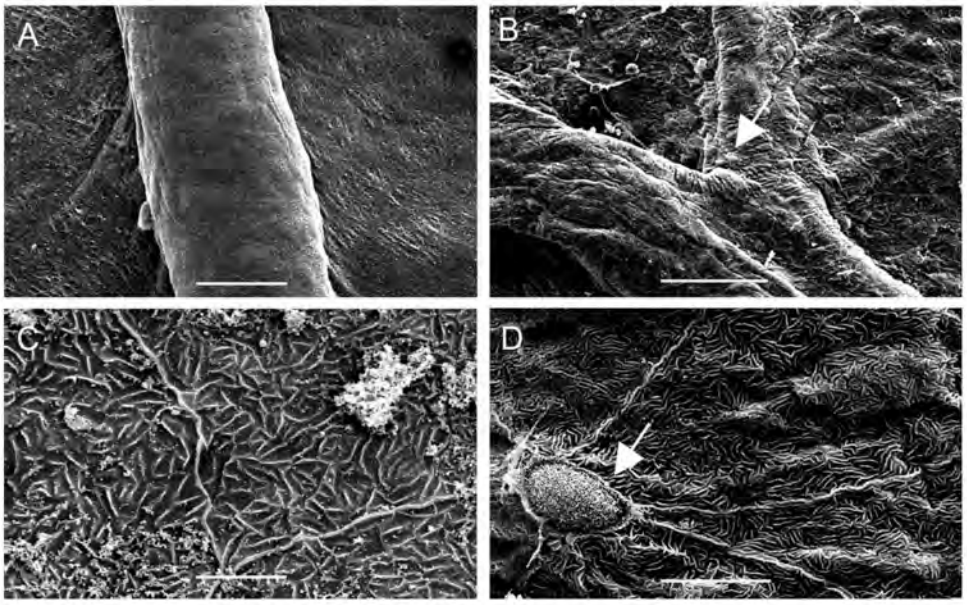

Fig. 3. Fetal components of the chorioallantoic placenta; SEM. Internal surface of allantois in *L. robustus* (**A,C**) and *L. walkeri* (**B,D**). A shows an allantoic blood vessel and endodermal cells. C shows a detail of endodermal cells lining the allantoic lumen at a higher magnification. B shows a branched blood vessel, endodermal cells and a small cell with highly packed microvilli (arrow). D shows a smaller microvillous cell surrounded by endodermal cells at a higher magnification. Microvillous cells were only observed in stage 35. Embryonic stages: A = 37; B, D, and E = 35. Scale bar: A = 50 μm; B = 100 μm; C = 5 μm; D = 10 μm.

Liolaemus walkeri

Only SEM differences with *L. robustus* are described below. *Chorioallantoic placenta.* In surface view, flat cells with small ridges or projections were only observed in stage 35. Scattered among flat cells are cells of similar size but with complex ridged-like surfaces; these cells were only observed between stages 34 and 35 (Fig. 2B,D).

Scattered among endoderm cells of the allantoic blood vessels lie small triangular cells with rounded apices and microvillous surfaces (Fig. 3B,D); they measure ~4 μm in width × 8 μm in length; these cells were only observed at stage 35.

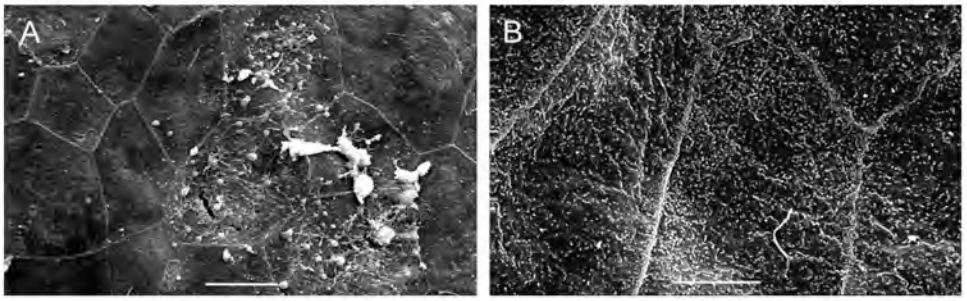

Fig. 4. Maternal components of the chorioallantoic placenta; SEM. **A** and **B** show the external surface of the uterus in *L. robustus* and *L. walkeri*, respectively. Surface of cells in B show small apical extensions. Embryonic stages: A = 33; B = 35. Scale bar: A = 10 μm; B = 5 μm.

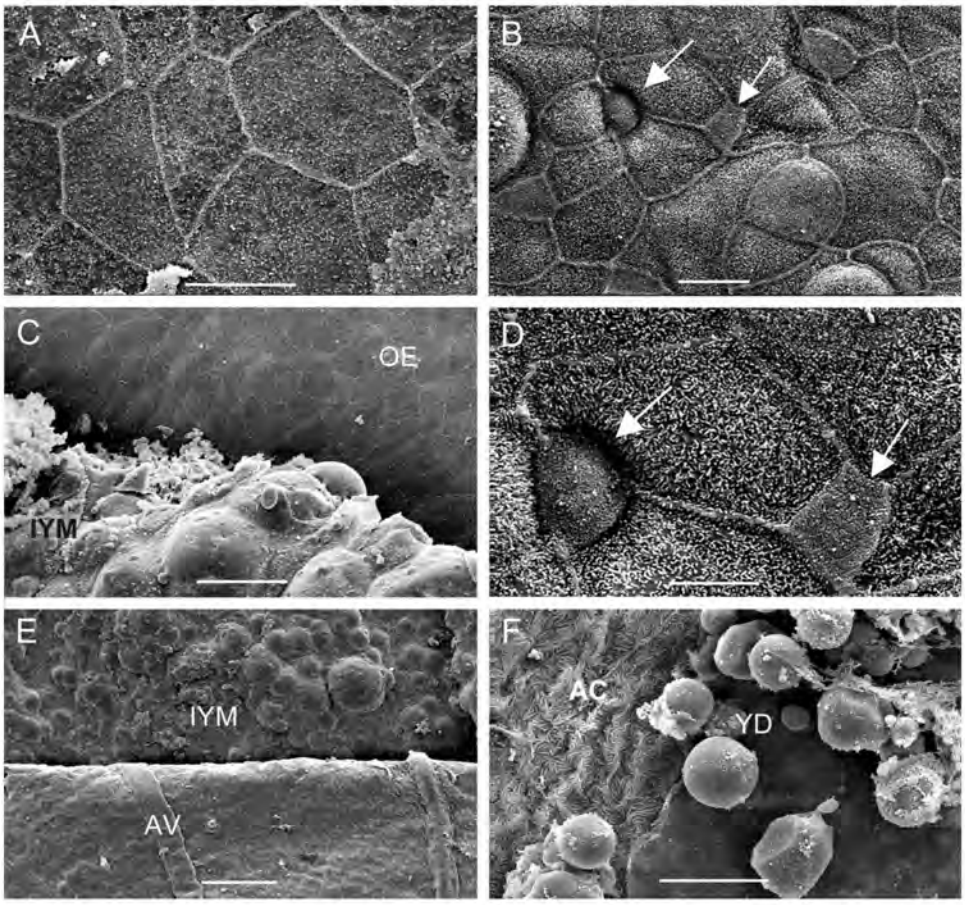

Fig. 5. Fetal components of the yolk sac placenta; SEM. From dorsal to ventral, the fetal components of yolk sac placenta are the allantois, isolated yolk mass (IYM) and omphalopleure. **A** and **C** show the external surface of the omphalopleure epithelium (OE) in *L. robustus*. **C** and **E** show the IYM. **E** shows the IYM and allantoic vessels (AV) in *L. robustus*. **B** and **D** (stage 35) show the external surface of OE at different magnifications with two populations of cells in *L. walkeri*: larger cells with less compacted microvilli and small cells with more compacted microvilli (arrows in B and D). **F** shows yolk droplets (YD) of IYM and allantoic cells (AC) in *L. walkeri*. Embryonic stages: A–D = 35, E = 39, F = 37. Scale bar: A, B, F = 10 μm; C = 50 μm; D = 5 μm; E = 200 μm.

The uterine epithelium shows surface cells with apical extensions (Fig. 4B), probably microplicae-like structures.

Yolk sac placenta. The external surface of the OE also forms a continuous layer, but two types of cells were observed in stage 35: small triangular-shaped cells with more compacted microvillous surfaces; and a network of large rounded or polygonal cells with less compacted microvillous surfaces (Fig. 5B,D). At stage 37, extracellular yolk droplets of the IYM form spherical bodies of various sizes (Fig. 5F).

The abembryonic uterus seems to show secretory activity. Secretory vesicles can be seen on the surface of cells of the uterine epithelium in many areas (Fig. 6B). SEM also shows a strip of shell membrane in the abembryonic pole (Fig. 6D).

Confocal laser scanning microscopy. In *L. walkeri*, a model without interaction but with placental tissue and stage as explanatory variables shows that there is no significant variation in Dv among stages (Figs. 7B,D,F,H and 8B,D), but significant intraspecific differences are present in Dv among placental tissues (Supporting Information

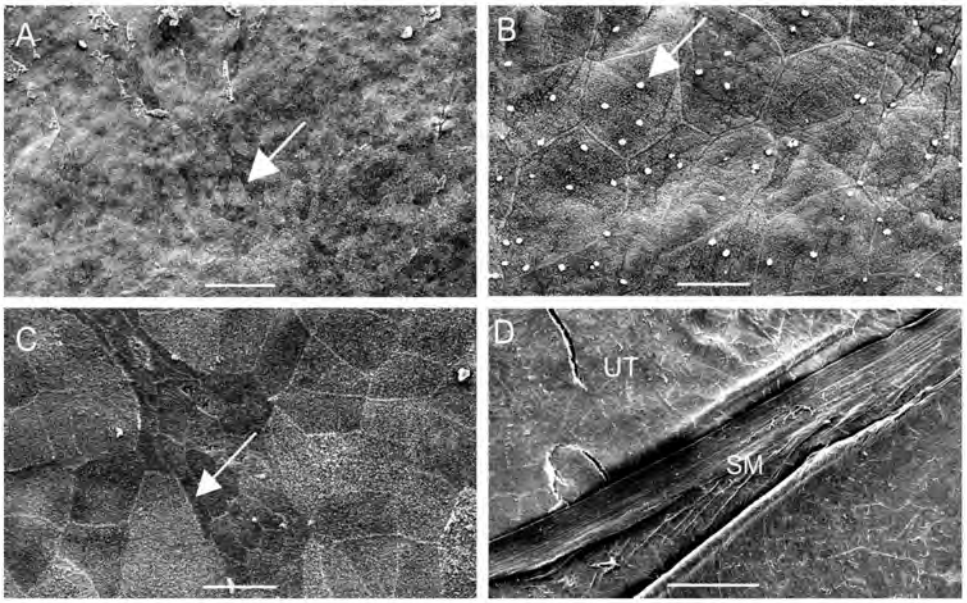

Fig. 6. Maternal components of the yolk sac placenta; SEM. **A** and **C** show the uterine epithelium area in *L. robustus* at lower and higher magnification, respectively. Note in A and C that most cells appear to be covered by thin uterine secretions (arrows indicate one of these cells). **B** shows cells of the uterine epithelium with what are probably secretory vesicles (arrow) in *L. walkeri*. **D** shows at low magnification, the uterine epithelium (UT) and a strip of shell membrane (SM) in the abembryonic pole of *L. walkeri*. Embryonic stages: A–D = 37. Scale bar: A = 100 μm; B, C = 20 μm; D = 500 μm.

Table S1). A Tukey HSD shows that these differences are between uterine embryonic and abembryonic tissues ($P = 0.004$; Fig. 7B,D,F,H; Supporting Information Table S1).

Interspecific comparisons show that overall uterine and chorioallantoic Dv is significantly higher in *L. robustus* than *L. walkeri* (Supporting Information Table S2), but there are no significant differences between tissues ($P = 0.1233$).

DISCUSSION

Phylogenetic Considerations

The aim of our study was to compare the placental morphology of two viviparous species of Andean lizards, *L. robustus* and *L. walkeri*, belonging to two different subgenera (*Eulaemus* and *Liolaemus*, respectively). Lack of detailed ancestral reconstructions of reproductive modes in a phylogenetic framework within each subgenus limits interpretation of our results. However, we propose working hypotheses that can be a starting point of further study until phylogenetic comparative hypotheses are available. Both species belong to clades within each subgenus that might have had viviparous ancestors. The phylogenetic relationships of *L. robustus* with other *Eulaemus* species are unknown, but it has been hypothetized to be part of the *L. montanus* species group in which most species are viviparous (Table 4; Schulte et al., 2000; Lobo et al., 2010; Pincheira-Donoso et al., 2013). Similarly, *L. walkeri* is included in the *L. walkeri* clade together with closely related viviparous species in the subgenus *Liolaemus* (Table 4; Aguilar et al., 2013). While the mode of reproduction of the common ancestor of the two subgenera is uncertain (Schulte et al., 2000; Pincheira-Donoso et al., 2013), it is likely that within each of the subgenera both species evolved viviparity independently from different most recent common ancestors. If true, then similar placental features in *L. robustus* and *L. walkeri* could represent either homoplasies or retention of shared ancestral characteristics. Alternatively, different placental features in both species might represent divergent phylogenetic history.

There are conspicuous differences in the microanatomy of the placentae as assessed by SEM that might reflect their divergent phylogenetic histories. SEM features present in *L. robustus*, but not in *L. walkeri*, include small cells scattered among larger flat cells in the chorion (Fig. 2A,C). Placental features present in *L. walkeri* but not in *L. robustus*, include cells with complex ridged-like

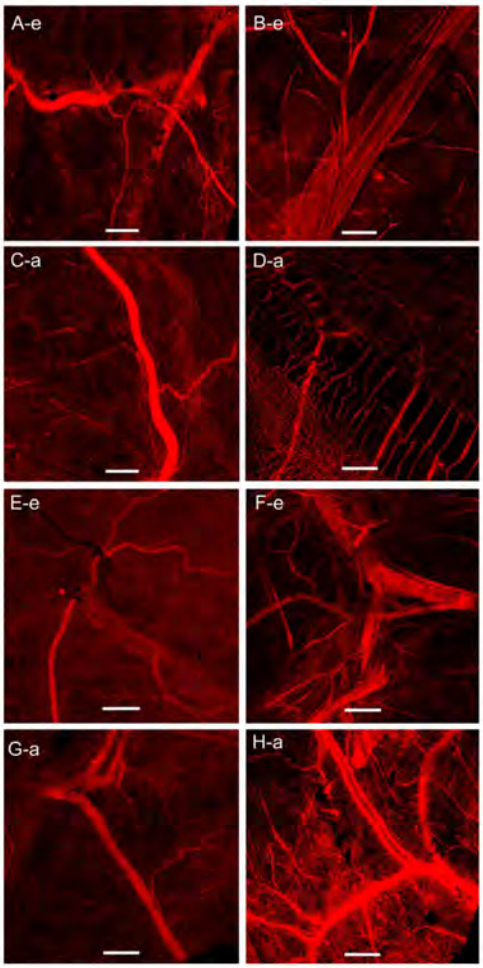

Fig. 7. Autofluorescent confocal micrographs of uterine microvasculature in the embryonic (e) and abembryonic hemisphere (a) of *L. robustus* (**A, C, E, G**) and *L. walkeri* (**B, D, F, H**). Embryonic stages: A, B, D = 33; C = 34; E–H = 39. Scale bar = 500 μm. [Color figure can be viewed in the online issue, which is available at wileyonlinelibrary.com.]

surfaces in the chorion (Fig. 2B,D), and microvillous cells present in the fetal allantois (Fig. 3B,D) and the omphalopleure (Fig. 5B,D). However, these cell types were only found in developmental stages 34 and 35.

Our results show that despite these differences, there are also some similarities in placental features between *L. robustus* and *L. walkeri*, and other oviparous and viviparous squamate species, that may be explained as retention of plesiomorphic traits (phylogenetic inertia). These similarities include: 1) the presence of a chorioallantois as a duplex membrane consisting of vascularized allantois fused to the chorion, and occupying the dorsal hemisphere of the egg (Figs. 2 and 3); 2) an avascular omphalopleure that consists of epithelium overlying the IYM and intravitelline cells (Fig. 5); and 3) a YC separating the omphalopleure and IYM from the YM (Figs. 1 and 5; Stewart and Thompson, 2003; Anderson et al., 2011; Blackburn, 2014). These are traits present during the development of other oviparous squamate species and likely reflect inheritance from an ancient but common oviparous substrate (Stewart and Thompson, 2003; Blackburn 2005; Thompson and Speake, 2006; Blackburn and Flemming, 2009; Stewart and Thompson, 2009). In addition, *L. elongatus*, a distant relative of *L. walkeri* within the subgenus *Liolaemus* (Table 4), has a divided YM above the YC, a trait similar to that in *L. walkeri* but different from *L. robustus* (Fig. 2C,D; Crocco et al., 2008); this similarity may be a synapomorphy for the subgenus *Liolaemus*, but the distribution of this character state is unknown in other species of the genus.

At least one similar feature might not be explained by retention of ancestral traits but as a shared homoplastic embryonic feature, the nearly complete reduction of the eggshell in *L. robustus* and *L. walkeri* (Figs. 1 and 6). Although a more detailed SEM study of closely related species and comparative phylogenetic analysis is needed, our working hypothesis is that both species have independently inherited this trait from their respective most recent viviparous ancestors (see above and Table 4). There is limited information about the character states of the eggshell (whether reduced or not) in other *Liolaemus* species, but in *L. elongatus*, a thin eggshell is present and is part of a clade with other closely related viviparous species in southern Argentina (Table 4; Crocco et al. 2008; Pincheira-Donoso et al., 2013; Medina et al., 2014). However, the condition of the eggshell is unknown in most species of this clade.

Divergent phylogenetic history might also explain significant differences in Dv as assessed by cLSM between placental tissues within each of the two focal species. In *L. robustus*, Dv is significantly larger in the allantois than in the uterine tissues, and in *L. walkeri* Dv is significantly larger in the embryonic than abembryonic uterine tissue (Figs. 7 and 8; Supporting Information Table S1). Significant differences are also present between placental tissues in some Australian skinks. For instance, in *Eulamprus quoyii* and *Niveoscincus coventryi* Dv is larger in the uterine abembryonic tissue than in the allantois and uterine embryonic tissue (Murphy et al., 2010; Ramirez-Pinilla et al., 2012), but in *Saiphos equalis* Dv is larger in the uterine embryonic than in the uterine abembryonic tissue (allantois not evaluated; Parker et al., 2010). These results suggest that different

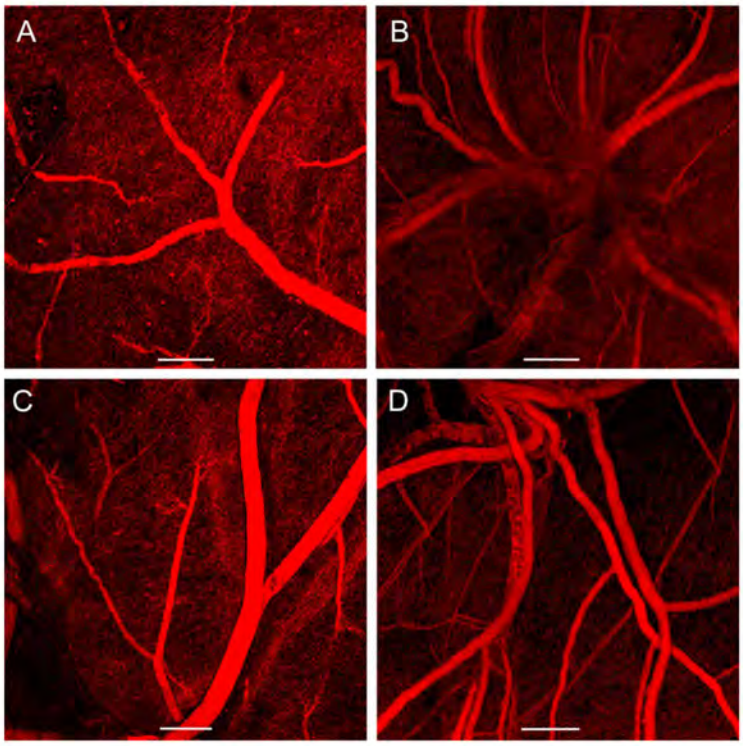

Fig. 8. Autofluorescent confocal micrographs of allantoic microvasculature of *L. robustus* (**A, C**) and *L. walkeri* (**B, D**). Embryonic stages: A = 33; B = 32; G and H = 39. Scale bar = 500 μm. [Color figure can be viewed in the online issue, which is available at wileyonlinelibrary.com.]

vascular dynamics with respect to Dv occur among placental tissues of these species, but as in this study, a more complete understanding of placental evolution will require comparative phylogenetic studies of many more taxa.

TABLE 4. Parenthetical relationships of main species groups within each subgenus of Liolaemus

Subgenera	Relationships within subgenus
Eulaemus	(((*L. montanus* group + *L. melanops* series) (*L. darwini* group + *L. anomalous* group)) (*L. lineomaculatus* section))
Liolaemus	((*L. walkeri* clade) + (((((*L. alticolor-bibronii* group + *L. chiliensis* clade) *L. coeruleus*)) (*L. kriegi-elongatus* group)) (*L. monticola-L. nitidus* clade))

L. robustus is part of the *L. montanus* group in the subgenus *Eulaemus*. *L. walkeri* and *L. elongatus* are part of the *L. walkeri* clade and the *L. kriegi-elongatus* group, respectively, in the subgenus *Liolaemus*. Relationships within major groups of the subgenus *Eulaemus* are based on Olave et al. (2015), and within subgenus *Liolaemus* are based on Aguilar et al. (2013) and Pincheira-Donoso et al. (2013).

There are also significant interspecific differences in Dv; *L. robustus* has an overall larger Dv than *L. walkeri* (Figs. 7 and 8; Supporting Information Table S2). These differences are irrespective of the location of the placental tissue. Only one study has compared the Dv of species belonging to the same family (Scindidae), and that comparison was made between oviparous (*Ctenotus taeniolatus*) and viviparous (*S. equalis*) species (Parker et al., 2010). In this case, there were no interspecific differences in Dv whether overall or between uterine tissue types. As in the case of SEM features, the most likely cause of the interspecific differences in Dv between *L. robustus* and *L. walkeri*, and between distinct placental tissues between species, must await more extensive phylogenetic comparative studies.

Functional Considerations

Even though functional interpretations of our results can be equivocal due to the lack of experimental and other observational (transmission electron

and light microscopy) evidence in these two species, functional hypotheses will be proposed based on our observations here and published literature from other viviparous squamate species.

Reduction of the eggshell is considered a selected feature and specialization to enhance gas exchange in the uterine environment (Blackburn 2005; Blackburn and Flemming, 2009; Stewart and Thompson, 2009). A complete reduction of the eggshell in the chorioallantoic placenta might have been selected in the respective common viviparous ancestors of *L. robustus* and *L. walkeri* to further improve physiological gas exchange in their similar highly hypoxic environments (both above 3,800 m). Although information about reduction of the eggshell is lacking in most species of *Liolaemus*, the thin eggshell that surrounds *L. elongatus* embryos might be correlated with its low elevation (≤1,800 m) habitats in southern Argentina (Crocco et al., 2008; Minoli et al., 2013), where hypoxia might not be a problem. Highland mammals also show placentae with modifications for shortening of diffusion distances between mothers and fetuses, favoring a reduction of the oxygen diffusion gradient (Monge and Leon-Velarde, 1991). For instance, in the epitheliochorial placenta of the South American Alpaca (*Vicugna pacos*), the minimum intercapillary distance between uterine and chorionic epithelia in late gestation is as little as 2 μm (Steven et al., 1980). Moreover, other viviparous squamates show attenuation of the intercapillary distance between uterine and chorionic epithelia (Blackburn and Lorenz, 2003; Adams et al., 2005; Wu et al., 2014).

In addition to the reduction of eggshell, small cells with microvillous surfaces were found in some stages in the allantois of *L. walkeri* that might enhance gas exchange. Microvilli increase the surface area of a cell, and thus, the respiratory area for diffusion (Adams et al., 2007a, 2007b). Moreover, Dv was larger in the embryonic than in the abembryonic uterus of *L. walkeri*. Thus, a combination of features (reduction of the eggshell, large Dv in the embryonic uterus, microvillous cells in the allantois when present) might increase gas exchange in the chorioallantoic placenta of *L. walkeri*. In contrast, *L. robustus* showed a Dv that was larger in the allantois than in both uterine regions, and lacked microvillous cells in the allantois. So in the *L. robustus* placenta, a combination of reduced egg shell and a large Dv in the allantois might enhance gas exchange in the chorioallantoic placenta.

Although there are different dynamics to improve gas exchange in the chorioallantoic placenta of *L. robustus* and *L. walkeri*, there were no significant differences in Dv between the evaluated stages (32–39) in all placental tissues within each species (Supporting Information Table S1; Figs. 7 and 8). These results suggest that between stage 32 and parturition, no significant increase in Dv occurs despite the fact that oxygen consumption might rise in the latest stages of development. If increased vessel diameter is a surrogate for enhanced blood flow and a mechanism to satisfy oxygen demand (Parker et al., 2010), then in *L. robustus* and *L. walkeri*, there should be another mechanism for this purpose. Increasing the surface area for gas exchange in the vascular bed of both fetal and maternal membranes might be such mechanism, as well as enhanced blood–oxygen-carrying capacity of embryonic and maternal blood, especially in the high-altitude hypoxic conditions of the Andes (Parker et al., 2010; Dubay and Witt, 2014). However, Chilean adult *Liolaemus* species from high and low elevations do not differ in red blood cell counts, hematocrit, or hemoglobin concentration (Ruiz et al., 1993). Mammals and birds genotypically adapted to live at high elevations also exhibit these physiological features that presumably were inherited from lowland ancestors (Monge and Leon-Velarde, 1991). However, embryonic oxygen demands in later stages of development might be accomplished by the high oxygen affinity of the fetal blood (Stewart and Blackburn, 2014), but such studies are unknown in any species of *Liolaemus*.

Besides respiratory traits to enhance gas exchange and the fact that uterine epithelia show features of simple lecithotrophic placentae (Fig. 4; Adams et al., 2007b) in the chorioallantoic placenta, both species also show surface chorionic epithelial cells of probable absorptive function, which suggests a possible subtle maternal–fetal transfer of nutrients or water (Fig. 2; Anderson et al., 2011). More evidence of a probable maternal–fetal transfer function, and not a respiratory one, is suggested by the SEM and cLSM features of the omphaloplacentae in both species. Dv in the abembryonic uteri were smaller than the allantois in *L. robustus*, and smaller than embryonic uterus in *L. walkeri*, suggesting that blood flow is not efficiently accomplished in this placental region (Figs. 7 and 8). However, lack of a shell membrane in most of the surface of the abembryonic uterus in both species might allow a direct contact of maternal and fetal tissues for histotrophic transfer (Fig. 6). In addition, cells covered with secretions or vesicles (Fig. 6) in the surface of the uterus of *L. robustus* and *L. walkeri*, respectively, also suggest a maternal–fetal histotrophic transfer (Fig. 6; Anderson et al., 2011). Moreover, the epithelium of the omphalopleure of *L. walkeri* shows microvillous cells that might increase the surface area for absorption of nutrients or water (Blackburn et al., 2002, 2009). However, other lines of evidence (experimental confocal, transmission, and light microscopy) in these and closely related species are needed to corroborate our functional interpretations.

ACKNOWLEDGMENTS

The authors thank two anonymous reviewers for greatly improving a previous version of this manuscript, M. Belk for valuable discussions on viviparity and placentation, P. Reynolds and M. Valdivia for allowing access in their laboratories, J. S. Gardner and H. Finch for assistance with SEM work, D. Robles and D. Olivera for assistance in the field.

LITERATURE CITED

Adams SM, Biazik JM, Thompson MB, Murphy CR. 2005. Cyto-epithelial placenta of the viviparous lizard *Pseudemoia entrecasteauxii*: A new placental morphotype. J Morphol 264: 264–276.

Adams SM, Lui S, Jones SM, Thompson MB, Murphy CR. 2007a. Uterine epithelial changes during placentation in the viviparous skink *Eulamprus tympanum*. J Morphol 268:385–400.

Adams SM, Biazik J, Stewart RL, Thompson MB, Murphy CR. 2007b. Fundamentals of viviparity: comparison of seasonal changes in the uterine epithelium of oviparous and viviparous *Lerista bougainvillii* (Squamata: Scincidae). J Morphol 268:624–635.

Aguilar C, Wood PL Jr, Cusi JC, Guzman A, Huari F, Lundberg M, Mortensen E, Ramirez C, Robles D, Suarez J, Ticona A, Vargas VJ, Venegas P, Sites JW Jr. 2013. Integrative taxonomy and preliminary assessment of species limits in the *Liolaemus walkeri* complex (Squamata, Liolaemidae) with descriptions of three new species from Peru. Zookeys 364:47–91.

Anderson KE, Blackburn DG, Dunlap KD. 2011. Scanning electron microscopy of the placental interface in the viviparous lizard *Sceloporus jarrovi* (Squamata: Phrynosomatidae). J Morphol 272:465–484.

Blackburn DG. 2005. Amniote perpectives on the evolutionary origins of viviparity and placentation. In: Grier HJ, Uribe MC, editors. Viviparous Fishes, Florida: New Life Publications. pp 301—322.

Blackburn DG. 2014. Evolution of vertebrate viviparity and specializations for fetal nutrition: A quantitative and qualitative analysis. J Morphol. DOI: 10.1002/jmor.20272.

Blackburn DG, Flemming AF. 2009. Morphology, development, and evolution of fetal membranes and placentation in squamate reptiles. J Exp Zool B Mol Dev Evol 312B:579–589.

Blackburn DG, Lorenz R. 2003. Placentation in garter snakes. III. Transmission EM of the omphalallantoic placenta of *Thamnophis radix* and *T. sirtalis*. J Morphol 256:187–204.

Blackburn DG, Stewart JR, Baxter DC, Hoffman LH. 2002. Placentation in garter snakes: Scanning EM of the placental membranes of *Thamnophis ordinoides* and *T. sirtalis*. J Morphol 252:263–275.

Blackburn DG, Anderson KE, Johnson AR, Knight SR, Gavelis GS. 2009. Histology and ultrastructure of the placental membranes of the viviparous brown snake, Storeria dekayi (Colubridae: Natricinae). J Morphol 270:1137–1154.

Crocco M, Ibarguengoytia NR, Cussac V. 2008. Contributions to the study of oviparity-viviparity transition: Placentary structures of *Liolaemus elongatus* (Squamata: Liolaemidae). J Morphol 269:865–874.

Dubay SG, Witt CC. 2014. Differential high altitude adaptation and restricted gene flow across a mid-elevation hybrid zone in Andean tit-tyrant flycatchers. Mol Ecol 23:3551–3565.

Dufaure JP, Hubert J. 1961. Table de development du lezard vivipare: *Lacerta (Zootoca) vivipara* Jaquin. Arch Anat Microsc Morphol Exp 50:309–328.

Ferner K, Mess A. 2011. Evolution and development of fetal membranes and placentation in amniote vertebrates. Respir Physiol Neurobiol 178:39–50.

Guillette LJ Jr. 1993. The evolution of viviparity in lizards. BioScience 43:742–751.

Lodé T. 2012. Oviparity or viviparity? That Is the Question. . .Reproductive Biology 12:259–264.

Lobo F, Espinoza RE, Quinteros S. 2010. A critical review and systematic discussion of recent classification proposal for liolaemid lizards. Zootaxa 2549:1–30.

Medina CD, Avila L, Sites JW Jr, Morando M. 2014. Multilocus phylogeography of the Patagonian lizard complex *Liolaemus kriegi* (Iguania: Liolaemini). Biol J Linn Soc 113: 256–269.

Minoli I, Medina CD, Frutos N, Morando M, Avila L. 2013. A revised geographical range for *Liolaemus elongatus* Koslowsky, 1896 (Squamata: Liolaemini) in Argentina: Review of reported and new-data based distribution with new localities. Acta Herpetol 8:159–162.

Monge C, Leon-Velarde F. 1991. Physiological adaptation to high altitude: Oxygen transport in mamals and birds. Physiolo Rev 71:1135–1172.

Morando M, Avila LJ, Perez CHF, Hawkins MA, Sites JW Jr. 2013. A molecular phylogeny of the lizard genus *Phymaturus* (Squamata, Liolaemini): Implications for species diversity and historical biogeography of southern South America. Mol Phylogenet Evol 66:694–714.

Murphy BF, Parker SL, Murphy CR, Thompson MB. 2010. Angiogenesis of the uterus and chorioallantois in the eastern water skink *Eulamprus quoyii*. J Exp Biol 213:3340–3347.

Olave M, Avila L, Sites JW Jr, Morando M. 2015. Model-based approach to test hard polytomies in the *Eulaemus* clade of the most diverse South American lizard genus *Liolaemus* (Liolaemini, Squamata). Zool J Linn Soc 174:169–184.

Parker SL, Manconi F, Murphy CR, Thompson MB. 2010. Uterine and placental angiogenesis in the Australian Skinks, *Ctenotus taeniolatus* and *Saiphos equalis*. Anat Rec 293:829–838.

Pincheira-Donoso D, Tregenza T, Witt MJ, Hodgson DJ. 2013. The evolution of viviparity opens opportunities for lizard radiation but drives it into a climatic cul-de-sac. Global Ecology and Biogeography 22:857–867.

Quinteros AS, Valladares P, Semham R, Acosta JL, Barrionuevo S, Abdala CS. 2014. A new species of *Liolaemus* of the *alticolor-bibronii* group from Northern Chile. South Am J Herpetol 9:20–29.

R Core Team. 2014. R: A language and environment for statistical computing. R Foundation for Statistical Computing, Vienna, Austria. Available at: http://www.R-project.org/. Accessed on April 2014.

Ramirez-Pinilla MP, Parker SL, Murphy CR. 2012. Uterine and chorioallantoic angiogenesis and changes in the uterine epithelium during gestation in the viviparous lizard, *Niveoscincus conventryi* (Squamata: Scincidae). J Morphol 273: 8–23.

Ruiz G, Rosenmann M, Nuñez H. 1993. Blood values of South American lizards from high and low altitudes. Comp Biochem Physiol 106:713–718.

Schulte JA, II MJR, Espinoza RE, Larson A. 2000. Phylogenetic relationships in the iguanid lizard genus *Liolaemus*: Multiple origins of viviparous reproduction and evidence for recurring Andean vicariance and dispersal. Biol J Linn Soc 69:75–102.

Steven DH, Burton GJ, Sumar J, Nathanielsz PW. 1980. Ultrastructural observations on the Placenta of the Alpaca (*Lama pacos*). Placenta 1:21–32.

Stewart JR, Blackburn DG. 2014. Viviparity and placentation in lizards. In: Rheubert JL, Siegel DS, Trauth SE, editors. Reproductive Biology and Phylogeny of Lizards and Tuatara. New York: CRC press. pp 448—563.

Stewart JR, Thompson MB. 2003. Evolutionary transformations of the fetal membranes of viviparous reptiles: A case study of two lineages. J Exp Zool A Comp Exp Biol 299:13–32.

Stewart JR, Thompson MB. 2009. Parallel evolution of placentation in Australian scincind lizards. J Exp ZoolMol Dev Evol 312B:590–602.

Thompson MB, Speake BK. 2006. A review of the evolution of viviparity in lizards: Structure, function and physiology of the placenta. J Comp Physiol B 176:179–189.

Van Dyke JU, Brandley MC, Thompson MB. 2014. The evolution of viviparity: Molecular and genomic data from squamate reptiles advance understanding of live birth in amniotes. Reproduction 147:R15–R26.

Wheeler B. 2010. lmPerm: Permutation tests for linear models. R Package Version 1:1–2. Available at: http://CRAN.R-project.org/package=lmPerm. Accessed on April 2014.

Whitlock MC, Schluter D. 2009. The Analysis of Biological Data. Colorado: Robert and Company publishers. pp 700

Wooding P, Burton G. 2008. Comparative Placentation. Structures, Functions and Evolution. Berlin: Springer. 301 p.

Wu Q, Fong CK, Thompson MB, Murphy CR. 2014. Changes to the uterine epithelium during the reproductive cycle of two viviparous lizard species (*Niveoscincus* spp.). Acta Zool DOI: 10.1111/azo.12096.

CHAPTER 3: Different roads lead to Rome: Integrative taxonomic approaches lead to the discovery of two new lizard lineages in the *Liolaemus montanus* group (Squamata: Liolaemidae)

Biological Journal of the Linnean Society, 2017, **120**, 448–467. With 7 figures.

Different roads lead to Rome: Integrative taxonomic approaches lead to the discovery of two new lizard lineages in the *Liolaemus montanus* group (Squamata: Liolaemidae)

CESAR AGUILAR[1,2,3]*, PERRY L. WOOD JR.[1], MARK C. BELK[1], MIKE H. DUFF[1] and JACK W. SITES JR.[1]

[1]*Department of Biology and M. L. Bean Life Science Museum, Brigham Young University (BYU), Provo, UT, 84602, USA*
[2]*Departamento de Herpetologia, Museo de Historia Natural de San Marcos (MUSM), Av. Arenales 1256, Jesus Maria, Lima, Peru*
[3]*Facultad de Ciencias Biologicas, Instituto de Ciencias Biologicas Antonio Raimondi, Universidad Nacional Mayor de San Marcos, Lima, Peru*

Received 21 February 2016; revised 30 July 2016; accepted for publication 30 July 2016

Integrative taxonomy (IT) is becoming a preferred approach to delimiting species boundaries by including different empirical criteria. IT methods can be divided into two types of procedures both of which use multiple kinds of evidence: step-by-step approaches test hypotheses by sequential evaluation in a hypothetic-deductive framework, while model-based procedures delimit groups based on statistical information criteria. In this study we used a step-by-step approach and a Gaussian clustering (GC) method to test species boundaries in the northernmost species of the *Liolaemus montanus* group. We used different methods based on mitochondrial and nuclear DNA sequence data, morphological measures and niche envelope variables. In contrast with GC, our step-by- step approach shows that one Andean population (Abra Apacheta) previously considered part of *L. melanogaster*, is actually nested within another clade; another Andean species, *L. thomasi*, is equivocally shown to be either a distinct species or conspecific with *L. ortizi*; and an additional Andean population (Abra Toccto) is delimited by concordance among most lines of evidence and different methods as a distinct lineage. However, one of the oldest and low-elevation populations (Nazca) is strongly delimited by all data sets and IT procedures as a new lineage distinct from any currently recognized species. © 2016 The Linnean Society of London, *Biological Journal of the Linnean Society*, 2017, **120**, 448–467.

KEYWORDS: lizards – Pacific lowland – Peruvian Andes – species boundaries.

INTRODUCTION

Integrative taxonomy (IT), the use of different kinds of data and methods for species discovery and hypothesis testing, is becoming a fundamental approach in species delimitation (Padial & De La Riva, 2010; Padial *et al.*, 2010; Mckay *et al.*, 2014; Pante, Schoelinck & Puillandre, 2015). This shift to IT as an alternative to species delimitation (SDL) studies based exclusively on molecular data is due to evidence that: (1) sequence data alone may not reflect accumulation of differences associated with reproductive isolation; (2) very young species or those that have diverged with ongoing gene flow in neutral regions of the genome may not be detected; (3) failures can occur when errors associated with initial assignment of individuals to species are not detected in upstream analyses; and (4) when molecular analyses, in general, are based on simplified assumptions about divergence processes (Camargo & Sites, 2013; Solís-Lemus, Knowles & Ané, 2014; Olave, Solà & Knowles, 2014a).

Integrative taxonomy approaches using different types of data should reveal cryptic diversity when divergence occurs (at least initially) along non-molecular axes of differentiation, or when divergence

*Corresponding author. E-mail: caguilarp@gmail.com

occurs with gene flow (Solís-Lemus *et al.*, 2014; Olave *et al.*, 2014a). IT also exposes potential conflicts among the different kinds of data, and leads to more deeply informed and statistically rigorous assessments of biodiversity (Mckay *et al.*, 2014). IT methods can be divided informally into two types of procedures: (1) step-by-step methods based on sequential analyses of independent data types, followed by a qualitative assessment of diversity in a hypothetico-deductive framework (Schlick-Steiner *et al.*, 2010; Yeates *et al.*, 2011; Andújar *et al.*, 2014); and (2) model-based methods that simultaneously evaluate multiple data types, followed by delimitation of species based on a statistical or information criterion (Guillot *et al.*, 2012; Edwards & Knowles, 2014; Solís-Lemus *et al.*, 2014). Both IT approaches can be used for the four focal areas of SDL: (1) validation of candidate species as evolutionary distinct lineages; (2) inferring species relationships; (3) detecting 'cryptic diversity'; and (4) individual specimen assignment to a species group (Edwards & Knowles, 2014; Leavitt, Moreau & Lumbsch, 2015).

These SDL issues are highly relevant in the large and ecologically prominent temperate South American lizard genus *Liolaemus* (Aguilar *et al.*, 2013), and in particular in the *L. montanus* group (Olave *et al.*, 2014b). These are mainly viviparous lizards ranging from northern Argentina, Chile and Bolivia to central Peru, and from near sea level to more than 5000 m elevation (Aguilar *et al.*, 2015). The group comprises 60 (24%) of the ~250 known species in the genus (Uetz & Hosek, 2016). The northernmost Peruvian component of this group includes 12 recognized species (Fig. 1): *L. annectens* Boulenger, 1901, *L. disjunctus* Laurent, 1990; *L. etheridgei* Laurent, 1998; *L. insolitus* Cei & Péfaur, 1982; *L. melanogaster* Laurent, 1998; *L. ortizi* Laurent, 1982; *L. poconchilensis* Valladares, 2004, *L. polystictus* Laurent, 1992; *L. robustus* Laurent, 1992; *L. signifer* (Dumeril and Bribon, 1837), *L. thomasi* Laurent, 1998 and *L. williamsi* Laurent, 1992. Most species descriptions in the northernmost species of this group have been based, at best, on only morphological data, and usually on a limited number of individuals from one or a few localities. In other cases, species descriptions were based on very small sample sizes or even a single specimen (e.g. *L. ortizi* and *L. thomasi*).

In addition to these issues, recent fieldwork and SDL studies have revealed examples of taxa representing a known species, but previously recognized as different based on a doubtful type locality (e.g. *Liolaemus disjunctus*; Aguilar *et al.*, 2013). This kind of taxonomic error reflects the fact that new populations collected between type localities of known species are often difficult to identify based on the limited morphological characters of earlier studies. More complete geographic sampling and multiple lines of evidence often identify new lineages that were 'hidden' due to insufficiently informative phenotypic traits (Aguilar *et al.*, 2013). Hypotheses of species limits based on adequate geographic sampling and multiple lines of evidence (molecular, ecological and morphological) are necessary for assigning populations to known species or for the discovery of new lineages as 'candidate species' requiring further study.

The *Liolaemus montanus* species group, like many others, exemplifies the need for a low-cost IT approach in megadiverse countries where research resources and infrastructure are limited, and immediate threats to biodiversity are an unfortunate reality. In the Peruvian Andes, habitat destruction and overexploitation are significant threats to some populations of the *L. montanus* species group, and some of these populations likely represent new species with restricted distributions. However, without formal descriptions and names, 'cryptic diversity', 'candidate species' and 'distinct evolutionary lineages' are not afforded legal protection or official recognition on species lists maintained by international conservation agencies (Pante *et al.*, 2015). For instance, a recent Peruvian list of threatened species and IUCN evaluation of Andean squamates (lizard and snakes) shows an increase in the number species in the *L. montanus* group listed as either 'threatened' (*L. insolitus* and *L. poconchilensis*) or 'near threatened' (*L. robustus* and *L. signifer*) due to habitat destruction, pollution and overexploitation in their geographic ranges (Ministerio de Agricultura, 2014; IUCN unpubl. data). These same threats are likely present in areas inhabited by distinct lineages of unrecognized species, but without formal names and descriptions they cannot be included in current conservation planning.

Species descriptions based on IT analyses of multiple lines of evidence (molecular, morphological and bioclimatic data) can be implemented at minimal cost, and these descriptions are of higher quality than conventional descriptions based on a single line of evidence (e.g. morphology) that are sometimes without statistical support (Aguilar *et al.*, 2013; Pante *et al.*, 2015). The goal of this study is to delimit species boundaries in the northernmost taxa of the *Liolaemus montanus* group using IT step-by-step and model-based SDL procedures based on molecular, morphological and bioclimatic data. Specifically we would like to test if: (1) an Andean population identified as 'Abra Apacheta' and currently assigned to *L. melanogaster*, is in fact part of this lineage, or conspecific with its geographically closest species, *L. polystictus*; (2) *L. ortizi* and *L. thomasi* actually represent one or two lineages; (3) an Andean population

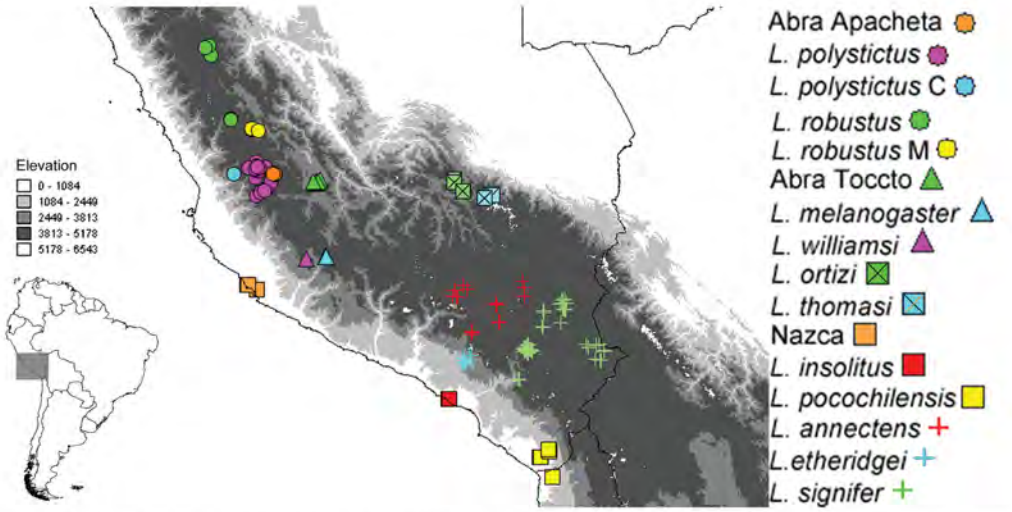

Figure 1. Distribution of northernmost species and populations of the *Liolaemus montanus* group based on museum records. *L. polystictus* C = *L. polystictus* 'Castrovirreyna'; *L. robustus* M = *L. robustus* 'Minas Martha'.

called 'Abra Toccto' represents a distinct lineage; and (4) a low-elevation population from the Pacific Andean slopes ('Nazca') represents a new lineage. Formal taxonomic changes and species descriptions will be treated in separate papers.

MATERIAL AND METHODS

SAMPLING OF SPECIMENS

Specimens were collected from *Liolaemus annectens*, *L. etheridgei*, *L. insolitus*, *melanogaster*, *L. ortizi*, *L. polystictus*, *L. robustus*, *L. signifer*, *L. thomasi* and *L. williamsi* type localities, localities of paratypes if different from the type locality, and other locations which are represented by previous museum records (Fig. 1) or mentioned in taxonomic publications. Type specimens of *L. ortizi*, *L. melanogaster*, *L. polystictus*, *L. robustus* and *L. williamsi* and other museum specimens (Supporting Information, Appendix S1) were also examined and compared with collected specimens to propose initial species hypothesis and perform morphological analyses (see below).

DNA SAMPLING AND EXTRACTION

Lizards were collected by hand, photographed and euthanized with an injection of sodium pentobarbital. After liver and muscle tissues were collected for DNA samples, whole specimens were fixed in 10% formaldehyde, and transferred to 70% ethanol for permanent storage in museum collections. Tissue samples were collected in duplicate, stored in 96% ethanol and deposited at the M. L. Bean Life Science Museum at Brigham Young University (BYU) and Museo de Historia Natural de San Marcos (MUSM) in Lima, Peru, and voucher specimens were shared between these same institutions on a 50:50 basis. Total genomic DNA was extracted from liver/muscle tissue using the animal tissue extraction protocol in the Qiagen protocol (Qiagen Inc., Valencia, CA).

For in-groups and outgroups we used selected species of the subgenus *Eulaemus* that are assigned to different species groups and for which mtDNA sequences of cyt-*b* and 12S fragments are available from the GenBank database. Our ingroup included ten taxa that have been assigned to the *Liolaemus montanus* group: *L. annectens*, *L. etheridgei*, *L. insolitus*, *L. melanogaster*, *L. ortizi*, *L. poconchilensis*, *L. robustus*, *L. polystictus*, *L. signifer*, and *L. williamsi* (Lobo, Espinoza & Quinteros, 2010). To further resolve the relationships of the northernmost species of the *L. montanus* group, we sampled other species assigned to this species group (*L. andinus* Koslowsky, 1895, *L. dorbignyi* Koslowsky, 1898, *L. famatinae* Cei, 1980), the *rothi* complex (*L. rothi* Koslowsky, 1898), and the *fitzingeri* group (*L. melanops* Burmeister, 1888; Olave *et al.*, 2014b). We used *L. ornatus*, a species belonging to the *darwini* group (Camargo *et al.*, 2012) as the outgroup.

DNA AMPLIFICATION AND SEQUENCING

We sequenced part of the mitochondrial cyt-*b* gene (643 bp for 138 individuals from 31 localities; Supporting Information, Appendix S2). Redundant cyt-*b* haplotypes were identified using DnaSP v5 (Librado & Rozas, 2009), and individuals representing non-redundant cyt-*b* haplotypes were then sequenced for the mtDNA 12S region (~660 bp), and five nuclear gene regions, including: protein-coding KIF24 (440 bp), MAXRA5 (776 bp), EXPH5 (747 bp), and anonymous A12D (~580 bp,) and A4B (~374 bp) DNA fragments. Individuals used for these fragments and sequencing primers are given in Supporting Information (Appendix S2) and Table 1, respectively. All new sequences are deposited in the GenBank database (accession numbers KX826506–KX826781; Supporting Information, Appendix S3) and alignments in Dryad. Double-stranded DNA polymerase chain reactions (PCR) amplified target regions under the conditions described in Aguilar *et al.* (2013) and Noonan & Yoder (2009), for mitochondrial and nuclear markers, respectively. PCR products were visualized on 10% agarose gels to ensure the targeted products were cleanly amplified, then purified using a MultiScreen PCR (μ) 96 (Millipore Corp., Billerica, MA), and directly sequenced using the BigDye Terminator v 3.1 Cycle Sequencing Ready Reaction (Applied Biosystems, Foster City, CA). The cycle sequencing reactions were purified using Sephadex G-50 Fine (GE Healthcare) and MultiScreen HV plates (Millipore Corp.). Samples were then analyzed on an ABI3730xl DNA Analyzer in the BYU DNA Sequencing Center.

Table 1. Molecular markers and primers used in this study (ANL, anonymous nuclear loci)

Locus	Kind of marker	Substitution model	Primers	References
CYTB	mtDNA	HKY + G	IguaF2, IguaR2	Corl *et al.* (2010)
12S	mtDNA	TrN + I + G	tphe, E	Wiens, Reeder & De Oca (1999)
A4B	ANL	HKY	F, R	Camargo *et al.* (2012)
A12D	ANL	TPM2uf	F, R	Camargo *et al.* (2012)
EXPH5	Coding	HKY	F1, R1	Portik *et al.* (2012)
KIF24	Coding	HKY	F1, R2	Portik *et al.* (2012)
MXRA5	Coding	HKY	F, R	Portik *et al.* (2012)

PHYLOGENETIC ANALYSES

All sequences were aligned in the MUSCLE (Edgar, 2004) plug-in in GENEIOUS PRO v5.6.6 (Kearse *et al.*, 2012), and protein-coding sequences were translated to check for premature stop codons. Bayesian Information Criteria in JMODELTEST v2.1.3 (Darriba *et al.*, 2012) were used to identify the best-fit models of evolution. The concatenated mitochondrial fragments (cyt-*b* and 12S; 1298 nt, 63 individuals) were run in MRBAYES v3.2 (Ronquist *et al.*, 2012). Two parallel runs were performed using four chains (one cold and three hot) for 1.1×10^6 generations with sampling every 200 generations from the Markov Chain Monte Carlo (MCMC) output. We determined stationarity by plotting the log likelihood scores of sample points against generation time; when the values reached a stable equilibrium and split frequencies fell below 0.01, stationarity was assumed. We discarded 100 000 samples and 10% of the trees as burn-in and a maximum clade credibility (MCC) tree was constructed using TREEANNOTATOR v2.1.2 (Bouckaert *et al.*, 2014); we interpreted Bayesian posterior probabilities (PP) > 95% as evidence of significant support for a clade (Wilcox *et al.*, 2002).

MULTILOCUS CONCATENATED AND DATING ANALYSIS

To estimate divergence times, we generated a concatenated tree that combined the mtDNA sequences and all nuclear region sequences using 117 terminals that include members of different species groups in the subgenus *Eulaemus*, and two species of the subgenus *Liolaemus* (Supporting Information, Appendix S3). Terminals include new sequences of 35 individuals of the northernmost species of the *L. montanus* group and sequences of 82 individuals downloaded from GenBank. Species of the subgenus *Liolaemus* were used as outgroups. We then calibrated the *Eulaemus* clade using a fossil (Albino, 2008) to date the divergence between *Liolaemus* (*s.s.*) and *Eulaemus* following Breitman *et al.* (2011) and Fontanella *et al.* (2012). This calibration prior was set to 20 Mya assuming a lognormal distribution and with a standard deviation of 0.13 (24.56–16.01), based on the recommendations of Ho (2007). This analysis was implemented in BEAST v1.8 (Drummond *et al.*, 2012) and run for 100 million generations for each of ten independent runs. To check for convergence, we used Tracer v1.6 (Drummond *et al.*, 2012) to ensure that all effective samples sizes (ESS) were greater than 200. We discarded 10% of the trees as burn-in and the remaining trees were combined using LogCombiner v1.8.0 and sampled at a lower frequency, resulting in 10 000 trees. An MCC

tree was then constructed using TreeAnnotator v1.8 (Drummond *et al.*, 2012), and keeping mean heights.

Species tree analysis

A species tree analysis was also performed for mtDNA and all nuclear region sequences. We used 15 terminals representing taxa of the northernmost species of the *Liolaemus montanus* group and *L. ornatus* as the outgroup. Each nuclear DNA fragment was tested for presence of recombination using RDP v3.44 (Martin & Rybicki, 2000) and haplotypes of nuclear markers were phased using DnaSP v5 (Librado & Rozas, 2009). Each locus was included as a separate data partition (the two mitochondrial loci were linked) in an estimate of the species tree using *BEAST in BEAST v2.0 (Bouckaert *et al.*, 2014). We used a relaxed log normal molecular clock model, a linear-with-constant-root model, and a Yule model for the species tree prior. Analyses were run for 100 million generations and samples taken every 4000 generations. We determined stationarity by plotting the log likelihood scores of sample points against generation time; when the values reached a stable equilibrium and split frequencies fell below 0.01, stationarity was assumed. We discarded 100 000 samples and 10% of the trees as burn-in, and constructed a MCC tree using TREEANNOTATOR v1.7.5 (Drummond *et al.*, 2012). Analyses were run in the BYU Fulton Supercomputer Lab.

Tree distance and Rosenberg's probability

We used the 'species delimitation' plug-in in the Geneious software (Masters, Fan & Ross, 2011) as an exploratory tool to assess populations and 'known' species in our mitochondrial gene tree. This algorithm estimates average pairwise interspecific tree distance (ITD) and the Rosenberg probability, P_{AB}, to test the null hypothesis that taxon A represented by a sequences is monophyletic, or in a clade of $a + b$ sequences the a sequences will be reciprocally monophyletic with the remaining b sequences, under a Yule model of random coalescence (Rosenberg, 2007). The rejection of the null hypothesis suggests that the random branching of the Yule model does not hold, perhaps because lineages were drawn from multiple genetically distinctive groups (Rosenberg, 2007). Specifically, we test whether monophyletic groups of populations might represent isolated lineages. We reject the null hypothesis of random branching when $P \leq 0.01$.

Morphological data and analyses

We collected three classes of morphological data from a total of 302 individuals (Supporting Information, Appendix S1). We scored the following 11 morphometric characters: (1; SVL) snout–vent length, (2; AGL) axilla–groin length (between the posterior insertion of forelimb and anterior insertion of thigh), (3; HL) head length (from snout to anterior border of auditory meatus), (4; HW) head width (at widest point), (5; FOL) forelimb length (distance from the attachment of the limb to the body to the terminus of the fourth digit), (6; HIL) hindlimb length (distance from the attachment of the limb to the body, to the terminus of the fourth digit), (7; SL) snout length (from snout to anterior border of eye), (8; AMW) auditory meatus width, (9; AMH) auditory meatus height, (10; RW) rostral width, and (11; RL) rostral length. We also scored five meristic characters, including: (1; MBS) number of midbody scales (counted transversely at the middle of the body), (2; DTS) dorsal trunk scales (counted from the level of anterior border of the ears to anterior border of the thighs), (3; DHS) dorsal head scales (counted from the rostral scale to anterior border of ear), (4; VS) ventral scales (counted from the mental scales to the cloaca), and (5; SCI) number of scales in contact with the interparietal.

Measurements and counts were taken from the right side of the animal using a stereomicroscope. Morphometric data were only taken for adult males and females (adults were identified by size using the largest female and male for each species/population). We explored differences between sexes using Principal Component Analyses (PCA; Supporting Information, Appendix S4), and if sexes formed distinct clusters, we performed all subsequent analyses for males and females separately; otherwise data from both sexes were pooled. Correlation of morphometric characters was performed to avoid redundancy and variables with linear Pearson higher than 0.9 were discarded. Size correction was done using SVL as an independent variable and remaining morphometric characters as dependent variables in a multivariate linear model. We used unstandardized residuals of the linear model as variables. Correlation and linear model were performed in PAST v3.0 (Hammer, Harper & Ryan, 2001).

The third category of morphological data was head shape, as quantified using geometric morphometric methods. Ten landmarks on the dorsal head view of lizards (Supporting Information, Appendix S4) were set on digital pictures using tpsDig v1.4 (Rohlf, 2004), and shape analyses were performed using PCA after a Generalized Procrustes approach. Procustes and PCA analyses were performed using MorphoJ v1.03d (Klingenberg, 2011), and PCA scores were extracted for further analyses (see below) using the Geomorph package (Adams & Otarola-Castillo, 2013) in R (R Core Team, 2014). We retained the

first two principal components for all classes of data as they are used in the gap morphological analysis (see below). The morphological data are deposited in the MorphoBank database.

We inferred gaps in morphology for the three types of data (morphometric, meristic and head shape) as described in Zapata & Jimenez (2012). This method uses the multivariate morphological space derived by a PCA to estimate a ridgeline manifold, the corresponding probability density function (PDF), and ellipsoids of tolerance regions for each pair of samples to test for discontinuities in phenotypic values. We assumed normality for the three classes of morphological data, and used the principal components on correlation (for measurements and counts) and covariance (for head shape data) matrices as mentioned above. The ridgeline manifold is a surface image that includes the main characteristics (e.g. peaks and saddles) of a PDF in a mixed distribution and identifies the number of modes (Ray & Lindsay, 2005). A mixed distribution is used to model the multivariate data in a set of two components (two groups of samples) that might have more than one mode. If the ridgeline manifold of a PDF suggests that there is more than one peak for different values of a variable α (which varies from 0 at the multivariate mean of one component, to 1 at the multivariate mean of the other), then one can infer two modes and a gap in morphological space (Zapata & Jimenez, 2012).

When the PDF along the ridgeline manifold exhibits two modes, ellipsoids of tolerance regions for each component are estimated with different values of β (a proportion of the multivariate distribution which varies from 0 to 1), and at fixed confidence level of 0.95 (Krishnamoorthy & Mondal, 2006; Krishnamoorthy & Mathew, 2009). Each tolerance region ellipsoid shares a single point along the ridgeline manifold (that corresponds to different values of α) with another ellipsoid that defines a tolerance region for the other distribution (Zapata & Jimenez, 2012). Overlap of these ellipsoids for different proportions β and values α along the ridgeline manifold can be visualized in a plot that shows the estimated phenotypic overlap between two samples. Following Wiens & Servedio (2000), we selected an *a priori* frequency cutoff of 10%, below which overlap of phenotypic values between samples indicates negligible gene flow. In other words, if the overlap in a plot is greater than $\beta = 0.9$, then the hypothesis that the sample of multivariate phenotypic values represents two taxa is supported.

Statistical analyses were performed using R packages ellipse (Murdoch & Chow, 2007), labdvs (Roberts, 2007), and mvtnorm (Genz *et al.*, 2009). Although *Liolaemus insolitus* and *L. poconchilensis* are recognized as distinct species, they overlapped in most meristic data (see below) suggesting that pooling morphological data is justified. Additionally, sample sizes were small for *Liolaemus insolitus* and *L. poconchilensis*, hence data for these two species were pooled to compare with a similar taxon (Nazca).

Distributional models and niche identity tests

We used bioclimatic variables from the WorldClim v1.4 dataset with a resolution of 2.5 min (Hijmans *et al.*, 2005) and to avoid over-parameterization of downstream analysis, we chose nine out of 19 variables that were not correlated with each other (Pearson coefficient $|r| < 0.7$). Bioclimatic variables were derived from monthly temperature and precipitation layers (Hijmans *et al.*, 2005). Occurrence points without duplicates are: 13 for Nazca, ten for Abra Apacheta, 12 for *L. robustus*, 22 for *L. polystictus*, 22 for Abra Toccto, nine for (*L. melanogaster* + *L. williamsi*), nine for *L. ortizi*, and 11 for *L. thomasi* (Supporting Information, Appendix S5).

To visualize potential niche divergence between populations and species in the northernmost species of the *Liolaemus montanus* group we conducted a PCA using bioclimatic data derived from occurrence points. We then used the maximum entropy model implemented in the program MAXENT v3.3.3e (Phillips, Anderson & Schapire, 2006) to estimate potential distribution of lineages in the northernmost species of the *Liolaemus montanus* group. MAXENT generates distributional models (or ecological niche models; ENMs) using presence-only records, contrasting them with background/pseudoabsence data sampled from the remainder of the study area. We chose this approach because of its overall better performance with presence-only data and with small sample sizes (Elith *et al.*, 2006). Because of small sample sizes some species occurrence points were pooled with closely related species (*L. melanogaster* + *L. williamsi*) enabling ENM development, but we were unable to develop ENMs for *L. insolitus* and *L. poconchilensis* because they are not hypothesized to be closely related.

Layers were trimmed to the areas surrounding each species or sample of populations that might represent candidate species, and then projected over a larger region that represents the whole geographic range of Peruvian species of the *Liolaemus montanus* group: $-10.793°$ to $-18.543°$ and $-75.423°$ to $-70.009°$.

For model calibration we used the default settings, but with a regularization multiplier of 2 to reduce overfitting (Radosavljevic & Anderson, 2014), with 1000 iterations, and the minimum training value averaged over the ten replicates as threshold with the default convergence threshold (10^{-5}). Due to our

small samples sizes, we used the cross-validation option with ten replicates for model calibration and evaluation, and averaged the results to estimate species niche and distributions. For model testing, we used occurrence points of closely related species (e.g. *Liolaemus thomasi* for *L. ortizi* and vice versa), or clades (e.g. *L. melanogaster* + *L. williamsi* for Abra Toccto and vice versa). We then used the area under the curve (AUC) to summarize the model's ability to rank presence localities higher than a sample of random pixels (Peterson *et al.*, 2011). AUC values ≤ 0.5 correspond to predictions that are equal or worse than random. AUC values > 0.5 are generally classed into: (1) poor predictors (0.5–0.7); (2) reasonable predictors (0.7–0.9); and (3) very good predictors (> 0.90; but see Peterson *et al.*, 2011, for caveats on use of AUC in presence/background data). Model clamping (the process by which variables are constrained to remain within the range of values in the training data) was checked with the 'fade by clamping' option available in MAXENT v 3.3.3e.

Finally, the Schoener's *D* metric was used as a measure of 'niche similarity' between pairs of populations (or species), and was estimated using the ENMTOOLS package (Warren, Glor & Turelli, 2010). We calculated these values by comparing the climatic suitability of each grid cell in the projected area obtained with MAXENT. This similarity measure ranges from 0 (niche 'envelopes' have no overlap) to 1 (niche 'envelopes' identical; Warren, Glor & Turelli, 2008). We estimated similarity measures and then tested whether the ENMs for two populations or species are 'identical' using the niche identity test in ENMTOOLS. One hundred randomly resampled pseudoreplicate data sets were generated to obtain a distribution of *D* scores under the null hypothesis that niche envelopes are random, and we reject the hypothesis of niche identity when the empirically observed value for *D* is significantly lower than the values expected from the pseudoreplicated data set (Warren *et al.*, 2010).

Gaussian clustering

For a small dataset of adults ($N = 20$ individuals) we used GC for our combined multilocus molecular, morphological (morphometric and meristic), and bioclimatic data. Most species and candidate species are known only from one or two localities, and bioclimatic data were redundant for most individuals within a locality, limiting the number of individuals that could be used for this method. We used the same individual for all datasets in most cases, but when this was not possible, we used another conspecific individual from the same locality. We used the same measurement and count variables as above, but two categorical variables were added: keeling in dorsal scales (absent/weak/strong), and enlarged ciliary scales (absent/present). We also used the 19 bioclimatic variables that were downloaded for each individual as mentioned above.

Euclidian and Gower distances were calculated for environmental and morphological data, respectively, using the cluster package in R (Maechler *et al.*, 2015). Genetic distances were estimated using MEGA v. 6.06 (Tamura *et al.*, 2013) with a Jukes–Cantor correction to account for multiple substitutions with substitution rates among sites following a Gamma distribution, and a Gamma parameter of 1. Genetic distances for individual loci were divided by mean pairwise distance to account for differences in substitution rates among loci, and individual distances were averaged across loci. Distance matrices for each data type were standardized using nonmetric multidimensional scaling (NMDS) using the MASS package (Venables & Ripley, 2002). We followed the recommendations of Hausdorf & Hennig (2010) and chose four NMDS dimensions because these had stress values below 10% for each dataset, and were considered to be accurate estimates of clusters (but see Discussion). We concatenated the four NMDS dimensions of each dataset and estimated species groups using GC with the number of clusters determined by the Bayesian Information Criteria (BIC), using the mclust package (Fraley & Raftery, 2002). Noise (outliers) in the NMDS data was detected by the 'noise' estimator in prabclus (Hennig & Hausdorf, 2015), and for this we chose a tuning constant of 2 to detect clusters with few individuals.

Integrative taxonomic procedure

Assuming a General Lineage Concept (de Queiroz, 1998, 2007) and using molecular, morphological and niche envelope differences as criteria to delimit species, we implemented a step-by-step approach to evaluate four hypothesized alternatives of species limits in the northernmost taxa of the *Liolaemus montanus* group. We then used our time-calibrated concatenated and species tree analyses, as well as the model-based GC approach, to further evaluate our step-by-step results.

Step-by-step approach

First, field collected and museum specimens were initially identified and grouped based on type material and species descriptions. When a sample could not be assigned to any known species (e.g. Abra Toccto and Nazca), it was referred to by the name of the locality where it was first discovered. Nominal species and populations were then used as our primary species hypotheses. Second, we used the mtDNA

gene tree to identify the number of well-supported haploclades, and then used this topology to estimate interspecific tree distances between these groups. We tested for significant deviation of these groups under the null model of random coalescence using Rosenberg probabilities, and offered alternate species hypotheses from this test. Third, we used our morphological analyses to test the hypothesized species limits obtained in this second step, and last, we used the niche similarity test to evaluate the species hypotheses resolved in the second and third steps. Finally we integrated all evidence and designated candidate species.

Species tree and dating analyses

Relationships in our mitochondrial gene tree were evaluated using the time-calibrated concatenated tree and the multilocus species tree. These multilocus analyses were implemented to provide a plausible history of the group, and to incorporate this history as an integral part of the SDL approach.

Comparison with Gaussian clustering and final delimitation

We compare our previous results with those derived from the GC analyses, to further test the proposed candidate species based on the mitochondrial tree, and results from the time-calibrated concatenated and species tree analyses. This procedure leads to our best-supported species hypotheses, and also highlights the incongruence among evidence and methods (see Table 3 and Discussion).

RESULTS

PRIMARY SPECIES HYPOTHESES

In total 302 specimens were examined (Supporting Information, Appendix S3) and five primary species hypotheses are proposed. Three primary species hypotheses correspond to samples that could not be assigned to any known species (Abra Apacheta, Abra Toccto and Nazca; see Integrative Taxonomy, for further details). A fourth sample is slightly different from *Liolaemus robustus* and we call it *L. robustus* 'Minas Martha'. One paratype of *L. polystictus* and our collected sample from the same locality are different from the holotype (and topotypes), and we call it *L. polystictus* 'Castrovirreyna'. Species limits between these two last populations, *L. robustus* and *L. polystictus* will be treated in a separate paper.

MITOCHONDRIAL TREE

Our mitochondrial tree recovers all populations and all named species as monophyletic groups with high posterior probability (pp) support (= 1, Fig. 2) with the exception of *Liolaemus polystictus* and *L. annectens*; *L. polystictus* is well resolved as paraphyletic to Abra Apacheta with the structure: (*L. polystictus* 'Castrovirreyna' (*L. polystictus* + Abra Apacheta)) with nodal support value of pp = 0.98 (Fig. 2). This clade is the sister clade (pp = 1) to (*L. robustus* + *L. robustus* 'Mina Martha') (pp = 1). This larger clade is in turn the sister group (pp = 1) of a [Abra Toccto (*L. melanogaster* + *L. williamsi*)] clade (pp = 0.98), which we refer to as the *L. robustus* clade. This group is the sister clade to a (*L. signifier* (*L. annectans* 'Lampa' (*L. annectans* + *L. etheridgei*))) clade (pp = 1 at the stem and all internal nodes). This large clade then forms an unresolved polytomy (pp < 0.9) with these other well supported clades: (*L. ortizi* + *L. thomasi*), *L. dorbignyi*, (*L. andinus* + *L. famatinae*), and (Nazca); pp = 1.0 for nodes of the three clades represented by two or more terminals. External to this larger clade is an unresolved polytomy with *L. insolitus* and two individuals of *L. poconchilensis*.

DIVERGENCE ESTIMATES, CONCATENATION AND SPECIES TREE PHYLOGENIES

Our concatenated (CT) and species tree (ST) analyses recovered topologies similar to the mtDNA gene tree, but with fewer strongly supported nodes and fewer paraphyletic terminals. Further, some relationships at deep nodes are more strongly supported in the ST relative to the CT (Fig. 3A, B; the complete tree of the dating analysis is shown in Supporting Information, Appendix S6). The CT (Fig. 3A) resolves the following clades with strong support: (*L. poconchilensis*), (Nazca), (*L. ortizi* + *L. thomasi*), (*L. williamsi* + *L. melanogaster*), (Abra Toccto), (*L. robustus*) and the *L. robustus* clade: (((*L. willliamsi* + *L. melanogaster*) + Abra Toccto) + (Abra Apacheta (*L. polystictus* (*L. polystictus* 'Castrovirreyna'))) + *L. robustus*).

In contrast, the ST recovers the two most deeply nested nodes with strong support, including (*L. poconchilensis* + (Nazca + *L. insolitus* + all Andean clades)) confirming paraphyly of the lowland groups. The Andean clade is not strongly supported, but well-supported nested clades include: the large ((*L. robustus* clade) + (*L. signifier* + (*L. annectans* + *L. etheridgei*))) and external to this clade is a strongly supported (*L. ortizi* + *L. thomasi*) clade.

Our time-calibrated analysis corroborates this topology in suggesting that Andean taxa originated in the Pleistocene (< 3 Myr), and the older low-elevation lineages having a Pliocene (5–3 Mya) origin, albeit there is extensive overlap in the highest posterior density (HPD) error bars of these estimates (Fig. 3A).

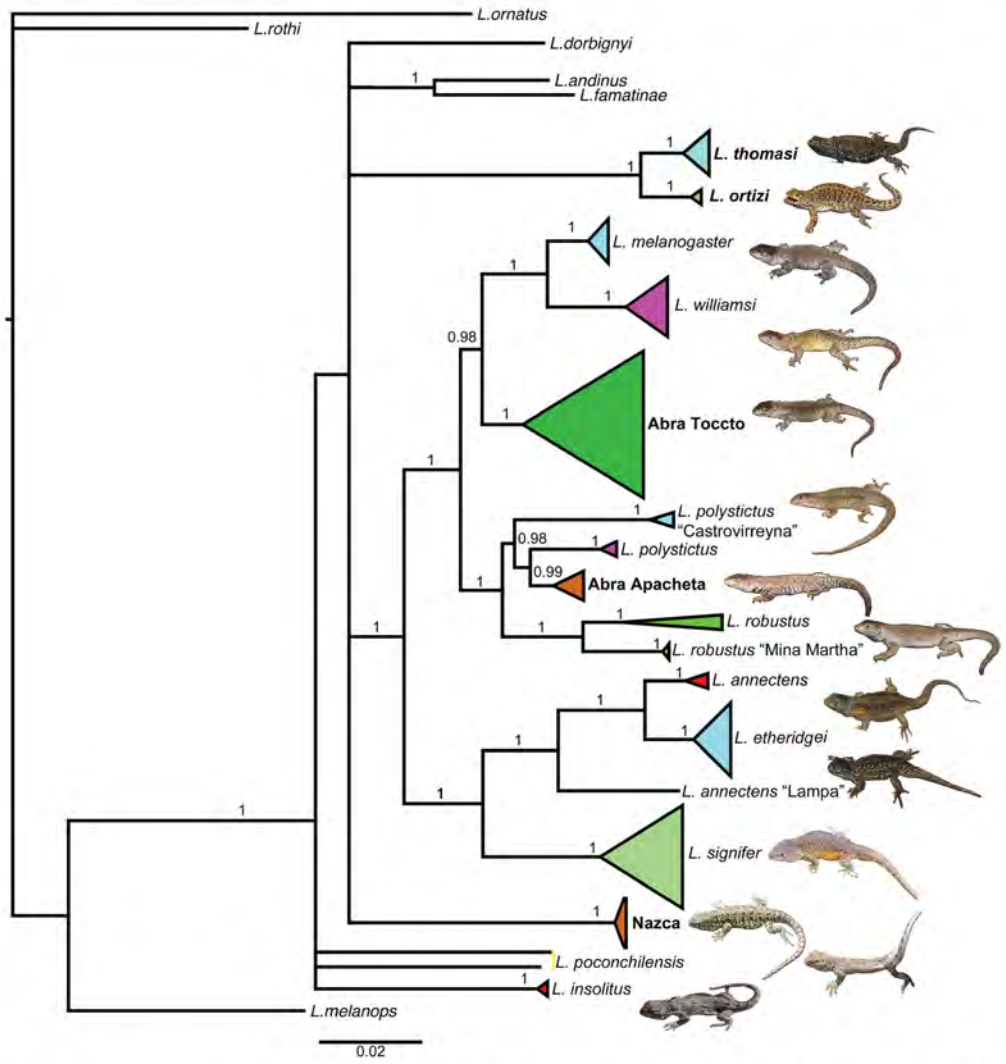

Figure 2. Bayesian mitochondrial gene tree (cyt-*b* and 12S) showing the relationships of northernmost species of the *Liolaemus montanus* group. Numbers on branches are posterior probability (PP) support values (values lower than 0.95 are not shown). The size of triangles is proportional to the sample size (see Supporting Information, Appendix S2). Focal taxa are in bold.

INTERCLADE DISTANCE AND ROSENBERG'S PROBABILITY

All interclade tree distances (ITD) show values equal or higher than 0.03 with the exception of *Liolaemus ortizi* and *L. thomasi* (Table 2). ITD between all combinations of lowland taxa (Nazca, *L. insolitus*, *L. poconchilensis*) are equal to or higher than 0.09. The Abra Toccto clade has ITD values of 0.05 and 0.06 with *L. melanogaster* and *L. williamsi*, respectively. The ITD between Abra Apacheta and *L. polystictus* is 0.03, between (*L. polystictus* 'Castrovirreyna' (Abra Apacheta + *L. polystictus*)) and *L. robustus* is 0.06. Rosenberg

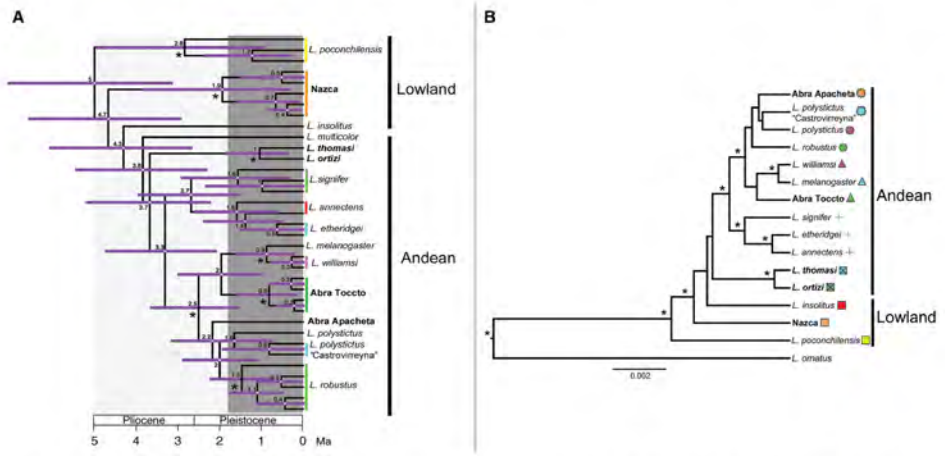

Figure 3. Concatenated time-calibrated (A) and species (B) trees showing the relationships among the northernmost species of the *Liolaemus montanus* group. In (A) and (B) asterisks are equal to posterior probabilities ≥ 0.95. In (A) number above branches and purple horizontal bars are means and 95% confidence intervals for node ages respectively. Focal taxa are in bold.

Table 2. Interspecific tree distances (ITD) and Rosenberg's probabilities *P*(*AB*) based on mitochondrial markers between focal taxa and selected northernmost species of the *L. montanus* group

Species	Closest species	ITD	Rosenberg's *P*(*AB*)
L. thomasi	*L. ortizi*	0.02	0.03
Abra Apacheta	*L. polystictus*	0.03	0.05
L. melanogaster	*L. williamsi*	0.03	1.98E-03
L. annectens	*L. etheridgei*	0.03	1.00E-02
L. melanogaster	Abra Toccto	0.05	6.20E-07
L. williamsi	Abra Toccto	0.06	1.98E-03
L. robustus	*L. polystictus**	0.06	6.00E-04
L. etheridgei	*L. signifer*	0.08	5.10E-06
L. insolitus	***L. poconchilensis***	**0.09**	**1.40E-05**
Nazca	***L. insolitus***	**0.11**	**5.00E-09**
Nazca	***L. poconchilensis***	**0.11**	**4.60E-04**

The bold rows indicate 'lowland' from all Andean taxa. *L. polystictus** includes the clade (*L. polystictus* "Castrovirreyna" (Abra Apacheta + *L. polystictus*)).

probabilities are small (i.e. reject the null hypothesis of random monophyletic groups at $P \leq 0.01$) for all pairwise comparisons except for *Liolaemus ortizi* vs. *L. thomasi*, and Abra Apacheta vs. *L. polystictus* (Table 2).

MORPHOLOGICAL GAP ANALYSES

In this section, we show the most relevant results, but see Supporting Information (Appendix S4) for the remaining gap analyses. In all cases, ellipsoids of tolerances regions at fixed confidence level of 0.95 overlapped below the frequency cutoff of 10% (Figs 4C, F, 6C, F; Supporting Information, Appendix S4). Morphometric and head shape gap analyses show one mode between Abra Apacheta and *Liolaemus polystictus* (Supporting Information, Appendix S4), whereas meristic gap analyses show two modes between these groups (Fig. 4A, B).

In gap analyses of morphometric and meristic data, *Liolaemus ortizi* and *L. thomasi* showed one mode (Supporting Information, Appendix S4), but two modes with the shape data (females only, Fig. 4D, E).

In gap analyses of morphometric, meristic and head shape data, Abra Toccto showed one mode with either *Liolaemus melanogaster* (Fig. 5A–F) or *L. williamsi* (Supporting Information, Appendix S4).

In gap analyses of meristic data, Nazca showed one mode with either *Liolaemus insolitus* or *L. poconchilensis*, (Supporting Information, Appendix S4) but two modes with each species in our gap analyses of the morphometric (*L. insolitus* and *L. poconchilensis* data were pooled; Supporting Information, Appendix S4) and head shape data (Fig. 6A–E).

In gap analyses of morphometric and head shape data, Nazca also showed one mode with either *Liolaemus ortizi* or *L. thomasi*, but two clear modes with each species in our gap analyses of the meristic data (Supporting Information, Appendix S4).

In gap analyses of morphometric, meristic and head shape data, Nazca showed one mode with

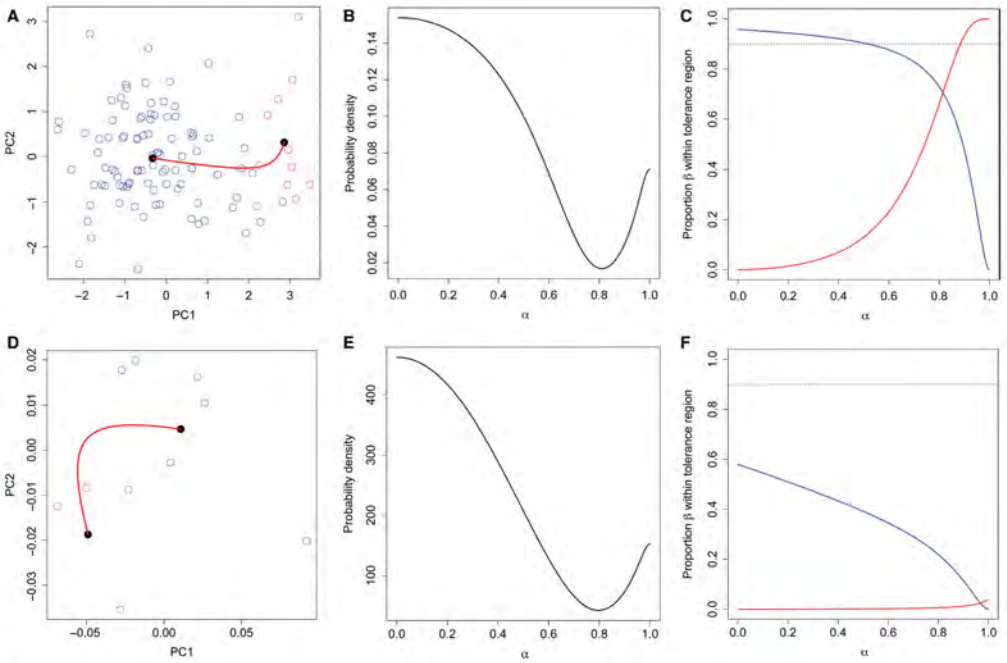

Figure 4. Inference of gaps between Abra Apacheta (red) and *Liolaemus polystictus* (blue) based on meristic data (A–C), and *L. thomasi* (red) and *L. ortizi* (blue) based on head shape data (D–F). A and D, show principal components 1 and 2, estimated multivariate means (black dots) and the ridgeline manifold (red continuous line). B and E, show the estimated probability density function evaluated at various points along the ridgeline manifold (α); note that the plot is bimodal. C and F, shows the estimated proportion β covered by tolerance regions sharing a single point at α in the ridgeline manifold; note that tolerance regions overlap below the frequency cutoff of 0.9 (horizontal dotted line).

Liolaemus robustus (Supporting Information, Appendix S4). In gap analyses of morphometric and meristic data, Nazca showed one mode with *L. polystictus*, but two clear modes with this species in our gap analyses of head shape data (Supporting Information, Appendix S4).

In gap analyses of morphometric and head shape data, Nazca showed one mode with Abra Apacheta, but two clear modes with this population in our gap analyses of meristic data (Supporting Information, Appendix S4).

In gap analyses of morphometric, meristic and head shape data, Nazca showed one mode with Abra Toccto (Supporting Information, Appendix S4). In gap analyses of head shape data, Nazca showed one mode with *L. williamsi*, but two modes with this species in our gap analyses of morphometric and meristic data (Supporting Information, Appendix S4).

In gap analyses of meristic data, Nazca showed one mode with *L. melanogaster*, but two modes with this species in our gap analyses of morphometric and head shape data (Supporting Information, Appendix S4).

Distributional models and niche identity tests

The first two principal components (PC) of the bioclimatic variables explained 99.7% of the variance in the data. The variables (Supporting Information, Appendix S5) contributing to most of the variation in both PCs are Temperature Seasonality (BIO4) and Annual Precipitation (BIO12). The PC plot (Supporting Information, Appendix S5) shows a clear break between lowland (Nazca, *Liolaemus poconchilensis* and *L. insolitus*) and Andean taxa (Abra Apacheta, Abra Toccto, *L. melanogaster*, *L. ortizi*, *L. polystictus*, *L. robustus*, *L. robustus* from Minas Martha, *L. thomasi* and *L. williamsi*).

All distributional models show AUC values > 0.90 with the exception of *Liolaemus ortizi* (AUC = 0.7284). Projections of niche models are shown in Supporting

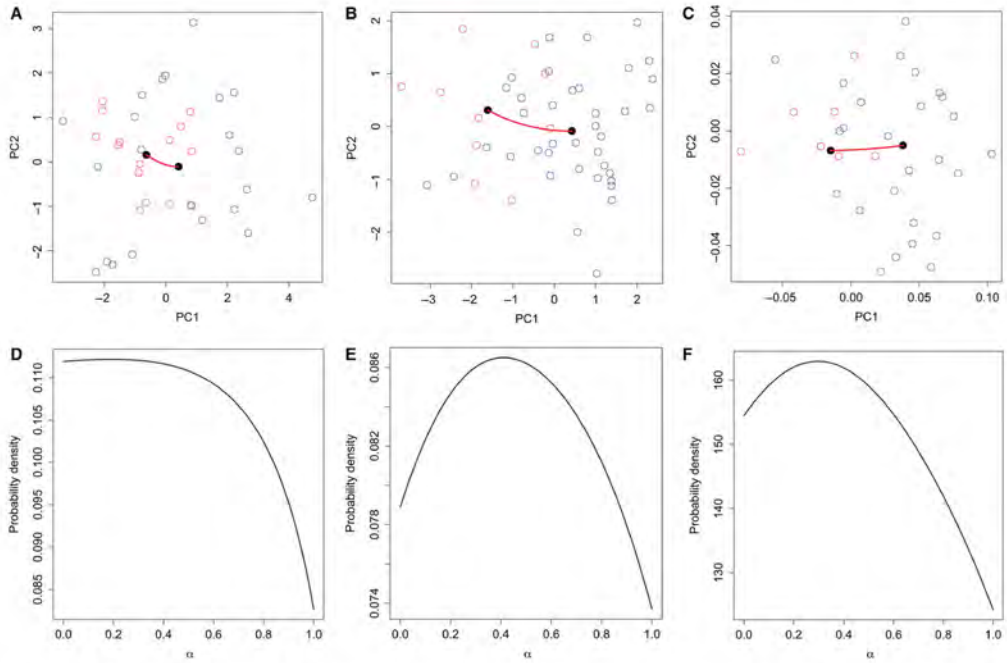

Figure 5. Gap analyses between *Liolaemus melanogaster* (red) and Abra Toccto (blue) based on morphometric (A, D), meristic (B, E) and head shape data (C, F). A–C, show principal components 1 and 2, estimated multivariate means (black dots) and ridgeline manifold (red continuous line) for each class of data. D–F, show the estimated probability density function evaluated at various points along the ridgeline manifold (α) for each class of data; note that in all cases the plot is unimodal.

Information (Appendix S5). Niche identity tests show that the observed Schoener's *D* metric of Abra Apacheta vs. *L. polystictus* (Fig. 7A), and of *L. ortizi* vs. *L. thomasi* (Fig. 7B) fall within the distribution of the pseudoreplicates, i.e. niche envelopes do not differ in either comparison. In contrast, niche identity tests show that the observed Schoener's *D* metric of Abra Toccto vs. (*L. melanogaster* + *L. williamsi*) (Fig. 7C) fall outside the distribution of the pseudoreplicates, i.e. niche envelopes differ between these lineages.

Gaussian clustering

NMDS stress values for each data type were below 5%. The best model (BIC = −246.5591) had six clusters: (1) Nazca; (2) *Liolaemus poconchilensis*; (3) *L. ortizi*, *L. thomasi* and *L. annectens*; (4) *L. melanogaster*, *L. williamsi*, *L. polystictus*, Abra Apacheta, and *L. signifer*; (5) Abra Toccto and *L. robustus* 'Mina Martha'; and (6) *L. polystictus* 'Castrovirreyna'. Taxa and number of individuals identified as noise were *L. insolitus* (1), *L. robustus* (2), and *L. etheridgei* (1). Using the step-by-step approach as a benchmark, 69% of the individuals were correctly identified.

Integrative taxonomy

Table 3 shows candidate species delimited through the step-by-step, concatenation, species tree analysis, and Gaussian clustering, and our consensus delimitation proposal. We summarize each final delimitation case below.

Abra Apacheta

Two individuals (one male adult and one juvenile) from Abra Apacheta were included as part of the paratype series in the species description of *Liolaemus melanogaster* (Laurent, 1998), but this locality is geographically closer to *L. polystictus* (Fig. 1). When these paratypes are compared with our collected samples, our primary hypothesis is that

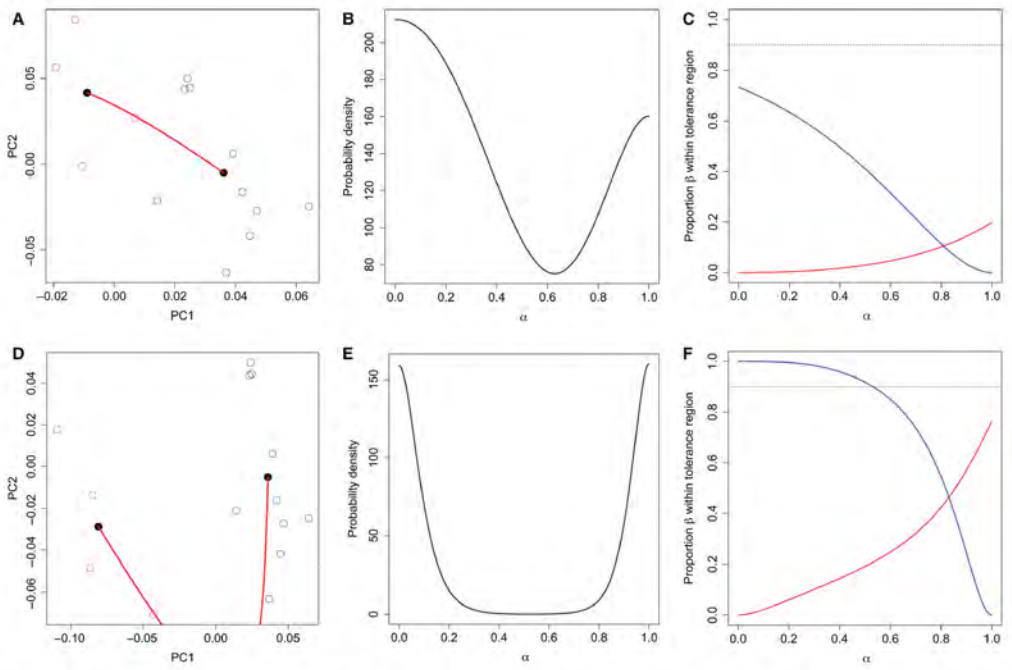

Figure 6. Inference of gaps based on head shape data between *Liolaemus insolitus* (red) and Nazca (blue) (A–C), and between *L. poconchilensis* (red) and Nazca (blue) (D–F). A and D, show principal components 1 and 2, estimated multivariate means (black dots) and ridgeline manifold (red continuous line). B and E, show the estimated probability density function evaluated at various points along the ridgeline manifold (α); note that the plot is strongly bimodal. C and F, show the estimated proportion β covered by tolerance regions sharing a single point at α in the ridgeline manifold; note that tolerance regions overlap below the frequency cutoff of 0.9 (horizontal dotted line).

Liolaemus individuals from this locality represent a population that cannot be assigned to *L. melanogaster*, *L. polystictus* or any known species. We identified this population 'Abra Apacheta' and the mtDNA gene tree recovers Abra Apacheta as the sister clade to *L. polystictus* (pp = 0.99), and distant from *L. melanogaster* by five strongly supported nodes (Fig. 2). Interclade tree distance (ITD) between Abra Apacheta and *L. polystictus* is similar to ITD between *L. melanogaster* and *L. williamsi* (0.03) from type localities, and lower than for all other pairs except for *L. ortizi* and *L. thomasi* (Table 2). Conversely, Rosenberg's probability is not significant between Abra Apacheta and *L. polystictus* suggesting that separation of these taxa is random (Table 2).

Gap analyses of meristic data reveal separation in the multivariate space between Abra Apacheta and *Liolaemus polystictus*, but there is overlap in their tolerance regions (Fig. 4A–C), and niche identity tests give an Abra Apacheta–*L. polystictus* Schoener's value within the distribution of the pseudoreplicate values (Fig. 7A). The CT and ST analyses recover Abra Apacheta grouped with *L. polystictus* 'Castrovirreyna', *L. polystictus* and *L. robustus*, but without significant support (Fig. 3A, B). Gaussian clustering of the concatenated four dimensions of each data set groups Abra Apacheta with *L. polystictus*, *L. williamsi* and *L. melanogaster*. Almost all available evidence suggests that Abra Apacheta should be a considered a distinct lineage related to (or conspecific with) *L. polystictus*, but not conspecific with *L. melanogaster* (Table 3).

Liolaemus thomasi

This species was described from a single specimen (Laurent, 1998), and is geographically close to *L. ortizi* (Fig. 1). However, our primary species hypothesis is that our collected topotypes should be considered *L. thomasi*. The mtDNA gene tree recovers *L. ortizi* and *L. thomasi* as distinct haploclades each

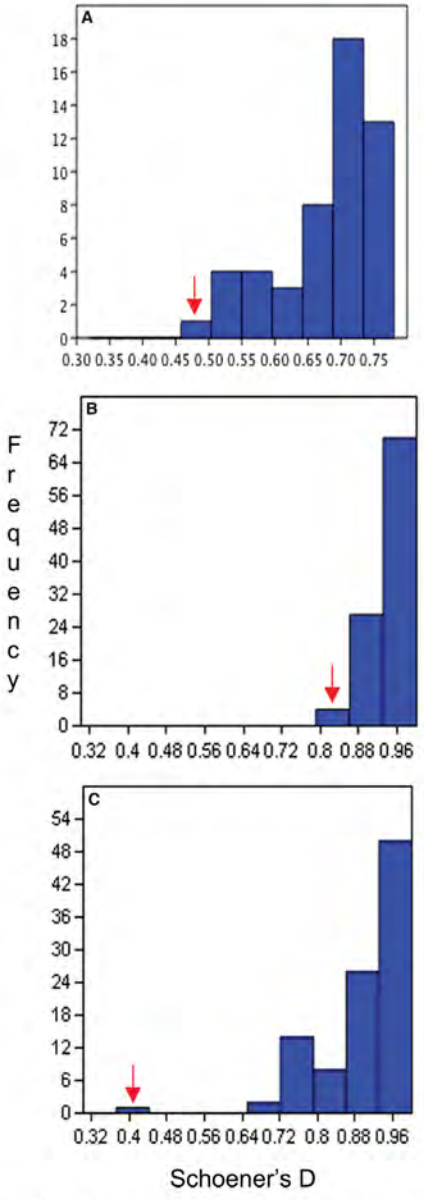

Figure 7. Histograms of the niche identity tests showing the observed Schoener's *D* values (red arrow) and frequencies of pseudoreplicates: (A) Abra Apacheta vs. *Liolaemus polystictus*, (B) *L. ortizi* vs. *L. thomasi*, (C) Abra Toccto vs. (*L. melanogaster* + *L. williamsi*).

with strong support and also as sister groups, but with the lowest ITD and Rosenberg's probability was not significant (Fig. 2, Table 2). Morphological gap analyses of shape data separate *L. thomasi* and *L. ortizi* in multivariate space, but with overlap in their tolerance regions (Fig. 4D–F), and the niche identity test recovers a Schoener's value between these species within the distribution of the pseudoreplicate values (Fig. 7B). The CT and ST analyses recover *L. thomasi* and *L. ortizi* as sister clades with high support (Fig. 3). Gaussian clustering of the concatenated four dimensions of each data set groups *L. thomasi* with *L. ortizi*, but also with *L. annectens*. In summary, all available evidence suggests that *L. thomasi* should either be considered a distinct lineage or conspecific with *L. ortizi*.

Abra Toccto

Our primary species hypothesis is that field collected and museum specimens of this locality form a distinct population. The mtDNA gene tree recovers the Abra Toccto samples as a well supported haploclade (pp = 1.0), and sister group to a *L. melanogaster* + *L. williamsi* clade (pp = 0.98; Fig. 2). This lineage also has a larger ITD with both *L. melanogaster* and *L. williamsi* than the ITD between these two last taxa, and significant Rosenberg probabilities separating it from these two species (Table 2). Gap analyses of morphometric, meristic and head shape data does not reveal any separation in multivariate space between Abra Toccto and *L. melanogaster*, and Abra Toccto and *L. williamsi* (Fig. 5). Niche identity tests give a Schoener's value for Abra Toccto vs. (*L. melanogaster* + *L. williamsi*) which falls outside of the pseudoreplicate values (Fig. 7C).

CT analysis recovers all Abra Toccto individuals as a strongly supported clade, and these are also recovered in the ST analysis (Fig. 3B). However, in both analyses there is only weak support for Abra Toccto as the sister group to the (*L. melanogaster* + *L. williamsi*) clade (pp < 0.9 in both; Fig. 3). Gaussian clustering of the concatenated four dimensions of each data set shows that Abra Toccto forms a distinct group from *L. melanogaster* and *L. williamsi*, but it also grouped with *L. robustus* 'Minas Martha'. In this example, niche identity tests and all phylogenetic and species tree analyses suggest that Abra Toccto is an independent lineage.

Nazca

Our primary species hypothesis is that field collected and museum specimens from Nazca form a distinct population. The mtDNA gene tree recovers all Nazca individuals as a clade with high support, and it falls outside of the well supported clade that includes all other taxa and populations of our ingroup (Fig. 2).

Table 3. Summary of species limits inferences from the step-by-step approach, multilocus divergence time and species tree, Gaussian clustering and final delimitation grouping

	Step-by-step approach						
Species boundary issue	Mitochondrial, tree distances and Rosenberg's probabilities	Morphological gap analysis	Niche identity test	Candidate species	Species/divergence time tree	Gaussian clustering	Final delimitation
Is Abra Apacheta part of *L. melanogaster* or *L. polystictus*?	*L. polystictus*	Uninformative	*L. polystictus*	*L. polystictus*	Abra Apacheta	Uninformative	Abra Apacheta/*L. polystictus*
Is *L. thomasi* a distinct lineage or conspecific with *L. ortizi*?	*L. ortizi*	Uninformative	*L. ortizi*	*L. ortizi*	*L. thomasi*	Uninformative	*L. ortizi*/*L. thomasi*
Is Abra Toccto a distinct lineage?	Abra Toccto	Uninformative	Abra Toccto	Abra Toccto	Abra Toccto	Uninformative	Abra Toccto
Is Nazca a distinct lineage?	Nazca	Uninformative	Not performed	Nazca	Nazca	Nazca	Nazca

Further, CT and ST analyses recover this clade well outside of strongly supported more nested clades, although fewer of these nested nodes have significant support in the concatenated than in the species tree (Fig. 3A, B). This sample also has a larger ITD in comparison with other old lowland *Liolaemus* (*L. insolitus* and *L. poconchilensis*, Table 2), and significant Rosenberg probabilities with both *L. insolitus* and *L. poconchilensis* (Table 2). Morphological gap analyses show a separation in the multivariate head shape space between Nazca and *L. insolitus*, and Nazca and *L. poconchilensis*, but with overlap in the tolerance regions of both paired tests (Fig. 6). There are also two modes in multivariate meristic space between Nazca vs. *L. ortizi*, *L. thomasi*, Abra Apacheta and *L. williamsi* (Supporting Information, Appendix S4); two modes in multivariate head shape space between Nazca vs. *L. polystictus* and *L. melanogaster* (Supporting Information, Appendix S4); and two modes in multivariate morphometric space between Nazca vs. *L. williamsi* and *L. melanogaster* (Supporting Information, Appendix S4). However, overlap in tolerance regions is present in all paired tests (Supporting Information, Appendix S4). Gaussian clustering of the concatenated four dimensions of each data set shows that Nazca forms a distinct group from all other species and populations. Most available evidence and methods (mitochondrial, concatenated, species trees and Gaussian clustering) suggest that Nazca is an independent lineage.

DISCUSSION

Robust hypotheses of species boundaries come from the inference of using multiple operational (empirical) criteria (Leavitt *et al.*, 2015). Different operational criteria emphasize the many contingent properties (monophyly, differences in morphological features, ecological niches, etc.) of diverging populations associated with the various evolutionary processes operating in various geographic contexts (de Queiroz, 2005a; Camargo & Sites, 2013). In contrast, using a single empirical criterion might artificially reduce the complexity of evolving lineages (de Queiroz, 2005b). In addition, the General Lineage Concept (de Queiroz, 1998, 2007) explicitly recognizes a 'grey zone' or fuzzy boundary where populations in various stages of divergence have not fully completed a speciation process, and under which all methods for delimiting species will occasionally fail or be discordant with each other (Sites & Marshall, 2003, 2004). However, an IT approach can provide evolutionary explanations for discordant species criteria and uncover complex evolutionary histories (Dejaco *et al.*, 2016; Karanovic, Djurakic & Eberhard, 2016).

Here we used different delimitation criteria within an integrative taxonomy framework to test for species limits in the northernmost lineages of the *Liolaemus montanus* group. We have found that the Abra Apacheta population, previously recognized as conspecific with *L. melanogaster*, is part of a different clade. In this case, the mitochondrial tree, Rosenberg probability and niche identity tests recover Abra Apacheta as conspecific with *L. polystictus*. In the same way, the mitochondrial tree distance, Rosenberg probability and niche identity tests recover *L. thomasi* as conspecific with *L. ortizi*. However, in both of these comparisons, relationships are not congruent (or not supported by) the concatenated and species tree analyses. This incongruence between data sets can reflect intricate evolutionary histories and can be explained considering Abra Apacheta as well as *L. thomasi* representing 'grey zone' lineages that have split from a common ancestor, but may not have fully diverged to the level of separate species. Although this is a limitation of IT approach to delimit species, it actually reflects the fact that speciation is a continuous process along different axes of divergence and for this reason some evolutionary entities will often be truly indistinct (Hey *et al.*, 2003; Nosil, Harmon & Seehausen, 2009; Huang & Knowles, 2016).

In contrast, the Abra Toccto and Nazca samples represent lineages at more advanced stages of speciation. Most empirical criteria and methods, particularly for Nazca, support these populations as distinct lineages. The Nazca population was also recovered as a significantly distinct group in the model-based GC algorithm, while Abra Toccto was not distinguished using this method. With the exception in the Nazca case, GC did not recover any other candidate species or isolated populations as distinct, even when they were recovered as separate lineages in our step-by-step, concatenated, and species tree methods. This lack of correspondence between GC and other approaches might be due to the small sample sizes we used for the four NMDS dimensions (1–3 individuals per species or population), in contrast to what is advised for this method (a minimum of five individuals; Hausdorf & Hennig, 2010).

Further, some populations or species are known from only single localities, thereby compromising the collection of sufficient bioclimatic, morphological or genetic data for this method. Additionally, GC might be better applied to closely related species or populations (species complex) than to taxa belonging to different species complexes, as is the case in our study (Edwards & Knowles, 2014; Hausdorf & Hennig, 2010). Moreover our results could simply be an idiosyncratic limitation of GC for this particular group of lizards, yet we still rely upon qualitative judgements of species boundaries in a hypothetico-deductive framework, even when IT model-based approaches are used (Sites & Marshall, 2004; Yeates *et al.*, 2011; Hausdorf & Hennig, 2010).

Our morphological gap analyses show different degrees of overlap using three different types of data [morphometric, meristic, and geometric morphometric (head shape)]. In these analyses Nazca, recovered as an older lineage in the time-calibrated concatenation analysis, shows the smallest degree of overlap among all of our paired gap analyses. Gap analyses between this taxon and lowland (*L. insolitus*, *L. poconchilensis*) and some Andean lineages, (*L. ortizi*, *L. thomasi*, *L. polystictus*, Abra Apacheta, *L. williamsi* and *L. melanogaster*) show two modes (Fig. 6, Supporting Information, Appendix S4) in comparison with the same analyses for other Andean taxa where a single mode is recovered (Figs 4, 5, Supporting Information, Appendix S4). However, tolerance regions overlapped between Nazca and these taxa probably due to small sample sizes. The general pattern here is that delimitation between the oldest lineages (4–5 Myr) and youngest lineages (1–2.5 Myr) in our gap analyses also show that, despite other criteria which clearly separate these lineages, morphological features commonly used in *Liolaemus* taxonomy do not differentiate taxa even when species appear to have had sufficient time to acquire morphological discontinuities. Alternatively, many species of *Liolaemus* may be under selective constraint, which is a particularly important point for taxonomic studies of *Liolaemus*, one of the most remarkable species-rich temperate lizards genera on earth. Until recently most species descriptions have been based only on gross comparisons of morphological features, and lacking statistical rigor (e.g. Cei & Péfaur, 1982; Laurent, 1982, 1990, 1992, 1998).

In contrast, the gap analyses we used here is probably one of the most comprehensive methods to detect species limits with morphological data and statistical rigor. It requires large samples sizes to infer no overlap (a gap) in the multivariate space of two taxa for 0.9 proportions of each statistical population (a surrogated for inferring limited gene flow) and at a confidence level of 95% (Zapata & Jimenez, 2012). Other univariate or multivariate methods that have been used to detect species limits with morphological data based on central tendencies (e.g. discriminant analyses, ANOVA) might have given statistically significant results, but they might not be appropriate as delimitation criteria for quantitative phenotypic characters. In an earlier study, we have shown that central tendency univariate methods for morphological characters might be misleading (even with statistically significant results) giving the

impression that a species have diverged to the point that diagnostic phenotypic characters have evolved (Aguilar *et al.*, 2013).

Although morphological gap analyses were uninformative for all four test of species boundaries in this study, ENMs and niche identity tests were useful to test species boundaries based on other lines of evidence (Fig. 7, Supporting Information, Appendix S5). However, the use of ENMs as non-heritable surrogates for ecological phenotypes in SDL studies has been questioned. Some researchers interpret these data as having limited (Tocchio *et al.*, 2014) or no relevance (Meik *et al.*, 2015). Whereas others show that ENMs provide an independent line of evidence in SDL studies and support of hypotheses based on heritable traits (e.g. Pelletier *et al.*, 2015; Huang & Knowles, 2016). We acknowledge the caution with which ENM data should be used in SDL studies, but these data might be useful as a proxy of some aspect of a species eco-physiological niche, and therefore relevant for studies of species boundaries (Warren, 2012).

We have shown, as have a growing number of previous studies in *Liolaemus* (Aguilar *et al.*, 2013; Medina, Avila & Morando, 2013; Medina *et al.*, 2014; Minoli, Morando & Avila, 2014; Breitman *et al.*, 2015), that an IT approach (together with evolutionary explanations in cases where different lines of evidence disagree) provides an empirically richer means of delimiting species, thereby improving the quality of species hypotheses, and associated descriptions.

ACKNOWLEDGEMENTS

We thank J. Córdova, C. Torres (MUSM), A. Resetar (FMNH), J. Losos, J. Rosado (MCZ), F. Glaw (ZSM), L. Welton and R. Brown (KU) for loans and accessions of specimens under their care. We thank Dr. D. Edwards for advice on Gaussian clustering, and C. Ramirez, C. Salas, A. Guzman, A. Mendoza, V. Vargas, F. Huari and J. C. Cusi for assistance in the fieldwork. We also thank an anonymous reviewer, J. A. Allen and C. L. Malone for improving with their comments a previous version of this paper. Fieldwork was supported by the Waitt Foundation-National Geographic Society (award W195-11 to CA and JWS), the BYU Bean Life Science Museum (JWS), and lab work by NSF-Emerging Frontiers award (EF 1241885 to JWS), Dr. C.G. Sites to JWS, and NSF-Doctoral Dissertation Improvement Grant (award #1501187 to JWS and CA). Permits (RD N° 1280-2012-AG-DGFFS-DGEFFS, RD N° 008-2014-MINAGRI-DGFFS-DGEFFS) were issued by the Ministerio de Agricultura, Lima, Peru, and the work was approved by the BYU Institutional Animal Care and Use Committee protocol number 12001 and in accordance with US law.

REFERENCES

Adams DC, Otarola-Castillo E. 2013. Geomorph: an R package for the collection and analysis of geometric morphometric shape data. *Methods in Ecology and Evolution* **4:** 393–399.

Aguilar C, Wood PL Jr, Cusi JC, Guzman A, Huari F, Lundberg M, Mortensen E, Ramirez C, Robles D, Suarez J, Ticona A, Vargas VJ, Venegas P, Sites JW Jr. 2013. Integrative taxonomy and preliminary assessment of species limits in the *Liolaemus walkeri* complex (Squamata, Liolaemidae) with descriptions of three new species from Peru. *ZooKeys* **364:** 47–91.

Aguilar C, Stark MR, Arroyo JA, Standing MD, Rios S, Washburn T, Sites JW Jr. 2015. Placental morphology in two sympatric andean lizards of the genus *Liolaemus* (Reptilia: Liolaemidae). *Journal of Morphology* **276:** 1205–1217.

Albino A. 2008. Lagartos iguanios del Colhuehuapense (MiocenoTemprano) de Gaiman (provincia del Chubut, Argentina). *Ameghiniana* **45:** 775–782.

Andújar C, Arribas P, Ruiz C, Serrano J, Gómez-Zurita J. 2014. Integration of conflict into integrative taxonomy: fitting hybridization in species delimitation of Mesocarabus (Coleoptera: Carabidae). *Molecular Ecology* **23:** 4344–4361.

Bouckaert R, Heled J, Kühnert D, Vaughan T, Wu C-H, Xie D, Suchard MA, Rambaut A, Drummond AJ. 2014. BEAST 2: a software platform for bayesian evolutionary analysis. *PLoS Computational Biology* **10:** e1003537.

Breitman MF, Avila LJ, Sites JW Jr, Morando M. 2011. Lizards from the end of the world: phylogenetic relationships of the *Liolaemus lineomaculatus* section (Squamata: Iguania: Liolaemini). *Molecular Phylogenetics and Evolution* **59:** 364–376.

Breitman MF, Bonino MF, Sites JW Jr, Avila LJ, Morando M. 2015. Morphological variation, niche divergence, and phylogeography of lizards of the *Liolaemus lineomaculatus* section (Liolaemini) from southern Patagonia. *Herpetological Monographs* **29:** 65–88.

Camargo A, Sites JW Jr. 2013. Species delimitation: a decade after the renaissance. In: Pavlinov IY, ed. *The species problem – ongoing issues*. Rijeka, Croatia: InTech – Open Access Publisher, 225–247.

Camargo A, Avila LJ, Morando M, Sites JW Jr. 2012. Accuracy and precision of species trees: effects of locus, individual, and base pair sampling on inference of species trees in lizards of the *Liolaemus darwinii* group (Squamata, Liolaemidae). *Systematic Biology* **61:** 272–288.

Cei JM, Péfaur JE. 1982. *Una especie nueva de Liolaemus (Iguanidae: Squamata): su sistemática, ecología y distribución*. Actas 8vo Congreso Latinoamericano de Zoología, Mérida, Venezuela, pp. 573–586.

Corl A, Davis AR, Kuchta SR, Comendant T, Sinervo B. 2010. Alternative mating strategies and the evolution of sexual size dimorphism in the side-blotched lizard, *Uta*

stansburiana: a population-level comparative analysis. *Evolution* **64:** 79–96.

Darriba D, Taboada GL, Doallo R, Posada D. 2012. jModelTest 2: more models, new heuristics and parallel computing. *Nature Methods* **9:** 772.

Dejaco T, Gassneri M, Arthoferi W, Schlick-Steineri BC, Steiner FM. 2016. Taxonomist's nightmare … evolutionist's delight: an integrative approach resolves species limits in jumping bristletails despite widespread hybridization and parthenogenesis. *Systematic Biology*. doi:10.1093/sysbio/syw003.

Drummond A, Suchard MA, Xie D, Rambaut A. 2012. Bayesian phylogenetics with Beauti and the Beast 1.7. *Molecular Biology and Evolution* **29:** 1969–1973.

Edgar R. 2004. MUSCLE: multiple sequence alignment with high accuracy and high throughput. *Nucleic Acids Research* **32:** 1792–1797.

Edwards D, Knowles LL. 2014. Species detection and individual assignment in species delimitation: can integrative data increase efficacy? *Proceedings of the Royal Society B* **281:** 20132765.

Elith J, Graham CH, Anderson RP, Dudik M, Ferrier S, Guisan A, Hijmans RJ, Huettmann F, Lethwick JR, Lehmann A, Li J, Lohmann LG, Loiselle BA, Manion G, Moritz C, Nakamura M, Nakazawa Y, McC OJ, Peterson AT, Phillips SJ, Richardson KS, Scachetti-Pereira R, Schapire RE, Soberon J, Williams S, Wisz MS, Zimmermann NE. 2006. Novel methods improve prediction of species' distributions from occurrence data. *Ecography* **29:** 129–151.

Fontanella F, Olave M, Avila LJ, Sites JW Jr, Morando M. 2012. Molecular dating and diversification of the South American lizard genus *Liolaemus* (subgenus *Eulaemus*) based on nuclear and mitochondrial DNA sequences. *Zoological Journal of the Linnean Society* **164:** 825–835.

Fraley C, Raftery AE. 2002. Model-based clustering, discriminant analysis and density estimation. *Journal of the American Statistical Association* **97:** 611–631.

Genz A, Bretz F, Miwa T, Mi X, Leisch F, Scheipl F, Hothorn T. 2009. *mvtnorm: multivariate normal and t distributions*. R package version 0.9-7. Available at: http://CRAN.Rproject.org/package=mvtnorm

Guillot G, Renaud S, Ledevin R, Michaux J, Claude J. 2012. A unifying model for the analysis of phenotypic, genetic, and geographic data. *Systematic Biology* **61:** 897–911.

Hammer Ø, Harper DAT, Ryan PD. 2001. PAST: Paleontological statistics software package for education and data analysis. *Palaeontologia Electronica* **4:** 1–9.

Hausdorf B, Hennig C. 2010. Species delimitation using dominant and codominant multilocus markers. *Systematic Biology* **59:** 491–503.

Hennig C, Hausdorf B. 2015. *The prabclus package version 2.1-2*. London: Department of Statistical Science, University College London. Available at: http://cran.r-project.org/

Hey J, Waples RS, Arnold ML, Butlin RK, Harrison RG. 2003. Understanding and confronting species uncertainty in biology and conservation. *Trends in Ecology & Evolution* **18:** 597–603.

Hijmans RJ, Cameron SE, Parra JL, Jones PG, Jarvis A. 2005. Very high resolution interpolated climate surfaces for global land areas. *International Journal of Climatology* **25:** 1965–1978.

Ho S. 2007. Calibrating molecular estimates of substitution rates and divergence times in birds. *Journal of Avian Biology* **38:** 409–414.

Huang JP, Knowles LL. 2016. The species versus subspecies conundrum: quantitative delimitation from integrating multiple data types within a single bayesian approach in hercules beetles. *Systematic Biology* **65:** 685–699.

Karanovic T, Djurakic M, Eberhard SM. 2016. Cryptic species or inadequate taxonomy? implementation of 2D geometric morphometrics based on integumental organs as landmarks for delimitation and description of copepod taxa. *Systematic Biology* **65:** 304–327.

Kearse M, Moir R, Wilson A, Stones-Havas S, Cheung M, Sturrock S, Buxton S, Cooper A, Markowitz S, Duran C, Thierer T, Ashton B, Mentjies P, Drummond A. 2012. Geneious basic: an integrated and extendable desktop software platform for the organization and analysis of sequence data. *Bioinformatics* **28:** 1647–1649.

Klingenberg CP. 2011. MorphoJ: an integrated software package for geometric morphometrics. *Molecular Ecology Resources* **11:** 353–357.

Krishnamoorthy K, Mathew T. 2009. *Statistical tolerance regions*. Hoboken, NJ: Wiley Series in Probability and Statistics.

Krishnamoorthy K, Mondal S. 2006. Improved tolerance factors for multivariate normal distributions. *Communications in Statistics – Simulation and Computation* **35:** 461–478.

Laurent R. 1982. Description de trois espèces nouvelles du genre *Liolaemus* (Sauria, Iguanidae). *Spixiana* **5:** 139–147.

Laurent R. 1990. Una especie apartada del género *Liolaemus* Wiegmann (Iguanidae, Lacertilia). *Acta Zoologica Lilloana* **39:** 79–84.

Laurent R. 1992. On some overlooked species of the genus *Liolaemus* Wiegmann (Reptilia Tropiduridae) from Peru. *Breviora* **494:** 1–31.

Laurent R. 1998. New forms of lizards of the subgenus *Eulaemus* of the genus *Liolaemus* (Reptilia: Squamata: Tropiduridae) from Perú and northern Chile. *Acta Zoologica Lilloana* **44:** 1–26.

Leavitt S, Moreau CS, Lumbsch HT. 2015. The dynamic discipline of species delimitation: progress toward effectively recognizing species boundaries in natural populations. In: Upreti D, Divakar PK, Shukla V, Bajpai R, eds. *Recent advances in lichenology. Modern methods and approaches in lichen systematics and culture techniques*. New Delhi, India: Springer, 11–44.

Librado P, Rozas J. 2009. DnaSP v5: a software for comprehensive analysis of DNA polymorphism data. *Bioinformatics* **25:** 1451–1452.

Lobo F, Espinoza R, Quinteros S. 2010. A critical review and systematic discussion of recent classification proposals for liolaemid lizards. *Zootaxa* **2549:** 1–30.

Maechler M, Rousseeuw P, Struyf A, Hubert M, Hornik K. 2015. *cluster: Cluster analysis basics and extensions*. R

package version 2.0.3. Available at: http://CRAN.Rproject.org/package= cluster

Martin D, Rybicki E. 2000. RDP: detection of recombination amongst aligned sequences. *Bioinformatics* **16:** 562–563.

Masters B, Fan V, Ross HA. 2011. Species delimitation – a Geneious plug-in for the exploration of species boundaries. *Molecular Ecological Resources* **11:** 154–157.

Mckay B, Mays HL Jr, Yao C, Wan D, Higuchi H, Nishiumi I. 2014. Incorporating color into integrative taxonomy: analysis of the varied tit (*Sittiparus varius*) complex in East Asia. *Systematic Biology* **63:** 505–517.

Medina CD, Avila LA, Morando M. 2013. Hacia una taxonomía integral: poniendo a prueba especies candidatas relacionadas a *Liolaemus buergeri* Werner 1907 (Iguania: Liolaemini) mediante análisis morfológicos. *Cuadernos de Herpetología* **27:** 27–34.

Medina CD, Avila LJ, Sites JW Jr, Morando M. 2014. Multilocus phylogeography of the patagonian lizard complex *Liolaemus kriegi* (Iguania: Liolaemini). *Biological Journal of the Linnean Society* **113:** 256–269.

Meik JM, Streicher JW, Lawing AM, Flores-Villela O, Fujita MK. 2015. Limitations of climatic data for inferring species boundaries: insights from speckled rattlesnakes. *PLoS ONE* **10:** e0131435.

Ministerio de Agricultura. 2014. *Decreto Supremo N° 004-2014-MINAGRI que aprueba la actualización de la lista de clasificación y categorización de las especies amenazadas de fauna silvestre legalmente protegidas. 520497–520504.* Lima: El Peruano.

Minoli I, Morando M, Avila LJ. 2014. Integrative taxonomy in the *Liolaemus fitzingerii* complex (Squamata: Liolaemini) based on morphological analyses and niche modeling. *Zootaxa* **3856:** 501–528.

Murdoch D, Chow ED, (portion to R by Frias Celayeta, JM). 2007. *Ellipse: functions for drawing ellipses and ellipses-like confidence regions*. R. package version 0.3-5. Available at: http://CRAN.Rproject.org/package=ellipse

Noonan P, Yoder AE. 2009. Anonymous nuclear markers for malagasy plated lizards (Zonosaurus). *Molecular Ecology Resources* **9:** 402–404.

Nosil P, Harmon LJ, Seehausen O. 2009. Ecological explanations for (incomplete) speciation. *Trends in Ecology & Evolution* **24:** 145–156.

Olave M, Solà E, Knowles LL. 2014a. Upstream analyses create problems with DNA-based species delimitation. *Systematic Biology* **63:** 263–271.

Olave M, Avila LJ, Sites JW Jr, Morando M. 2014b. Multilocus phylogeny of the widely distributed South American lizard clade *Eulaemus* (Liolaemini, *Liolaemus*). *Zoologica Scripta* **43:** 323–337.

Padial JM, De La Riva I. 2010. A response to recent proposals for integrative taxonomy. *Biological Journal of the Linnean Society* **101:** 747–756.

Padial JM, Miralles A, De la Riva I, Vences M. 2010. The integrative future of taxonomy. *Frontiers in Zoology* **7:** 1–14.

Pante E, Schoelinck C, Puillandre N. 2015. From integrative taxonomy to species description: one step beyond. *Systematic Biology* **64:** 152–160.

Pelletier TA, Crisafulli C, Wagner S, Zellmer AJ, Cartens BC. 2015. historical species distribution models predict species limits in western Plethodon salamanders. *Systematic Biology* **64:** 909–925.

Peterson AT, Soberon J, Pearson R, Anderson RP, Martinez-Meyer E, Nakamura M, Araujo MB. 2011. *Ecological niches and geographic distributions*. Princeton: Princeton University Press.

Phillips S, Anderson RP, Schapire RE. 2006. Maximum entropy modeling of species geographic distributions. *Ecological Modelling* **190:** 231–259.

Portik DM, Wood PL Jr, Grismer JL, Stanley EL, Jackman TR. 2012. Identification of 104 rapidly-evolving nuclear protein-coding markers for amplification across scaled reptiles using genomic resources. *Conservation Genetics Resources* **4:** 1–10.

de Queiroz K. 1998. The General Lineage Concept of species, species criteria, and the process of speciation. In: Howard DJ, Berlocher SH, eds. *Endless forms: species and speciation*. New York: Oxford University Press, 57–75.

de Queiroz K. 2005a. Ernst Mayr and the modern concept of species. *Proceedings of the National Academy of Sciences of the United States of America* **102:** 6600–6607.

de Queiroz K. 2005b. A unified concept of species and its consequences for the future of taxonomy. *Proceedings of the National Academy of Sciences of the United States of America* **56:** 196–215.

de Queiroz K. 2007. Species concepts and species delimitation. *Systematic Biology* **56:** 879–886.

R Core Team. 2014. *R: a language and environment for statistical computing*. Vienna, Austria: R Foundation for Statistical Computing. Available at: http://www.R-project.org/

Radosavljevic A, Anderson RP. 2014. Making better MAXENT models of species distributions: complexity, overfitting and evaluation. *Journal of Biogeography* **41:** 629–643.

Ray S, Lindsay BG. 2005. The topography of multivariate normal mixtures. *The Annals of Statistics* **33:** 2042–2065.

Roberts DW. 2007. *labdsv: ordination and multivariate analysis for ecology*. R package version 1.3-1. Available at: http://ecology.msu.montana.edu/labdsv/R

Rohlf F. 2004. *tpsDig 1.4*. Stony Brook, NY: Department of Ecology and Evolution, State University of New York at Stony Brook.

Ronquist F, Teslenko M, van der Mark P, Ayres DL, Darling A, Höhna S, Larget B, Liu L, Suchard MA, Huelsenbeck JP. 2012. MrBayes 3.2: efficient Bayesian phylogenetic inference and model choice across a large model space. *Systematic Biology* **61:** 539–542.

Rosenberg NA. 2007. Statistical tests for taxonomic distinctiveness from observations of monophyly. *Evolution* **61:** 317–323.

Schlick-Steiner B, Steiner FM, Seifert B, Stauffer C, Christian E, Crozier RH. 2010. Integrative taxonomy: a multisource approach to exploring biodiversity. *The Annual Review of Entomology* **55:** 421–438.

Sites JW Jr, Marshall JC. 2003. Delimiting species: a renaissance issue in systematic biology. *Trends in Ecology & Evolution* **18:** 462–470.

Sites JW Jr, Marshall JC. 2004. Operational criteria for delimiting species. *Annual Review of Ecology Evolution and Systematics* **35:** 199–227.

Solís-Lemus C, Knowles LL, Ané C. 2014. Bayesian species delimitation combining multiple genes and traits in a unified framework. *Evolution* **69:** 492–507.

Tamura K, Stecher G, Peterson D, Filipski A, Kumar S. 2013. MEGA6: molecular evolutionary genetics analysis version 6.0. *Molecular Biology and Evolution* **30:** 2725–2729.

Tocchio LJ, Gurgel-Goncalves R, Escobar LE, Peterson AT. 2014. Niche similarities among white-eared opossums (Mammalia, Didelphidae): is ecological niche modelling relevant to setting species limits? *Zoologica Scripta* **44:** 1–10.

Uetz P, Hosek J. 2016. *The reptile database*. Available at: http://www.reptile-database.org

Venables W, Ripley BD. 2002. *Modern applied statistics with S*. New York, NY: Springer.

Warren DL. 2012. In defense of 'niche modeling'. *Trends in Ecology & Evolution* **27:** 497–500.

Warren D, Glor RE, Turelli M. 2008. Environmental niche equivalency versus conservatism: quantitative approaches to niche evolution. *Evolution* **62:** 2868–2883.

Warren DL, Glor RE, Turelli M. 2010. ENMTools: a toolbox for comparative studies of environmental niche models. *Ecography* **33:** 607–611.

Wiens J, Servedio MR. 2000. Species delimitation in systematics: inferring diagnostic differences between species. *Proceedings of the Royal Society of London B* **267:** 631–636.

Wiens JJ, Reeder TW, De Oca ANM. 1999. Molecular phylogenetics and evolution of sexual dichromatism among populations of the Yarrow's spiny lizard (*Sceloporus jarrovii*). *Evolution* **53:** 1884–1897.

Wilcox T, Zwickl DJ, Heath TA, Hillis DM. 2002. Phylogenetic relationships of the dwarf boas and a comparison of Bayesian and bootstrap measures of phylogenetic support. *Molecular Phylogenetics and Evolution* **25:** 361–371.

Yeates D, Seago A, Nelson L, Cameron SL, Joseph L, Trueman JWH. 2011. Integrative taxonomy, or iterative taxonomy? *Systematic Entomology* **36:** 209–217.

Zapata F, Jimenez I. 2012. Species delimitation: inferring gaps in morphology across geography. *Systematic Biology* **61:** 179–194.

SUPPORTING INFORMATION

Additional Supporting Information may be found online in the supporting information tab for this article:

Appendix S1. Specimens used in this study for morphological analyses (if yes marked with an X) including museum number, types, sex, reproductive stage for each individual.
Appendix S2. Tissues used in this study including molecular markers (if yes marked by an X), museum numbers and locality for each individual.
Appendix S3. GenBank accession numbers used in this study.
Appendix S4. Landmarks used in shape analysis and other gap analyses..
Appendix S5. Geographic information, principal component analysis of bioclimatic data and Maxent projections of selected species..
Appendix S6. Extended time calibrated phylogenetic tree including 117 terminals.

CHAPTER 4: The shadow of the past: convergence of young and old South American desert lizards as measured by quantitative and categorical traits

The shadow of the past: convergence of young and old South American desert lizards as measured by quantitative and categorical traits.

Cesar Aguilar[1,2], Luciano J. Avila[3], Ignacio de la Riva[4], Noemi Goicoechea[4], Leigh Johnson[1], Mariana Morando[3], Jaime Troncoso[5], Jack W. Sites Jr[1].

[1]Department of Biology and M. L. Bean Life Science Museum, Brigham Young University (BYU), Provo, UT, 84602, USA
[2]Departamento de Herpetologia, Museo de Historia Natural de San Marcos (MUSM), Av. Arenales 1256, Jesus Maria, Lima, Peru
[3]Centro Nacional Patagónico (CENPAT-CONICET). Bv. Alte. Brown 2915, U9120, Puerto Madryn, Chubut, Argentina.
[4]Museo Nacional de Ciencias Naturales, CSIC. C/ Jose Gutierrez Abascal, 2. 28006 Madrid, Spain
[5]Programa de Fisiologia y Biofisica, Instituto de Ciencias Biomedicas (ICBM), Facultad de Medicina, Universidad de Chile, Independencia 1027, Santiago, Chile

Abstract

Convergence is a pervasive phenomenon in the Tree of life. The study of convergence has improved with the development of methods that identify and quantify this phenomenon. However most methods that measure the strength of convergence have relied on quantitative data, and limited use of categorical data. Here we use non-metric multidimensional scaling (NMMS) to combine categorical and quantitative traits and estimate new multivariate quantitative variables. We applied this approach to test putative convergent evolution of desert traits in several species of South American lizards in the *Liolaemus montanus* and *L. anomalous* groups, and *Ctenoblepharys adpersa*. We estimated a multilocus time-calibrated phylogeny based on seven molecular markers and including 44 species. We collected quantitative head shape and categorical data for 401 specimens, and used three phylogenetic comparative methods (SURFACE, CONVEVOL and WHEATSHEAF index) to test for and estimate the strength of convergence based on NMMS dimensions. We found strong evidence for convergence among *C. adspersa, L. lentus, L. manueli, L. poconchilensis* and *L. stolzmanni,* which we hypothesize as adaptation to a "sand-diving" behavior for predator avoidance. We hypothesize that these traits evolved first in *C. adspersa* (~93 My) and more recently independently in two different *Liolaemus* groups (≤25 My), suggesting that constraints to achieve a similar phenotype might have also been involved in this evolutionary convergence.

Introduction

Evolutionary convergence is a pervasive phenomenon in the Tree of Life and can be defined as the repeated, independent evolution of the same trait (or complex of traits) in two or more clades at different points in geological time (McGhee, 2011). However, some definitions of convergence are linked to methods used to identify and quantify it (Stayton, 2015; Speed and Arbuckle, 2016; Arbuckle and Speed, 2016). For instance, convergence is sometimes defined as result of a process (in contrast to a pattern), and methods that identify cases of convergence assume an adaptive process (e.g., Ingram and Mahler, 2013). Because convergence might be due to processes other than natural selection, it should be defined as a process-neutral pattern, and then independently tested for adaptation or other processes (Losos, 2011; Stayton 2015; Pontarotti and Hue, 2016).

Two possible goals in the study of evolutionary convergence are its identification (whether convergence is present) and quantification (estimating its frequency and strength); (Arbuckle and Speed, 2016). The frequency of convergence can be achieved by enumerating the cases in a group of taxa, while the strength of convergence estimates how similar is/are the trait(s) of the convergent taxa. Categorical traits have only been used to identify convergence or quantify its frequency (Speed and Arbuckle, 2016; Arbuckle and Speed, 2016), but not to estimate its strength in combination with quantitative traits. Here we standardize quantitative and categorical traits using Gower distances and Non-Metric Multidimensional Scaling (NMMS), and use the NMMS dimensions as quantitative traits.

We used these NMMS dimensions to identify and measure the strength of convergence in South American lizards of the *Liolaemus montanus* group (Fig. 1). Some species in this group are toad-like ("phrynosauroid") in head shape, have a pronounced serrated combs formed by the projecting outer ciliary scales, and smooth (not keeled) dorsal scales (Fig. 2). These lizards inhabit the extremely arid desert environments of the South American Pacific coast, and are morphologically different from remaining (mostly Andean) species of the *montanus* group. Moreover, they resemble another linage present in the same arid desert, the monotypic *Ctenoblepharys adspersa*, as well as species of the *L. anomalous* group indigenous to the Monte Desert of Argentina (Abdala and Juarez-Heredia, 2013).

The taxonomic history of these desert species is a good example of how convergence has confused taxonomists. Lizards from the *montanus* and *anomalous* groups were originally

considered distinct from *Liolaemus* and recognized as different genera were created for them (*Abas*, *Ceiolaemus, Phynosaura*), or assigned to *Ctenoblepharys* within Liolaemidae. These putative new genera were later rejected and all species except *C. adspersa* were returned to *Liolaemus* (reviewed in Etheridge, 1995). Independent evolution of this lizard phenotype in the *montanus* group as a local adaptation to sandy habitats has been suggested previously (Valladares, 2004), but quantative analysis of these phenotypes within a phylogenetic context has not been done for this species group of *Liolaemus*.

The aims of this paper are to: 1) test the monophyly of "phrynosauroid" lizards of the *montanus* group and estimate their divergence times; and 2) test for phenotypic convergence in desert lizards of the *montanus* and *anomalous* groups, and *Ctenoblepharys adspersa*, using head shape and qualitative traits.

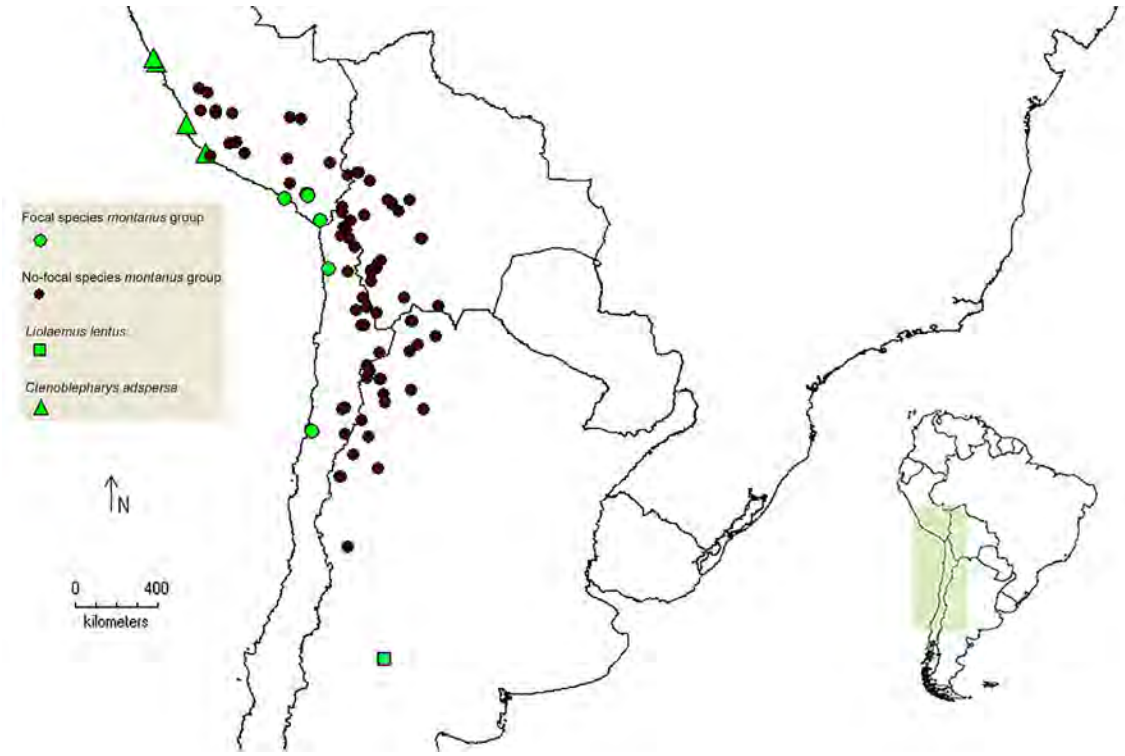

Figure 1. Distribution map of *Liolaemus* species of the *montanus* group, *L. lentus* (*anomalous* group) and *Ctenoblepharys adspersa*. Focal species of the *montanus* group (*L. insolitus, L. manueli, L. poconchilensis, L. stolzmanni* and *Liolaemus* "Moquegua") are represented by green dots, and non-focal species by black dots.

Figure 2. Morphological traits in non-focal (left) versus focal (right) species of the *Liolaemus montanus* group: A (*L. melanogaster*) and B (*L. poconchilensis*) show differences in head shapes; C and D show eyes framed by reduced ciliary scales in C (*Liolaemus* "Nazca") versus conspicuous comb-like ciliaries in D (*L. poconchilensis*). E and F show keeled dorsal body scales in E (*L. thomasi*) and smooth in F (*L. poconchilensis*).

Material and Methods

DNA EXTRACTION, AMPLIFICATION AND SEQUENCING

Lizards were collected by hand, photographed and euthanized with an injection of sodium pentobarbital. After liver and muscle tissues were collected for DNA samples, whole specimens were fixed in 10% formaldehyde, and transferred to 70% ethanol for permanent storage in museum collections. Tissue samples were collected in duplicate, stored in 96% ethanol and deposited at the M. L. Bean Life Science Museum at Brigham Young University (BYU) and Museo de Historia Natural de San Marcos (MUSM) in Lima, Peru, and voucher specimens were shared between these same institutions on a 50:50 basis.

Total genomic DNA was extracted from liver/muscle tissue using the animal tissue extraction protocol in the Qiagen protocol (Qiagen, Inc., Valencia, CA). The mitochondrial cyt-b gene (652 bp) was sequenced for all individuals and non-redundant haplotypes were sequenced for the mtDNA 12S region (~788 bp), and five nuclear gene regions: CMOS (398 bp), EXPH5 (888 bp), KIF24 (478 bp), MXRA5 (776 bp), and PRLR (~534 bp). All new sequences will be deposited in GenBank and Dryad, respectively. Double stranded polymerase chain reactions (PCR) amplified target regions under the conditions described in Aguilar et al. (2016). PCR products were visualized on 10% agarose gels to ensure the targeted products were cleanly amplified, then purified using a MultiScreen PCR (mu) 96 (Millipore Corp., Billerica, MA), and directly sequenced using the BigDye Terminator v 3.1 Cycle Sequencing Ready Reaction (Applied Biosystems, Foster City, CA). The cycle sequencing reactions were purified using Sephadex G-50 Fine (GE Healthcare) and MultiScreen HV plates (Millipore Corp.). Samples were then analyzed on an ABI3730xl DNA Analyzer in the BYU DNA Sequencing Center.

TAXON SAMPLING FOR PHYLOGENETIC INFERENCE

Some individuals of the *montanus* group could not be assigned to any known species because they are juveniles or females lacking diagnostic morphological features, or they may represent new species. All individuals sequenced in this study, along with their taxonomic assignments and localities, are summarized in Appendix 1. To resolve taxonomic uncertainties, we implemented a maximum likelihood (ML) phylogenetic analysis (see below for details) of the mitochondrial data (12S and cyt-b combined) using all individuals (198 terminals, Appendix 2); and from this analysis we estimated tree distances and Rosenberg probabilities for clades or

terminals representing unnamed taxa. Clades recovered with bootstrap support ≥ 70 and single terminals were considered candidate species when tree distances ≥ 3% and Rosenberg probabilities ≤ 0.01 (Aguilar et al., 2016). We subsampled the mtDNA gene tree by selecting single individuals representing either species or candidate species of the *L. montanus* group for further analyses.

PHYLOGENETIC ANALYSES

Our analyses included 42 taxa assigned to the *montanus* group (Lobo et al., 2010) and 13 candidate species (see above, Aguilar et al., 2016). We also included *Liolaemus lentus* (*anomalous* group), *L. puelche*, *L. canqueli*, *L. ornatus*, *L. rothi* and *L. baguali* (representing other species groups in the subgenus *Eulaemus*)*, L. walkeri* (subgenus *Liolaemus*), and *Phymaturus sitesi* (Liolaemidae) were also included in the analyses. *Ctenoblepharys adspersa* (Liolaemidae) was selected as the outgroup to root the tree (Schulte, 2013). For some of these taxa homologous regions were obtained from GenBank.

All sequences were aligned in the MUSCLE (Edgar, 2004) plugin in GENEIOUS®PRO v5.6.6 (Kearse et al., 2012), and protein coding sequences were translated to check for premature stop codons. Bayesian Information Criteria in JMODELTEST v2.1.3 (Darriba et al., 2012) were used to identify the best-fit models of evolution. ML phylogenetic analyses were performed using RAXML (Stamadakis, 2014) partitioned by gene, and 1000 bootstrap replications were estimated using CIPRES. The ML analysis based on all markers was completed for all taxa and a subset of 42 species for which morphological data are available for convergence analyses (see below).

To estimate divergence times, a concatenated tree was generated using the same terminals but including members of different families as outgroups. The *Eulaemus* clade was calibrated as in Aguilar et al. (2016), but two fossils were added to calibrate: 1) the Pleurodont clade formed by Liolaemidae, *Leiosaurus catamarcensis* (Leiosauridae), *Anolis carolinensis* (Polychrotidae) and *Phrynosoma platyrhinos* (Phrynosomatidae), setting a prior to 48 million years (My) (Conrand and Norell, 2007; Jones et al., 2013); and 2) the Iguania clade formed by the Pleurodont clade + *Chamaeleo calyptratus* (Chamaeleonidae), and setting a prior to 168.9 My (Evans et al., 2002).

This analysis was implemented in BEAST v1.8 (Drummond et al., 2012) and run for 100 million generations. We used TRACER v1.6 (Drummond et al., 2012) to ensure effective samples sizes (ESS) were greater than 200. We discarded 10% of the trees as burn-in and the remaining trees were combined using LOGCOMBINER v1.8.0 and sampled at a lower frequency, resulting in 10,000 trees. A maximum clade credibility tree (MCC) was then constructed using TREEANNOTATOR v1.8 (Drummond et al., 2012), and keeping mean and 95% confident intervals for node ages.

MORPHOLOGICAL DATA

To examine convergence traits in the *L. montanus* group, the ML tree was combined with head shape data as quantified using geometric morphometric methods. Ten landmarks on the dorsal head view (Aguilar et al., 2016) of 401 lizards representing 44 species (Appendix 3) were set on digital pictures using TPSdig v1.4 (Rohlf, 2004), and shape analyses were performed using PCA after a Generalized Procrustes approach. Because specimens of *Liolaemus lentus* and *Phymaturus sitesi* were not available we used another species of the same group (*L. pseudoanomalus*) or same genus (*P. patagonicus*), respectively. Procustes and PCA analyses were performed using MORPHOJ v1.03d (Klingenberg, 2011), and PCA scores were extracted for further analyses using the GEOMORPH package (Adams and Otarola-Castillo, 2013) in R (R Development Core Team, 2014). The first two principal components explained 58.9% of the variance and were retained. Average of PC1 and PC2 scores for specimens representing each species were estimated.

Two discrete traits for each species were examined and added to the data set: scales keeling (present/absent) and enlarged ciliary scales (present/absent). Euclidian and Gower distances were calculated for PC1, PC2 and the two discrete variables using the CLUSTER package in R (Maechler et al., 2015). The distance matrix was standardized using non-metric multidimensional scaling (NMDS) using the MASS package (Venables and Ripley, 2002), and retained the two dimensions with stress values below 10%. These two quantitative dimensions (V1 and V2) were used for the convergence analyses. Morphological data will be deposited in MorphoBank.

CONVERGENCE ANALYSES

Three convergence analyses were performed using traits V1 and V2 and the phylogeny of 44 terminals. The first analysis was performed using the R package SURFACE (Ingram and Mahler, 2013); this algorithm employs a Ornstein-Uhlenbeck (OU) process to identify cases without the *a priori* designation of convergent taxa. The method has a forward phase in which selective regimes are inferred using a phylogenetic tree and quantitative traits, and a backward phase in which taxa having the same (convergent) regime are identified. In the forward phase, selective regimes are added to a Hansen model (Hansen, 1997) and then further regime shifts (models) are added in a stepwise process. Model performance is evaluated using a corrected Akaike Information Criterion (AICc). In the backward phase, all selective regimes obtained in the first phase are combined in a pairwise manner and collapsed into a shared regime. This procedure is repeated until no more stepwise combinations improve the models, and convergent (collapsed) regimes are estimated (again using AICc). The SURFACE model (OUm) was compared with simpler stochastic models such a single regime (OU1) and Brownian motion (BM) models.

Convergence regimes found in SURFACE were used to code taxa and map PC1 and PC2 scores onto the ML phylogeny employing a squared-change parsimony (Maddison, 1991) method in MORPHOJ. This method was selected to visualize the convergent evolutionary changes in head morphology.

Convergence regimes found in SURFACE were also used to estimate convergent metrics with CONVEVOL (Stayton, 2015). This method estimates four distances (C1, C2, C3, C4) and one frequency-based (C5) measure of convergence. C1 is based on the idea that the more dissimilar the ancestors, and the more similar the descendants, the more stronger is the convergence. C1 represents the proportion of the maximum distance between two lineages that has been brought together by subsequent evolution, and ranges from 0 to 1 as convergence increases. A value of 1 indicates that lineages are fully convergent, and a value of 0 means that lineages are phenotypically different and convergence is absent. C2 is another measure representing the absolute amount of evolution that has occurred during convergence, with larger values indicating greater convergence. C3 and C4 are based on C2 and allow comparison between datasets (in contrast to within datasets). C3 is the proportion between C2 and the total amount of evolutionary change along the lineages leading from the common ancestor of the convergent taxa to those taxa. C4 is the proportion between C2 and the total amount of evolution

in the entire clade defined by the common ancestor of the convergent taxa (Stayton, 2015).

C5 is a frequency-based measure and is defined as the number of focal taxa that reside within a limited but convergent region of a phylomorphospace (the phylogenetic connections between taxa represented graphically in a plot of morphological space).

Statistical tests of convergence as measured by C1, C2, C3 and C4 were evaluated using 1000 evolutionary simulations via a BM model. Specifically we tested whether the simulated measures are significantly different from the observed values. In the same way, the statistical significance of convergence as measured by C5 was tested using 1000 simulations. Results of all test were considered significant at a p-value ≤ 0.05.

We implemented a WHEATSHEAF analysis to measure the strength of convergent evolution, as implemented in the R package WINDEX (Arbuckle et al., 2014; Arbuckle and Minter, 2015). This index calculates the similarity of focal (convergent) species to each other and the separation in phenotypic space of the focal group from non-convergent species, all corrected for phylogenetic relatedness. Convergence is stronger when focal species are more phenotypically similar to each other, and when focal species are more disparate to the non-focal species. As in the previous analysis, convergence cases found in SURFACE were used to estimate the WHEATSHEAF Index and 95% confidence intervals. The null hypothesis that the observed WHEATSHEAF index is no higher than those expected by chance is rejected when $p \leq 0.05$ (indicating exceptionally strong convergence). Expected WHEATSHEAF indexes were derived from 1000 bootstrap replications. Calculations and tests of the WHEATSHEAF index were based on an ultrametric tree. The ML tree was converted to an ultrametric tree using the R package APE (Paradis et al., 2004). We evaluated ultrametric trees with different values of λ (0, 0.1, 1) and alternative models (correlated, relaxed, discrete), and selected the one with the best penalized-log likehood score ($\lambda = 0$, correlated).

Results

PHYLOGENETIC RELATIONSHIPS AND DIVERGENCE TIMES

Results of the multilocus maximum likelihood (ML; Fig. 3) tree with bootstrap support values (BS) and main differences with the Bayesian divergence time tree (DT; Appendix 4) are mentioned below. The ML shows a well-supported (BS $\geq$ 70) *Liolaemus montanus* group formed by most species currently assigned to this group, with the exception of *L. chlorostictus*. This

species is more closely related to species of the *darwini* group (*L. ornatus*, *Liolaemus* sp. 1 and *Liolaemus* sp. 6) than those of the *montanus* group. The *montanus* group includes three major clades; one of which (*L. andinus*, *L. famatinae, L. foxi, L. gracielae*, *L. nigriceps*, *L. manueli, L. patriciaiturrae*, *L. rosenmanni*, *L. rubiali*, and *L. vallecurensis*), is only weakly supported (BS ≤ 70). However this clade is well supported in the DT tree with posterior probability (PP) ≥ 0.9 (Appendix 4).

This clade is sister to a well supported (BS ≥ 70) clade that in turn includes two subclades: one of these includes (BS ≤ 70) *L. annectens*, *L. etheridgei*, *L. melanogaster*, *L. ortizi*, *L. polystictus*, *L. robustus*, *L. signifer, L. thomasi*, *L. williamsi*, *L.* "AbraApacheta", *L.* "AbraToccto", *L.* "Castrovirreyna", *L.* "Lampa", *L.* "MinasMartha", *L.* "Parinacochas", *L.* "Apurimac", *L. forsteri*, *L.* sp. 2, and *L.* sp. 3. In addition to these taxa, the DT tree also includes a group with low support (PP ≤ 0.9) formed by *L. islugensis, L. multicolor*, *L. pleopholis, L. orientalis*, *L.* cf. *schmidti,* and *L.* sp. 4 (Appendix 4).

The second subclade (BS ≤ 70) is composed of *L. aymararum*, *L. cazianae*, *L. insolitus*, *L. hajeki*, *L. halonastes*, *L. huacahuasicus*, *L. inti, L. islugensis, L. jamesi, L. multicolor*, *L. orientalis*, *L. pachecoi, L. pleopholis, L. poconchilensis*, *L. poecilochromus*, *L. porosus*, *L. scrocchii, L. stolzmanni*, *L. vulcanus*, *L.* cf. *dorbigny*, *L.* cf. *schmidti, Liolaemus* "Moquegua", *L.* "Nazca", *L.* sp. 4., and *L.* sp. 5. However, this subclade without *L. islugensis, L. multicolor*, *L. pleopholis, L. orientalis*, *L.* cf. *schmidti* and *L.* sp. 4. This clade is well supported in the DT tree (PP ≥ 0.9).

The ML and DT trees show that "Phrynosauroids" *Liolaemus poconchilensis*, *L. stolzmanni* and *L. manueli* do not form a monophyletic group, but instead are recovered in three distinct clades, all with strong support in the DT tree. *Liolaemus lentus* form a well-supported group (BS ≤ 70) with the *L. montanus* group, *L. canqueli*, *L. chlorostictus*, *L. ornatus*, *L. puelche*, *L. rothi*, *L.* sp. 1 and *L.* sp. 6. However in the DT tree (Appendix 4), *L. lentus* is more closely related to *L. rothi* but with low support (PP ≤ 0.9).

The ML tree resolves a well supported (*Liolaemus* + *Phymaturus sitesi*). The DT (Appendix 4) tree shows a sister relationship of *C. adspersa* with (*Phymaturus sitesi* (*Liolaemus* + *Leiosaurus catamarcensis*)) but with low support (PP ≤ 0.9).

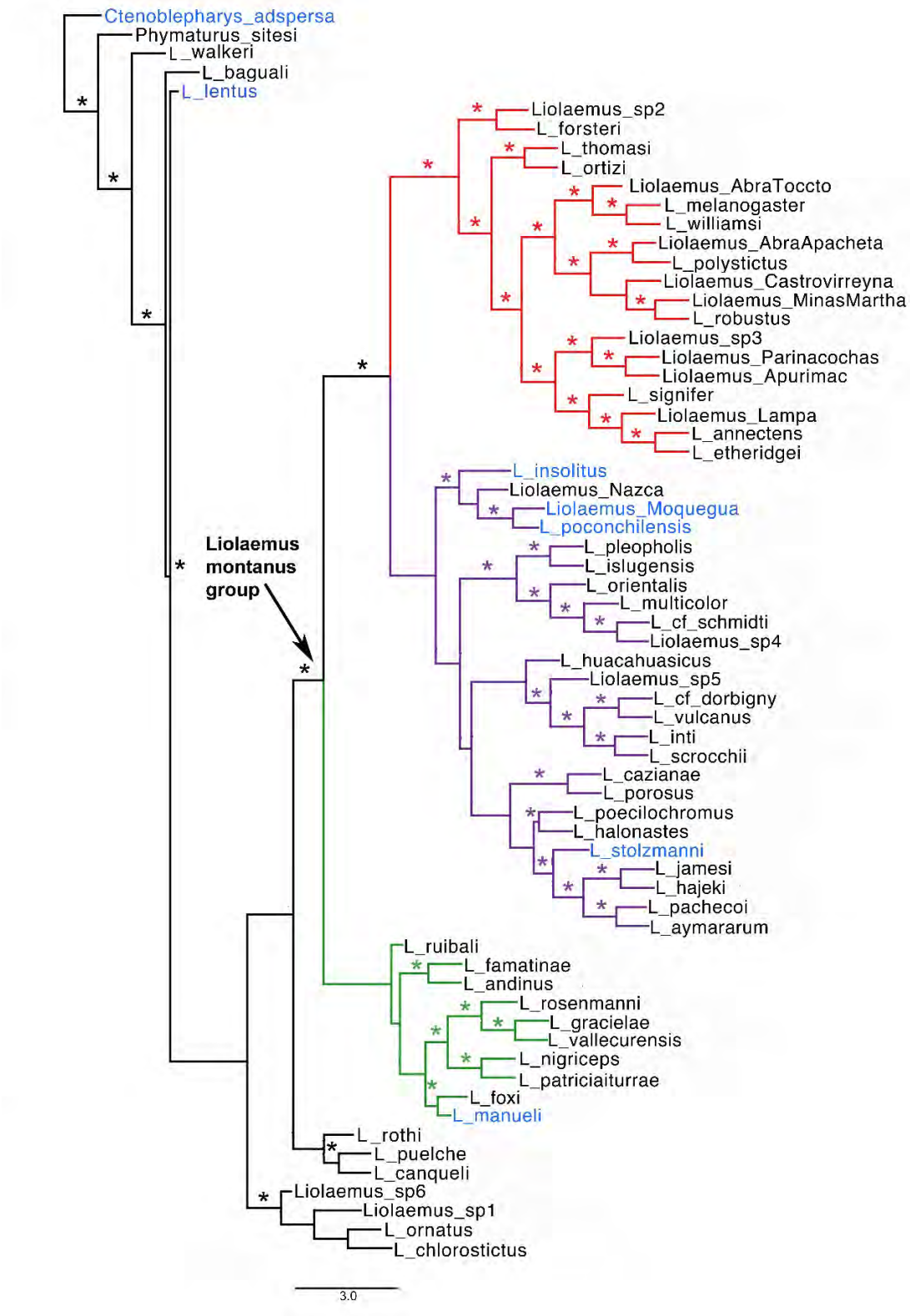

Figure 3. Maximum likelihood tree of the *montanus* group (high-lighted) and its relationship with other taxa. Putative convergent taxa are in blue. Asterisks (*) indicate bootstrap values ≥ 70.

This clade diverged from *C. adspersa* at ~ 80 My (Appendix 4). In the DT tree *Liolaemus lentus* (*anomalus* group) and the *rothi* complex (represented by *L. rothi*) diverged at about 22 My (Appendix 4). The *montanus* group and its sister group (species representing the *darwini, melanops* and *donosobarroi "*groups") diverged at about 25 My (Appendix 4). The clade (*L. insolitus* (*Liolaemus* "Moquegua" + *L. poconchilensis*)) has a mean age of 10 My (Appendix 4). The clade (*L. stolzmanni* ((*L. pachecoi* + *L. aymararum*) (*L. jamesi* + *L. hajeki*))) has a mean age of 9 My. The clade (*L. manueli* + *L. foxi*) has a mean age of 5 My (Appendix 4).

CONVERGENT ANALYSES

Our SURFACE analyses identify five phenotypic regimes, two of which are convergent (Table 1; Fig. 4A,B). One convergent regime is achieved independently by *Ctenoblepharys adspersa*, *Liolaemus lentus*, *L. manueli*, *L. poconchilensis*, and *L. stolzmanni*, while *L. insolitus* and *Liolaemus* "Moquegua" reach the other convergent regime independently (Fig. 4A,B). The best model found by SURFACE (OUm; AICc = -301.9182) is an improvement over the one peak model (OU1; AICc = -130.3372) and Brownian model (BM; AICc = -87.79926). Other model parameters are shown in Table 1.

Geometric morphometric scores of the first two principal components (PC1 and PC2) mapped onto the phylogeny are shown in Figure 5. This phylomorphospace shows *Ctenoblepharys adspersa*, *L. lentus, L. manueli*, *L. poconchilensis, L. stolzmanni* (red)*, Liolaemus insolitus* and *Liolaemus* "Moquegua" (blue) having mid- to high PC1and PC2 scores in comparison with most of the taxa (Fig 5C). This independent evolution in head morphology reflects a reduction from the tip of the snout to the nostrils (landmarks 1-3; Fig 5A,B), and a widening of the head at the level of the parietal scale (landmarks 5,7-8; Fig 5A,B).

C1-C5 metrics of convergences are shown in Table 2. C1-C5 measures were estimated for the two convergent regimes found in SURFACE analyses, and when taxa of these two regimes are pooled. C1-C4 values show that *Cteblepharys adspersa*, *Liolaemus lentus, L. manueli*, *L. poconchilensis* and *L. stolzmanni* have a significant stronger similarity than taxa *L. insolitus* and *Liolaemus* "Moquegua", or when all convergent taxa are pooled together (Table 2). The C5 metric of the selective regime that includes *Cteblepharys adspersa*, *L. lentus, Liolaemus manueli*, *L. poconchilensis* and *L. stolzmanni* shows that all five taxa significantly cluster in a region of the phylomorphospace (Table 2, Fig. 6).

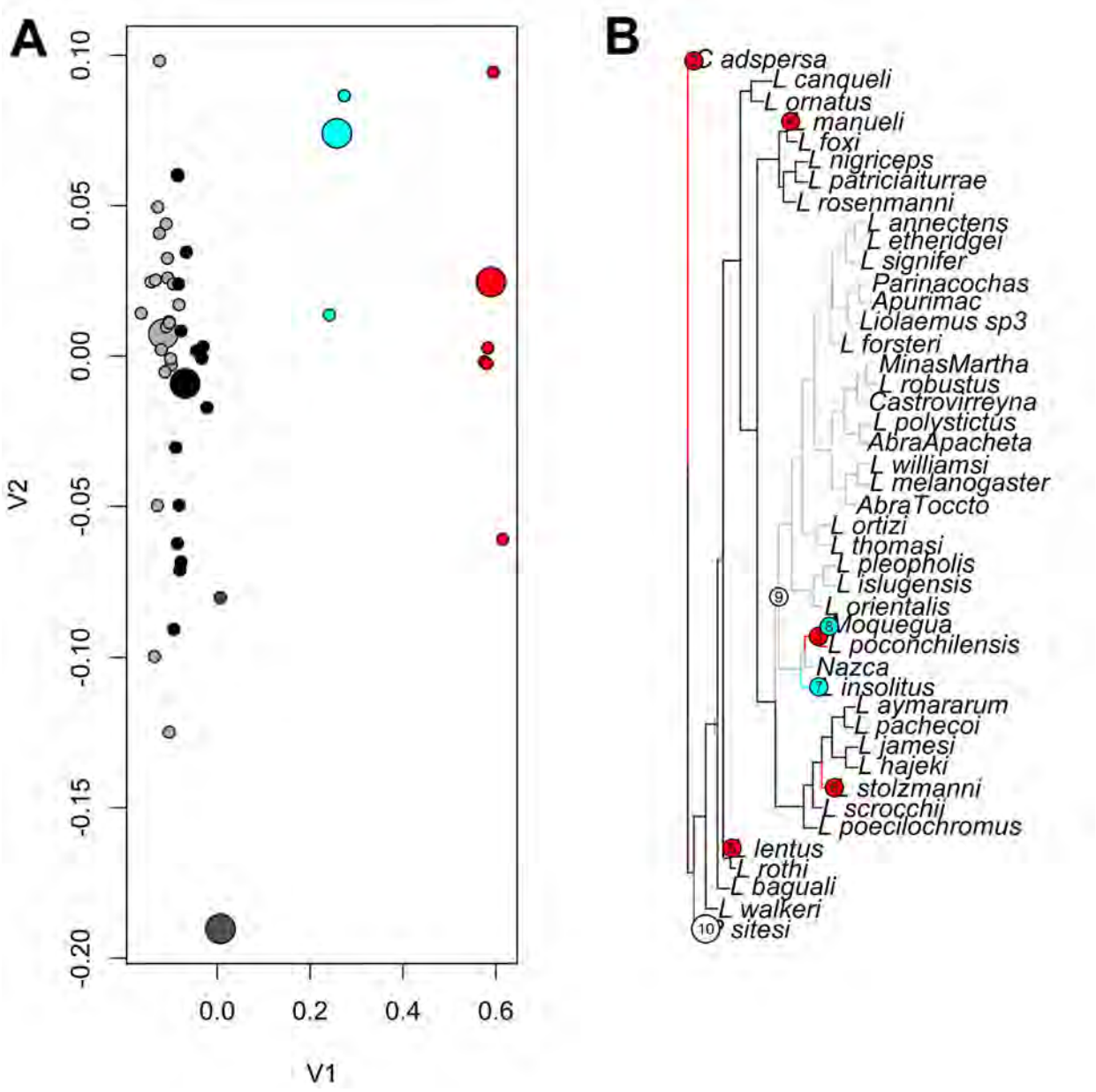

Figure 4. Results of SURFACE analysis. A = NMMS plot of trait values: small circles identify species and large circles are estimated adaptive optima; blue and red circles identify species and estimated optima for convergent regimes, respectively. B = phylogeny (reduced from Fig. 1) showing placement of convergent regimes (colored) as in A.

Table 1. SURFACE analysis parameters for different models of evolution: OUm (model obtained in the backward phase), OU1 (model with one adaptative peak) and BM (Brownian motion model).

Parameters	Models		
	OUm	OU1	BM
k (regime shifts)	10	1	0
k' (number of distinct regimes)	5	1	0
Δk (k-k', the reduction in complexity of the adaptive landscape when accounting for convergence)	5	0	0
c (number of shifts that are towards convergent regimes occupied by multiple lineages)	7	0	0
k'_conv (number of convergent regimes reached by multiple shifts	2	0	0
AICc (corrected Akaike Information Criteria)	-301.9182	-130.3372	-87.79926

The C5 value for all seven taxa combined also includes the same five species, but it is not significant (Table 2). C5 could not be estimated to the convergent regime formed by *L. insolitus* and *Liolaemus* “Moquegua”.

Table 2. C1-C5 convergence metrics derived from CONVEVOL analyses. High numbers in C1-C4 indicates strong convergence and C5 shows the number of convergent taxa that occupy a distinct region in phylomorphospace. Numbers in bold are statistically significant. NA = not applicable.

Convergent taxa	C1	C2	C3	C4	C5
C. adspersa, L. lentus, L. stolzmanni, L. poconchilensis, L. manueli	**0.723**	**0.197**	**0.025**	**0.027**	**5**
All	**0.563**	**0.276**	**0.022**	**0.038**	5
L. insolitus, Liolaemus "Moquegua"	**0.506**	**0.081**	**0.010**	**0.090**	NA

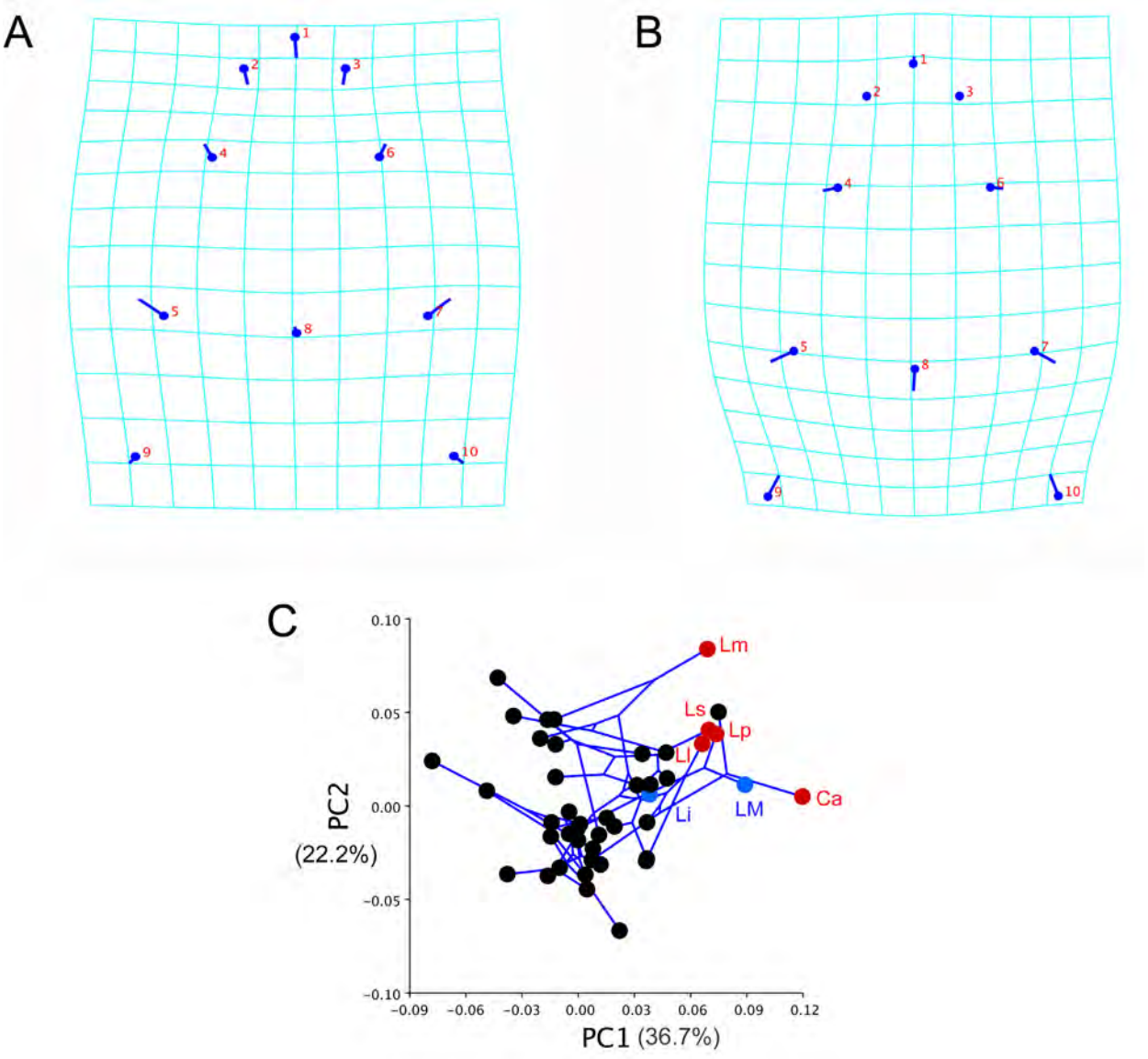

Figure 5. Phylomorphospace of head shape. A and B show the grid configurations of head shape for scores of principal components (PC) 2 and 1 respectively. C shows the averaged species scores of PC1 and PC2 mapped onto the phylogeny. Focal species are colored as in convergent regimes found in the SURFACE analysis (Fig. 4). Ca = *Ctenoblepharys adspersa*, Li = *Liolaemus insolitus*, LM = *Liolaemus* "Moquegua", Ll = *L. lentus*, Lm = *L. manueli*, Lp = *L. poconchilensis*, Ls = *L. stolzmanni*.

The WHEATSHEAF index is also higher for *Cteblepharys adspersa*, *Liolaemus lentus, L. manueli*, *L. poconchilensis* and *L. stolzmanni* than when all convergent taxa are pooled, but these differences were not significant (Table 3). The WHEATSHEAF index could not be estimated to the case *L. insolitus* and *Liolaemus* "Moquegua".

Table 3. Results of WHEATSHEAF index. Higher values of this index indicate that the convergent taxa are more similar to each other than non-focal taxa. CI= confidence interval, NA = not applicable.

Convergent taxa	Wheatsheaf Index	Lower 95% CI	Upper 95% CI	*p*-value
C. adspersa, L. lentus, L. stolzmanni, L. poconchilensis, L. manueli	2.398	2.153	2.975	0.44
All	0.820	0.737	0.843	0.45
L. insolitus, Liolaemus ″Moquegua″	0.521	0.468	NA	NA

Discussion

QUANTITATIVE AND CATEGORICAL TRAITS IN MEASURING CONVERGENCE

Quantifying convergence (frequency and strength) is important for one of the most important question in evolutionary biology: is biodiversity constrained and hence predictable (McGhee, 2011; Speed and Arbuckle, 2016)? Categorical traits have only been used for estimating the frequency of convergence, and methods to measure the strength of convergence focused on continuous traits (Ingram and Mahler, 2013; Stayton, 2015; Speed and Arbuckle, 2016; Arbuckle and Speed, 2017).

Here we employed non-metric multidimensional scaling (NMMS) to estimate convergence by combining continuous head shape traits (estimated via geometric morphometric methods) and categorical traits. One concern about using the NMMS approach is whether this data transformation will confound the biological significance of the original variables.

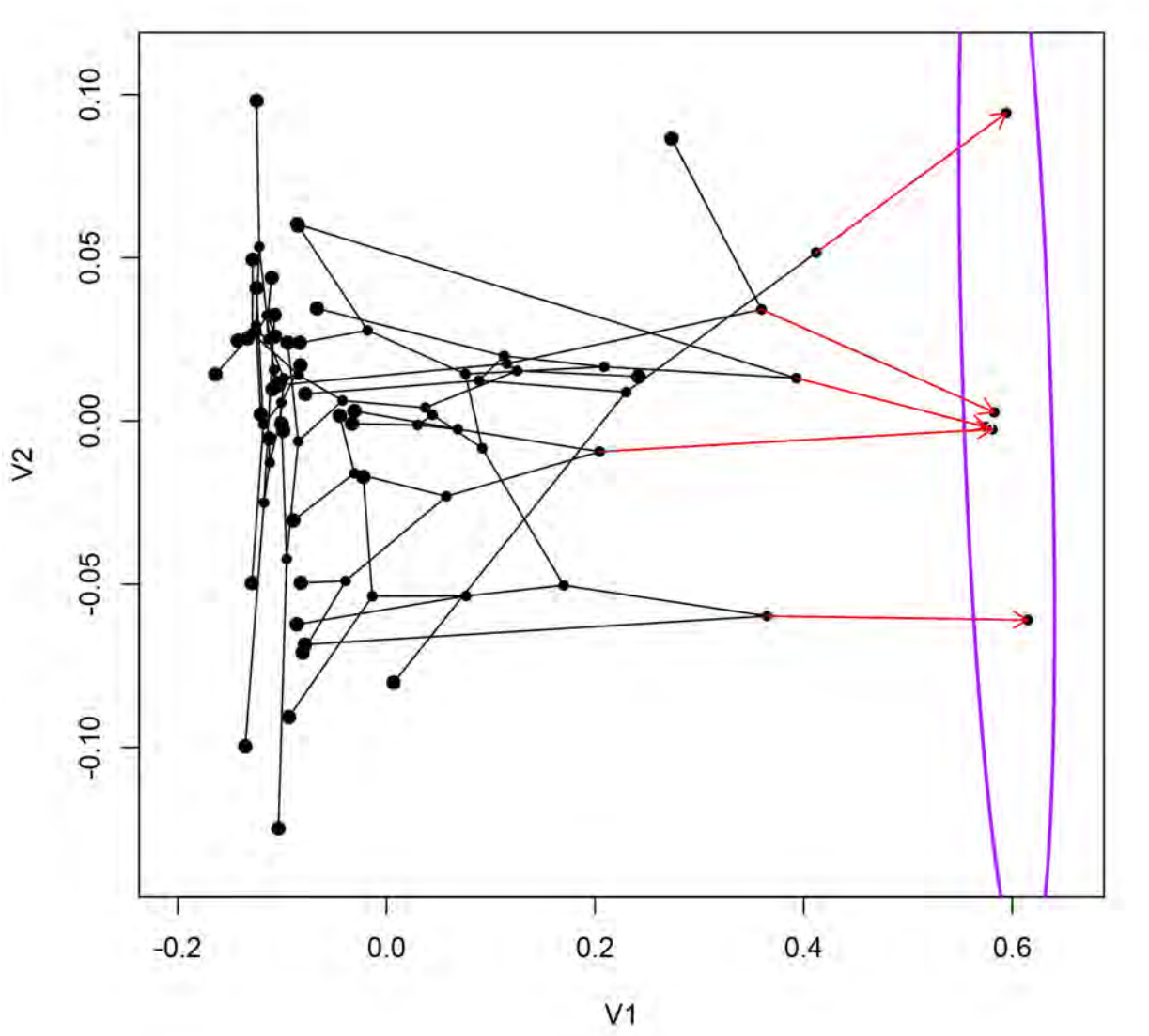

Figure 6. CONVEVOL phylomorphospace of 42 species in two NMMS dimensions (V1 and V2). The black lines connect only non-focal species and red arrows connect non-focal species to 5 convergent species (*Ctenoblepharys adspersa*, *Liolaemus lentus*, *L. manueli*, *L. poconchilensis* and *L. stolzmanni*). The location of these five taxa defines a separate distinct region in the phylomorphospace, defined by the violet ellipse.

First, shape data are necessarily a multivariate trait (Collyer et al., 2015). Geometric morphometric (GM) variables are usually reduced using principal components (PC) analyses, and the first two or three PC axes that explain most of the variance are employed instead of the original data (e.g., Muschick et al., 2012; Esquerre and Scott, 2016). The use of PC scores in phylogenetic comparative studies has been criticized in cases of high dimensional data (when more variables are used to describe a phenotype than the number of phenotypes analyzed), or when only a few PC axes have been selected (Uyeda et al., 2015). Although here we have chosen only the first two principal components that explain more than 50% of the variance, the number of variables (10 landmarks) selected for our study does not exceed the number of phenotypes (42 species).

Second, for taxa differing in qualitative characteristics, such as the presence or absent of traits, quantification is not possible because the variables only have a categorical scale (Chartier et al., 2014). This lack of mensuration is probably why categorical variables are only used for identification and frequency of evolutionary convergence (Arbuckle and Speed, 2017). However, the inclusion of categorical traits might be important in the construction of a phylomorphospace and in quantifying convergence. NMMS is one of the methods suited for categorical and quantitative data as long as a notion of similarity (e.g. Gower distance) can be expressed numerically (Chartier et al., 2014). The objective of NMMS is to determine the configuration of objects (e.g., taxa) in a distance space of minimal dimensions that best represents the original objects distances (Atchley and Bryant, 1975). One issue in applying distances is that the number of chosen categorical or quantitative variables might have an impact on its estimation (Huttegger and Mitteroecker, 2011). What if instead of two PC axes from GM analysis we had chosen three or four? If a different number of measurements or discrete traits is taken from distinct parts of a species morphology, this decision can affect the interpretation of the data when it is transformed into distances and NMMS dimensions. Further research is needed to address this and others issues. For instance, a possible concern that should be examined is the use of standard NMMS scores instead of scores that take into account phylogenetic dependence between taxa, as it is done for PC scores before any comparative analysis (Uyeda et al., 2015).

ADAPTIVE CONVERGENCE OR CONSTRAINTS?

Convergence might be due to chance, developmental constraints or natural selection

(Losos, 2011). Adaptive convergence implies that natural selection have produced the same phenotype in similar environments in unrelated taxa (Losos, 2011). Two of the three methods applied in our study, SURFACE and the WHEATSHEAF index, are based on the assumption that convergence is adaptive (Ingram and Mahler, 2013; Arbuckle et al., 2014). Both of these methods employ the metaphor of Wright and Simpson that evolution is a local search by fitter geno/phenotypes climbing higher peaks in an adaptive landscape (Niklas, 1995; Arnold et al., 2001). These methods identify convergent taxa via their occupation of the same adaptive peak, which is then taken to characterize a selective regime (Ingram and Mahler, 2013; Arbuckle et al., 2014).

Results of our SURFACE analysis identify two convergent selective regimes, one of them reached by five species: *Ctenoblepharys adspersa*, *Liolaemus lentus*, *L. manueli*, *L. stolzmanni* and *L. poconchilensis* (Fig. 4). Convergence of these five taxa is strongly supported by C1-C4 metrics, and all occupy a separate region of the phylomorphospace as measured by C5 (Table 2, Fig. 6). In contrast, the WHEATSHEAF Index, although high, was not significant, indicating that their phenotypic similarity is not enough to qualify as strong convergence (Table 3). Despite this, it seems that these five species have reached a convergent adaptive peak.

Ctenoblepharys adspersa, *Liolaemus manueli*, *L. stolzmanni* and *L. poconchilensis* are distributed in the Peruvian and Atacama Desert (Fig. 1), while *L. lentus* and all members of the monophyletic *anomalous* group (*L. acostai, L. anomalous, L. ditadai, L. millcayac, L. pipanaco, and L. pseudoanomalus*) occupy the Monte Desert (Abdala and Juarez-Heredia, 2013). These are the most prominent arid and semiarid regions of South America; the Peruvian and Atacama Desert are characterized by a mean annual rainfall ~1–15 mm while this ranges from ~ 30–350 mm in the Monte Desert (Rundel et al., 2007). Further, the origin of the hyper-aridity in the Peruvian and Atacama Deserts (~ 25 My) and semiarid conditions in Monte (~ 56 My) is consistent with the ages of focal *Liolaemus* clades in our time-calibrated tree (Appendix 4; Rundel et al., 2007).

The arid conditions and sandy substrates of these deserts likely have exerted strong selective pressures for the evolution of convergent phenotypes in these five taxa. A distinct head shape with a blunt snout, enlarged ciliaries and smooth scales may have facilitated an escape behavior characterized by diving under the sand, and exclusion of sand from the eyes while diving (Etheridge, 2000). Sand diving is in turn a mechanism for predator avoidance (Arnold,

1995). However, details of sand diving in this group of five species are only known in *Ctenoblepharys adspersa* (CA, personal observation), and sand diving is known in other *Liolaemus* species characterized by different morphologies (Etheridge, 2000). Assuming sand diving is present in desert species of the *anomalous* and *montanus* groups, our time-calibrated phylogeny resolves the origin of traits associated with this predator-scape mechanism first in *C. adspersa*, later in the *anomalous* group, and finally three times in the *montanus* group. This suggests that, in addition to natural selection, developmental constraints may also limit phenotypes in these clades of arid zone lizards.

Our SURFACE analysis also recovered another selective regime for *L. insolitus* and *Liolaemus* "Moquegua", but the C1-C4 values and WHEATSHEAF index for these two taxa were lower than the above case, and when all taxa are forced to be convergent (Table 2). This lack of statistical support for the convergence of *L. insolitus* and *Liolaemus* "Moquegua" may be due their phylogenetic relationship and recency of divergence (Figs. 3 and 4B). If so, these species may represent intermediate "steps" toward a more derived sand diving morphology. *Liolaemus insolitus* is included in a well-supported clade with *Liolaemus* "Nazca", *Liolaemus* "Moquegua" and *L. poconchilensis* (Figs. 3 and 4). *Liolaemus* "Nazca" and *L. insolitus* have a more "normal" head shape as most species of the *montanus* group, compared to *Liolaemus* "Moquegua" and *L. poconchilensis* (Fig. 5). For example, both *L. insolitus* and *Liolaemus* "Moquegua" have smooth scales and lack enlarged comb-like ciliaries, but enlarged ciliaries are present in *L. poconchilensis*. This may again represent transitional states within this small clade: *L. insolitus* and *Liolaemus* "Moquegua" may represent "intermediate stages", between normal phenotypes and those fully modified for "sand diving".

Acknowledgments

We thank J. Córdova, C. Torres (MUSM), Herman Nuñez (MNHN), A. Resetar (FMNH), J. Losos, J. Rosado (MCZ), F. Glaw (ZSM), L. Welton and R. Brown (KU) for loans and accessions of specimens under their care. Fieldwork was supported by the Waitt Foundation-National Geographic Society (award W195-11 to CA and JWS, Jr.), the BYU Bean Life Science Museum (JWS, Jr.), and lab work by NSF-Emerging Frontiers award (EF 1241885 to JWS, Jr.), Dr. C.G. Sites to JWS, Jr., and a NSF-Doctoral Dissertation Improvement Grant (award #1501187 to JWS, Jr. and CA). Permits (RD N˚ 1280-2012-AG-DGFFS-DGEFFS, RD N˚ 008-2014-MINAGRI-DGFFS-DGEFFS) were issued by the Ministerio de Agricultura, Lima, Peru, and the work was approved by the BYU Institutional Animal Care and Use Committee protocol number 12001 and in accordance with US law.

References

Abdala C.S, Juárez-Heredia, V.I. 2013. Taxonomía y filogenia de un grupo de lagartos amenazados: el grupo de Liolaemus anomalus (Iguania: Liolaemidae). *Cuadernos de Herpetología* **27:** 109-153.

Adams D.C, Otarola-Castillo E. 2013. geomorph: an R package for the collection and analysis of geometric morphometric shape data. *Methods in Ecology and Evolution.* **4:** 393-399.

Aguilar C., Wood Jr. P.L. Belk, M.C., Duff M.H., Sites Jr. J.W. 2016. Different roads lead to Rome: Integrative taxonomic approaches lead to the discovery of two new lizard lineages in the Liolaemus montanus group (Squamata: Liolaemidae). *Biological Journal of the Linnean Society*.

Arbuckle K, Bennett, C.M., Speed M.P. 2014. A simple measure of the strength of convergent evolution. *Methods in Ecology and Evolution* **5:** 685–693.

Arbuckle K, Minter, A. 2015. Windex: analyzing convergent evolution using the Wheatsheaf index in R. *Evolutionary Bioinformatics* **11:** 11-14.

Arbuckle K, Speed M. P. 2016. Analysing Convergent Evolution: A Practical Guide to Methods. In: Pontarotti P, ed. *Evolutionary Biology. Convergent Evolution, Evolution of Complex Traits, Concepts and Methods*. Switzerland: Springer Nature. 23-36.

Arnold N. 1995. Identifying the effects of history on adaptation - origins of different sand-diving techniques in lizards. *Journal of Zoology* **235:** 351-388.

Arnold S.J., Pfrender M.E., Jones A. G. 2001. The adaptive landscape as a conceptual bridge between micro and macroevolution. *Genetica* **112–113**.

Atchey W.R., Bryant E.H. 1975. *Multivariate Statistical Methods*. Halsted Press: Pennsylvania.

Chartier M., Jabbour F., Gerber S., Mitteroecker P., Sauquet H., von Balthazar, M., Staedler Y., Crane P. R., Schonenberger, J. 2014. The floral morphospace – a modern comparative approach to study angiosperm evolution. *New Phytologist* **204:** 841–853.

Collyer M.L., Sekora D.J., Adams D.C. 2015. A method for analysis of phenotypic change for phenotypes described by high-dimensional data. *Heredity* **115:** 357-365.

Conrad J.L, Norell M.A. 2007. A Complete Late Cretaceous Iguanian (Squamata, Reptilia) from the Gobi and Identification of a New Iguanian Clade. *American Museum Novitates* **3584:** 47 pp.

Drummond A., Suchard M.A, Xie D., Rambaut A. 2012. Bayesian Phylogenetics with Beauti and the Beast 1.7. . *Molecular Biology and Evolution* **29:** 1969–1973.

Edgar R. 2004. MUSCLE: multiple sequence alignment with high accuracy and high throughput. *Nucleid Acids Research* **32:** 1792-1797.

Esquerre D., Keogh J. S. 2016. Parallel selective pressures drive convergent diversification of phenotypes in pythons and boas. *Ecology Letters* **19:** 800–809.

Etheridge R. 1995. Redescription of Ctenoblepharys adspersa Tschudi, 1845, and the Taxonomy of Liolaeminae (Reptilia: Squamata: Tropiduridae). *American Museum Novitates* **3142:** 34 pp.

Etheridge R. 2000. A Review of Lizards of the Liolaemus wiegmannii Group (Squamata, Iguania, Tropiduridae), and a History of Morphological Change in the Sand-Dwelling Species. *Herpetological Monographs* **14** 293-352.

Evans S.E, Prasad G.V.R., Manhas B.K. 2002. Fossil lizards from the jurassic kota formation of India. *Journal of Vertebrate Paleontology* **22:** 299-312.

Hansen T. 1997. Stabilizing selection and the comparative analysis of adaptation. *Evolution***:** 1341-1351.

Huttegger SM, Mitteroecker P. Invariance and Meaningfulness in Phenotype spaces. *Evolutionary Biology* **38:** 335–351.

Ingram T, Mahler D. L. 2013. SURFACE: detecting convergent evolution from comparative data by fitting Ornstein-Uhlenbeck models with stepwise Akaike Information Criterion. *Methods in Ecology and Evolution* **4:** 416–425.

Jones M.E.H., Anderson C.J., Hipsley C.A., Müller J., Evans S.E, Schoch R.R. 2013. Integration of molecules and new fossils supports a Triassic origin for Lepidosauria (lizards, snakes, and tuatara). *BMC Evol. Biol.* **13:** 1-21.

Kearse M., Moir R., Wilson A., Stones-Havas S., Cheung M., Sturrock S., Buxton S., Cooper A., Markowitz S., Duran C., Thierer T., Ashton B., Mentjies P., Drummond A. 2012. Geneious Basic: an integrated and extendable desktop software platform for the organization and analysis of sequence data. *Bioinformatics* **28:** 1647–1649.

Klingenberg C.P. 2011. MorphoJ: an integrated software package for geometric morphometrics. *Molecular Ecology Resources* **11:** 353-357.

Lobo F., Espinoza R.E., Quinteros S. 2010. A critical review and systematic discussion of recent classification proposals for liolaemid lizards. *Zootaxa* **2549:** 1–30.

Losos J.B. 2011. Convergence, Adaptation, And Constraint. *Evolution* **65:** 1827–1840.

Maddison W.P. 1991. Squared-change parsimony reconstructions of ancestral states for continuous-valued characters on a phylogenetic tree. *Systematic Zoology* **40:** 304–314.

Maechler M., Rousseeuw P., Struyf A., Hubert M., Hornik K. 2015. cluster: Cluster Analysis Basics and Extensions. R package version 2.0.3.

McGhee G. 2011. *Convergent evolution: limited form most beautiful*. The MIT Press: Cambridge.

Muschick M., Indermaur, A., Salzburger W. 2012. Convergent evolution within an adaptive radiation of cichlid fishes. *Current Biology* **22:** 2362–2368.

Niklas K.J. 1995. Morphological Evolution Through Complex Domains of Fitness. In: Fitch WM, Ayala F. J., ed. *Tempo And Mode In Evolution. Genetics And Paleontology 50 Years After Simpson*. Washington D.C.: National Academy Press. 145-166.

Paradis E., Claude J., Strimmer K. 2004. APE: analyses of phylogenetics and evolution in R language. *Bioinformatics* **20:** 289–290.

Pontarotti P., Hue, I. 2016. Road Map to Study Convergent Evolution: A Proposition for Evolutionary Systems Biology Approaches. In: Pontarotti P, ed. *Evolutionary Biology. Convergent Evolution, Evolution of Complex Traits, Concepts and Methods*. Switzerland: Springer Nature. 3-21.

Rohlf F. 2004. tpsDig 1.4. *Stony Brook, NY: Department of Ecology and Evolution, State University of New York at Stony Brook*.

Rundel P.E, Villagra, P.E., Dillon, M.O., Roig-Juñent, S., Debandi G. 2007. Arid and Semi-Arid Ecosystems. In: Veblen TT, Young, K. R., Orme A.R, ed. *The Physical Geography of South America*. New York: Oxford Regional Environments.

Speed MP, Arbuckle K. 2016. Quantification provides a conceptual basis for convergent evolution. *Biological Reviews*. doi: 10.1111/brv.12257

Stamatakis A. 2014. RAxML version 8: a tool for phylogenetic analysis and post-analysis of large phylogenies. *Bioinformatics* **30:** 1312–1313.

Stayton C.T. 2015. The definition, recognition, and interpretation of convergent evolution, and two new measures for quantifying and assessing the significance of convergence. *Evolution* **69:** 2140–2153.

Uyeda J.C, Caetano D.S., Pennell M.W. 2015. Comparative analysis of principal components can be misleading *Systematic Biology* **64:** 677–689.

Valladares J.P. 2004. Nueva especie de lagarto del género Liolaemus (Reptilia: Liolaemidae) del norte de chile, previamente confundido con Liolaemus (=phrynosaura) reichei. *Cuadernos de Herpetología* **18:** 41-51.

Venables W., Ripley B.D. 2002. *Modern Applied Statistics with S.* Springer: New York.

Appendixes

Appendix 1. Specimens sequenced for this study, their museum or field numbers and country.

	Museum/Field Acronym	Number	Genus	Species	Country
1	CAP	1346	Ctenoblepharys	adspersa	Peru
2	CAP	1398	Ctenoblepharys	adspersa	Peru
3	LJAMM-CNP	5019	Liolaemus	cf.dorbigny	Argentina
4	LJAMM-CNP	5018	Liolaemus	cf.dorbigny	Argentina
5	LJAMM-CNP	14395	Liolaemus	andinus	Argentina
6	LJAMM-CNP	14394	Liolaemus	andinus	Argentina
7	LJAMM-CNP	15797	Liolaemus	cazianae	Argentina
8	LJAMM-CNP	15690	Liolaemus	porosus	Argentina
9	LJAMM-CNP	14735	Liolaemus	poecilochromus	Argentina
10	LJAMM-CNP	14730	Liolaemus	sp5	Argentina
11	LJAMM-CNP	14725	Liolaemus	poecilochromus	Argentina
12	LJAMM-CNP	14731	Liolaemus	sp5	Argentina
13	LJAMM-CNP	14727	Liolaemus	sp5	Argentina
14	LJAMM-CNP	12025	Liolaemus	sp4	Argentina
15	LJAMM-CNP	14720	Liolaemus	poecilochromus	Argentina
16	LJAMM-CNP	14734	Liolaemus	poecilochromus	Argentina
17	LJAMM-CNP	12464	Liolaemus	ruibali	Argentina
18	LJAMM-CNP	15767	Liolaemus	famatinae	Argentina
19	LJAMM-CNP	14728	Liolaemus	poecilochromus	Argentina
20	LJAMM-CNP	12827	Liolaemus	huacahuasicus	Argentina
21	LJAMM-CNP	14743	Liolaemus	poecilochromus	Argentina
22	LJAMM-CNP	12555	Liolaemus	gracielae	Argentina
23	LJAMM-CNP	12465	Liolaemus	ruibali	Argentina
24	LJAMM-CNP	12466	Liolaemus	sp	Argentina
25	LJAMM-CNP	12008	Liolaemus	multicolor	Argentina
26	LJAMM-CNP	14726	Liolaemus	sp5	Argentina
27	LJAMM-CNP	14715	Liolaemus	poecilochromus	Argentina
28	LJAMM-CNP	12006	Liolaemus	multicolor	Argentina
29	LJAMM-CNP	14718	Liolaemus	poecilochromus	Argentina
30	LJAMM-CNP	13978	Liolaemus	ruibali	Argentina
31	LJAMM-CNP	14696	Liolaemus	poecilochromus	Argentina
32	LJAMM-CNP	12007	Liolaemus	multicolor	Argentina
33	LJAMM-CNP	16081	Liolaemus	porosus	Argentina
34	LJAMM-CNP	16032	Liolaemus	sp	Argentina
35	LJAMM-CNP	15768	Liolaemus	famatinae	Argentina
36	LJAMM-CNP	15766	Liolaemus	famatinae	Argentina
37	LJAMM-CNP	15750	Liolaemus	nigriceps	Argentina
38	LJAMM-CNP	12826	Liolaemus	huacahuasicus	Argentina
39	LJAMM-CNP	15759	Liolaemus	nigriceps	Argentina

40	LJAMM-CNP	12828	Liolaemus	huacahuasicus	Argentina
41	LJAMM-CNP	15756	Liolaemus	nigriceps	Argentina
42	LJAMM-CNP	16075	Liolaemus	chlorostictus	Argentina
43	LJAMM-CNP	16055	Liolaemus	chlorostictus	Argentina
44	LJAMM-CNP	16056	Liolaemus	chlorostictus	Argentina
45	LJAMM-CNP	16077	Liolaemus	chlorostictus	Argentina
46	LJAMM-CNP	16057	Liolaemus	chlorostictus	Argentina
47	LJAMM-CNP	16054	Liolaemus	sp3	Argentina
48	LJAMM-CNP	15761	Liolaemus	nigriceps	Argentina
49	LJAMM-CNP	15662	Liolaemus	inti	Argentina
50	LJAMM-CNP	15664	Liolaemus	inti	Argentina
51	LJAMM-CNP	15659	Liolaemus	inti	Argentina
52	LJAMM-CNP	15661	Liolaemus	inti	Argentina
53	LJAMM-CNP	16105	Liolaemus	cazianae	Argentina
54	LJAMM-CNP	16079	Liolaemus	porosus	Argentina
55	LJAMM-CNP	16034	Liolaemus	orientalis	Argentina
56	LJAMM-CNP	16090	Liolaemus	sp4	Argentina
57	LJAMM-CNP	16033	Liolaemus	orientalis	Argentina
58	LJAMM-CNP	16093	Liolaemus	porosus	Argentina
59	LJAMM-CNP	16094	Liolaemus	porosus	Argentina
60	LJAMM-CNP	2709	Liolaemus	vallecurensis	Argentina
61	LJAMM-CNP	2034	Liolaemus	famatinae	Argentina
62	LJAMM-CNP	12022	Liolaemus	sp6	Argentina
63	LJAMM-CNP	12023	Liolaemus	sp6	Argentina
64	LJAMM-CNP	12024	Liolaemus	sp4	Argentina
65	LJAMM-CNP	12026	Liolaemus	sp4	Argentina
66	LJAMM-CNP	12027	Liolaemus	sp4	Argentina
67	LJAMM-CNP	12740	Liolaemus	sp4	Argentina
68	LJAMM-CNP	12741	Liolaemus	sp4	Argentina
69	LJAMM-CNP	2033	Liolaemus	famatinae	Argentina
70	LJAMM-CNP	15691	Liolaemus	halonastes	Argentina
71	LJAMM-CNP	15792	Liolaemus	halonastes	Argentina
72	LJAMM-CNP	12818	Liolaemus	huacahuasicus	Argentina
73	LJAMM-CNP	12821	Liolaemus	huacahuasicus	Argentina
74	LJAMM-CNP	15721	Liolaemus	multicolor	Argentina
75	LJAMM-CNP	15723	Liolaemus	multicolor	Argentina
76	LJAMM-CNP	15803	Liolaemus	scrocchii	Argentina
77	LJAMM-CNP	15801	Liolaemus	scrocchii	Argentina
78	LJAMM-CNP	2696	Liolaemus	vallecurensis	Argentina
79	LJAMM-CNP	2697	Liolaemus	vallecurensis	Argentina
80	LJAMM-CNP	14736	Liolaemus	vulcanus	Argentina
81	MNCN	34755	Liolaemus	sp.3	Bolivia
82	MNCN	34757	Liolaemus	sp.3	Bolivia

83	MNCN	34758	Liolaemus	sp.3	Bolivia
84	MNCN	34762	Liolaemus	sp.3	Bolivia
85	MNCN	34763	Liolaemus	sp.3	Bolivia
86	MNCN	34775	Liolaemus	sp.3	Bolivia
87	MNCN	34776	Liolaemus	sp.3	Bolivia
88	MNCN	34753	Liolaemus	sp.3	Bolivia
89	MNCN	34803	Liolaemus	sp.3	Bolivia
90	MNCN	34802	Liolaemus	sp.3	Bolivia
91	MNCN	48521	Liolaemus	sp.3	Bolivia
92	MNCN	48522	Liolaemus	sp.3	Bolivia
93	MNCN	48540	Liolaemus	sp.3	Bolivia
94	MNCN	48541	Liolaemus	sp.3	Bolivia
95	MNCN	48556	Liolaemus	sp.3	Bolivia
96	MNCN	48557	Liolaemus	sp.3	Bolivia
97	MNCN	48569	Liolaemus	sp.3	Bolivia
98	MNCN	48571	Liolaemus	sp.3	Bolivia
99	MNCN	48572	Liolaemus	sp.3	Bolivia
100	MNCN	39892	Liolaemus	pachecoi	Bolivia
101	MNCN	39893	Liolaemus	pachecoi	Bolivia
102	MNCN	39898	Liolaemus	pachecoi	Bolivia
103	MNCN	39899	Liolaemus	pachecoi	Bolivia
104	MNCN	39902	Liolaemus	pachecoi	Bolivia
105	MNCN	39903	Liolaemus	pachecoi	Bolivia
106	MNCN	39906	Liolaemus	pachecoi	Bolivia
107	MNCN	39907	Liolaemus	pachecoi	Bolivia
108	MNCN	39909	Liolaemus	pachecoi	Bolivia
109	MNCN	39910	Liolaemus	pachecoi	Bolivia
110	MNCN	39915	Liolaemus	pachecoi	Bolivia
111	MNCN	39916	Liolaemus	pachecoi	Bolivia
112	MNCN	39894	Liolaemus	islugensis	Bolivia
113	MNCN	39895	Liolaemus	islugensis	Bolivia
114	MNCN	39912	Liolaemus	islugensis	Bolivia
115	MNCN	39913	Liolaemus	islugensis	Bolivia
116	MNCN	48666	Liolaemus	islugensis	Bolivia
117	MNCN	48667	Liolaemus	islugensis	Bolivia
118	MNCN	48674	Liolaemus	islugensis	Bolivia
119	MNCN	48506	Liolaemus	signifer	Bolivia
120	MNCN	48507	Liolaemus	signifer	Bolivia
121	MNCN	48602	Liolaemus	signifer	Bolivia
122	MNCN	5588	Liolaemus	forsteri	Bolivia
123	MNCN	5589	Liolaemus	forsteri	Bolivia
124	MNCN	5598	Liolaemus	forsteri	Bolivia
125	MNCN	34747	Liolaemus	forsteri	Bolivia

126	MNCN	34748	Liolaemus	forsteri	Bolivia
127	MNCN	48584	Liolaemus	forsteri	Bolivia
128	MNCN	48585	Liolaemus	forsteri	Bolivia
129	MNCN	48603	Liolaemus	forsteri	Bolivia
130	MNCN	48613	Liolaemus	sp.2	Bolivia
131	MNCN	48614	Liolaemus	sp.2	Bolivia
132	MNCN	39889	Liolaemus	sp.1	Bolivia
133	MNCN	39890	Liolaemus	sp.1	Bolivia
134	MNCN	39891	Liolaemus	sp.1	Bolivia
135	SSUC	151	Liolaemus	rosenmanni	Chile
136	SSUC	394	Liolaemus	rosenmanni	Chile
137	SSUC	162	Liolaemus	patriciaiturrae	Chile
138	SSUC	362	Liolaemus	hajeki	Chile
139	SSUC	388	Liolaemus	foxi	Chile
140	SSUC	569	Liolaemus	pleopholis	Chile
141	SSUC	622	Liolaemus	stolzmanni	Chile
142	JT	98	Liolaemus	aymararum	Chile
143	JT	326	Liolaemus	jamesi	Chile
144	JT	285	Liolaemus	manueli	Chile
145	JT	328	Liolaemus	islugensis	Chile
146	JT	327	Liolaemus	islugensis	Chile
147	SSUC	337	Liolaemus	cf.schmidti	Chile
148	SSUC	135	Liolaemus	cf.schmidti	Chile
149	BYU	50507	Liolaemus	Nazca	Peru
150	BYU	50508	Liolaemus	Nazca	Peru
151	BYU	51569	Liolaemus	Moquegua	Peru
152	BYU	51566	Liolaemus	Moquegua	Peru
153	BYU	51568	Liolaemus	Moquegua	Peru
154	MUSM	31547	Liolaemus	Moquegua	Peru
155	MUSM	31528	Liolaemus	Moquegua	Peru
156	AQILO	2	Liolaemus	poconchilensis	Peru
157	MUSM	31545	Liolaemus	poconchilensis	Peru
158	MUSM	31543	Liolaemus	poconchilensis	Peru
159	MUSM	31544	Liolaemus	poconchilensis	Peru
160	MUSM	31490	Liolaemus	insolitus	Peru
161	BYU	50462	Liolaemus	insolitus	Peru
162	MUSM	31510	Liolaemus	ortizi	Peru
163	MUSM	31513	Liolaemus	ortizi	Peru
164	BYU	50469	Liolaemus	thomasi	Peru
165	BYU	50466	Liolaemus	thomasi	Peru
166	MUSM	31504	Liolaemus	robustus	Peru
167	MUSM	31508	Liolaemus	robustus	Peru
168	BYU	50438	Liolaemus	MinasMartha	Peru

169	MUSM	31446	Liolaemus	polystictus	Peru
170	MUSM	31452	Liolaemus	polystictus	Peru
171	MUSM	31455	Liolaemus	Castrovirreyna	Peru
172	MUSM	31481	Liolaemus	AbraApacheta	Peru
173	MUSM	31371	Liolaemus	AbraToccto	Peru
174	MUSM	31374	Liolaemus	AbraToccto	Peru
175	BYU	50426	Liolaemus	AbraToccto	Peru
176	MUSM	31461	Liolaemus	AbraToccto	Peru
177	MUSM	31373	Liolaemus	AbraToccto	Peru
178	BYU	50151	Liolaemus	melanogaster	Peru
179	BYU	50152	Liolaemus	melanogaster	Peru
180	BYU	50463	Liolaemus	williamsi	Peru
181	MUSM	31485	Liolaemus	williamsi	Peru
182	BYU	50489	Liolaemus	annectens	Peru
183	BYU	50486	Liolaemus	annectens	Peru
184	MUSM	31433	Liolaemus	annectens	Peru
185	BYU	50494	Liolaemus	etheridgei	Peru
186	BYU	50495	Liolaemus	etheridgei	Peru
187	MUSM	31443	Liolaemus	signifer	Peru
188	MUSM	31434	Liolaemus	signifer	Peru
189	MUSM	27688	Liolaemus	Apurimac	Peru
190	MUSM	27694	Liolaemus	Apurimac	Peru
191	MUSM	26393	Liolaemus	Parinacochas	Peru
192	MUSM	26387	Liolaemus	Parinacochas	Peru
193	LJAMM-CNP	12190	Phrymaturus	sitesi	Argentina

Appendix 2. Maximum likelihood tree based on cyt-b and 12S mitochondrial markers including 198 terminals. Terminals in red and blue are those found to be convergent in our SURFACE analysis. Asterisks represent ≥70% bootstrap support.

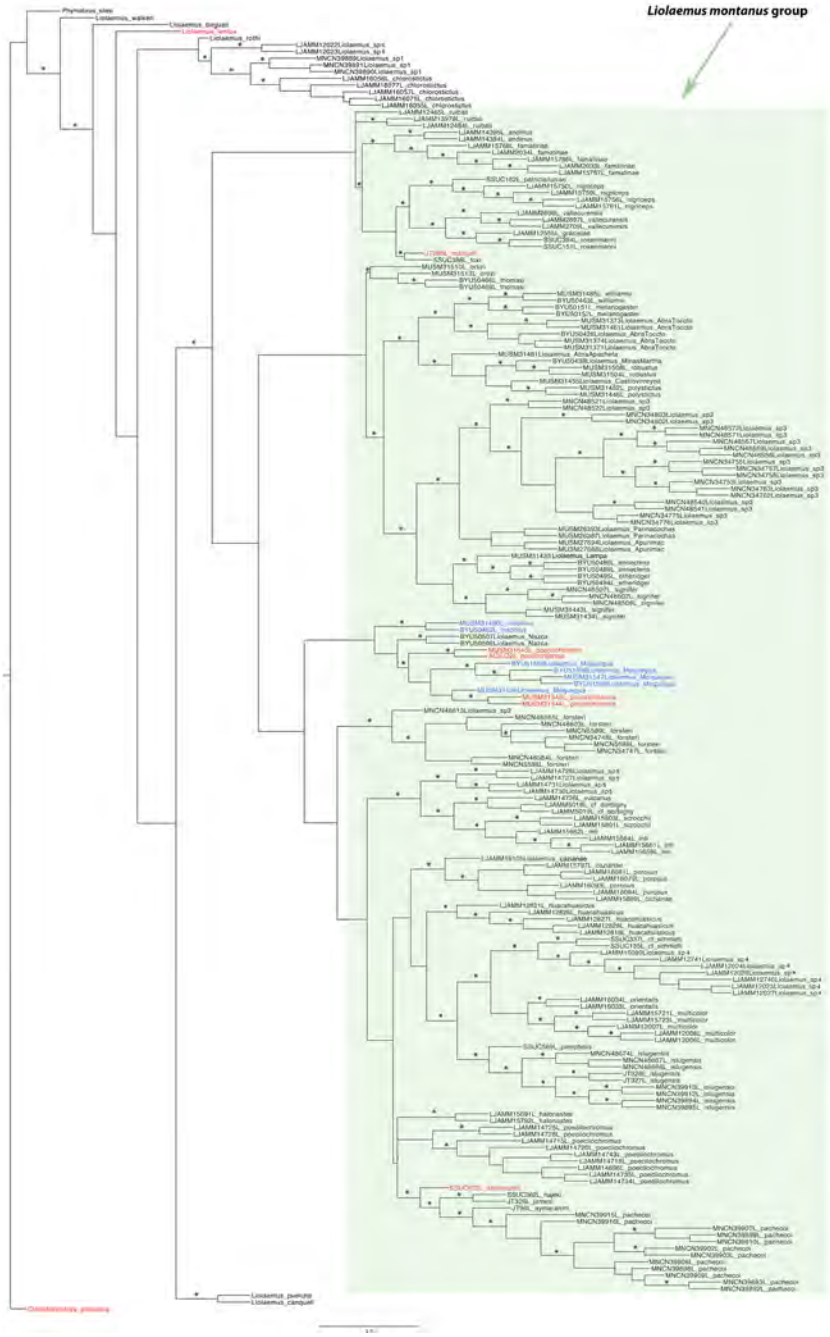

Appendix 3. Number of specimens per species examined for geometric morphometric and categorical traits.

	Taxa	Number of specimens
1	*Ctenoblepharys adspersa*	6
2	*Liolaemus* "Abra Apacheta"	10
3	*Liolaemus* "Abra Toccto"	24
4	*Liolaemus* "Apurimac"	31
5	*Liolaemus* "Castrovirreyna"	1
6	*Liolaemus annectens*	35
7	*Liolaemus aymararum*	9
8	*Liolaemus baguali*	2
9	*Liolaemus canqueli*	2
10	*Liolaemus etheridgei*	9
11	*Liolaemus forsteri*	9
12	*Liolaemus foxi*	9
13	*Liolaemus hajeki*	2
14	*Liolaemus insolitus*	9
15	*Liolaemus islugensis*	16
16	*Liolaemus jamesi*	2
17	*Liolaemus pseudoanomalus*	1
18	*Liolaemus manueli*	11
19	*Liolaemus melanogaster*	9
20	*Liolaemus nigriceps*	4
21	*Liolaemus orientalis*	3
22	*Liolaemus ornatus*	3
23	*Liolaemus ortizi*	7
24	*Liolaemus pachecoi*	11
25	*Liolaemus patriciaiturrae*	5
26	*Liolaemus pleopholis*	1
27	*Liolaemus poconchilensis*	8
28	*Liolaemus poecilochromus*	5
29	*Liolaemus polystictus*	37
30	*Liolaemus robustus*	20
31	*Liolaemus rosenmanni*	4
32	*Liolaemus rothi*	3
33	*Liolaemus scrocchii*	1
34	*Liolaemus signifer*	13
35	*Liolaemus stolzmanni*	6
36	*Liolaemus* sp.3	10
37	*Liolaemus thomasi*	4
38	*Liolaemus walkeri*	5

39	*Liolaemus williamsi*	12
40	*Liolaemus* "MinasMartha"	9
41	*Liolaemus* "Moquegua"	9
42	*Liolaemus* "Nazca"	10
43	*Liolaemus* "Parinacochas"	12
44	*Phymatarus patagonicus*	2
	Total	401

Appendix 4. Bayesian time calibrated tree of the *montanus* group (green rectangle), and its relationship with *Liolaemus lentus*, *Ctenblepharys adspersa* and other taxa. Focal taxa are colored according to the same convergent regimes found in SURFACE (see below). Asterisks (*) indicate posterior probabilities ≥ 0.9